KU Leuven
Biomedical Sciences Group
Faculty of Pharmaceutical Sciences
Drug Delivery and Disposition

TRACKING DOWN COLONIC DRUG DISPOSITION

THE LAST STATION FOR ACCUMULATION

Glenn **LEMMENS**

Jury:

Supervisor:	Prof. Dr. Patrick Augustijns
Co-supervisor:	Prof. Dr. Tim Vanuytsel
	Prof. Dr. Ricard Farré
Chair:	Prof. Dr. Ann Van Schepdael
Jury members:	Prof. Dr. Erwin Adams
	Prof. Dr. Kristin Verbeke
	Prof. Dr. Maria Vertzoni
	Dr. An Van den Bergh

Dissertation presented in partial fulfilment of the requirements for the degree of Doctor in Pharmaceutical Sciences

April 2021

Dankwoord

Het is eigenaardig hoe één zenuwachtige klik op ‘verzenden’ vier levensjaren kan vastleggen. Hoe een simpele ‘ja’ bepaalt wat ik doe, wie ik ontmoet, en wie ik zal worden. Zoveel kracht in één klein en schijnbaar onbeduidend moment. In dit dankwoord wil ik even stilstaan bij de mensen die me een ‘ja’ hebben gegeven, en de mensen die me geholpen hebben om het een ‘ja’ te laten blijven.

Patrick, dank u om mij deze kans te geven. Als promotor heb je me vier jaar lang in goede banen geleid, af en toe op de rem gaan staan, af en toe wat gas bij moeten geven, zodat ik nu met een mooie doctoraatsthesis de finishlijn kan oversteken. Je hebt er voor gezorgd dat ik in een toonaangevend labo onderzoek mocht verrichten, en je hebt er voor gezorgd dat ik mocht deelnemen aan meerdere internationale congressen in prachtige landen. Je hebt me ook getoond wat is het om gepassioneerd en gedreven te zijn. Maar bovenal is het prachtig dat ik ook mocht ‘falen’ in jouw labo. Zoals elke wetenschapper weet, lukken niet al de experimenten. Dan gaf je aan dat dat OK is, dat het een leercurve is, en dat we gewoon opnieuw proberen. Want ook dat is wetenschap; doorzetten. Dat terzijde, wil ik je er tevens een laatste keer aan herinneren dat het aantal trappisten dat je me moet al hoger dan 10 is.

Tim, ook jij bedankt om als copromotor mij deze kans te geven. Wat ik me het meest zal herinneren is hoe extatisch we waren toen we voor de eerste keer colonvochten konden collecteren. Wie had geweten dat *dat* je zo blij kon maken. Iedereen weet ook dat je een toonaangevend persoon bent in het gastro-intestinale domein, maar ik wil graag ook wat aandacht opeisen voor je werkethiek. Een heel passende quote om jou te omschrijven is ‘Lead by example’. Ik kon van dichtbij meemaken hoe je vele late/vroege uren draait, weekends opoffert voor het onderzoek, en je kost wat kost blijft doorzetten. Als ik het even niet kon opbrengen om door te werken, herinnerde ik mezelf er aan dat terwijl ik één zin neertik, jij waarschijnlijk al één onderzoeksartikel hebt geschreven, één eindeloos lange review hebt nagelezen, twee internationale lezingen hebt gegeven, ondertussen een coloscopie doet, en een koffietje drinkt. Want ontspannen moet natuurlijk ook. Daardoor vond ik het meer dan normaal om ook weekendshiften te draaien. Als je omringd bent door gemotiveerde mensen, dan ben je zelf ook gemotiveerd; je zorgde ervoor dat ik beter wou zijn. En daarvoor dank.

Ricard, I am also very grateful to have had you as a co-promoter. You have always greeted me with a smile, provided me with guidance, and helped me optimize several *in vitro* techniques that are vital to this thesis.

Joachim, ontzettend bedankt om steeds een kritische blik te werpen op de experimenten en artikels. Raf, bedankt voor de vele analyses, en *in situ* experimenten uit te voeren. Zonder jullie had deze thesis er heel anders uit gezien.

Mijn interne jury, Ann Van Schepdael, Kristin Verbeke, en Erwin Adams, bedankt om mijn project jaarlijks op te volgen, om mijn doctoraatsthesis met een kritisch oog te lezen, en steeds

hulpvolle feedback te geven. Ook hartelijk dank aan mijn externe jury, An Van den Bergh en Maria Vertzoni. An, we maakten beiden deel uit van het TRAIN project, wat betekent dat we op hetzelfde moment deadlines moesten halen, presentaties moesten voorbereiden, en zoveel mogelijk data wouden analyseren om dan te kunnen presenteren. Ik stond altijd versteld van het mooie en doordachte onderzoek dat je had uitgevoerd. Wat me bijblijft is dat zelfs als je mijn presentatie niet kon bijwonen, je op me afstapte tijdens de pauze om me uit te horen over mijn onderzoek. Het is altijd mooi om zien dat je onderzoek met oprechte interesse gevolgd wordt, en daarvoor dank. Also a massive thank you to Maria Vertzoni. You are one of the pioneers in the colon-department, and your research was of incredible use for this PhD project. I have always read your research with a lot of interest, and I will surely hold an eye out for your upcoming papers!

I also want to express my thanks to the entire TRAIN team. It was wonderful to witness how all of us were steadily discovering the uncharted territory that is the colon. In particular I would like to thank Jan Snoeys for being closely involved with my research, and to guide this project with the greatest care. I would also like to request a round of applause for Stephanie Kourula. Writing a review of 50+ pages is an intense and painstaking process, but we could always rely on you to deliver top notch texts, and to give valuable insight and feedback. Steffi, you set an example for a lot of aspiring researchers; you are persistent in your curiosity, and you are one of the kindest persons I have had the chance to meet. Forgive me for the pun, but I'm curious to see where the TRAIN will take us!

Ook een heel harde merci aan de verplegers op endoscopie, en al de vrijwilligers. Sommige vrijwilligers hebben al mijn studies meegemaakt, sommigen zijn zelfs vrienden geworden.

Superlatieven zijn onlosmakelijk verbonden met een dankwoord, maar het kan langdradig zijn om opnieuw en opnieuw te lezen. Vandaar dat ik nu een stukje tekst wil opdragen aan mijn collega's, die ik steevast associeer met het woord 'Meh'. Echter heeft mijn doctoraat me ook dit bijgebracht: iedere interactie is een opportuniteit om te leren.

Marlies, door jou weet ik nu dat de nauwkeurigheid van een Zwitsers zakhorloge in het niet valt in vergelijking met het knorren van jouw maag, elke dag stipt om 11 uur. Arno, door jou leerde ik dat Club Brugge het slechter doet dan ik dacht. Tom, van jou leerde ik dat het menselijke brein maar één taal heel goed kan beheren. Bij jou is die taal sarcasme. Matthias, de les die ik van jou kan leren moet nog komen…denk ik. Wanneer je een nieuwe job aanneemt, hoop je dat je collega's meevallen, want je zit er mee opgescheept voor vier jaar en je kan er niet aan ontsnappen. En ik had pech, want het zal verdomd moeilijk zijn om betere collega's te vinden. Jullie zijn stuk voor stuk prachtige mensen, die ik naast collega's ook graag vrienden noem.

Er zijn natuurlijk ook al veel collega's die momenteel niet meer op het DDD lab vertoeven. Jef, Jens, Jari, Philippe, Bart, jullie hebben me laten kennis maken met de wereld van de biofarmacie, en ook jullie draag ik een warm hart toe.

Het is ook belangrijk om ook de bijdrage van vrienden en familie te erkennen, mijn fan base. Zij hebben mij de nodige ontspanning gebracht doorheen de jaren, en me bijgestaan waar nodig.

Sofie, Sarah, Astrid: jullie hebben elke kilometer van mijn academische marathon mogen aanschouwen. Jullie zagen mijn interesse in wetenschap op de middelbare schoolbanken ontstaan, vierden het behalen van een bachelorsdiploma, een masterdiploma, en nu dit. Ontzettend bedankt om steeds sponzen, waterflesjes en bananen naar mij te gooien zodat ik zou blijven gaan. I made it.

Eline, Matthias, Inke, Asmin, Chloë, Yamina: mijn biochemievrienden, allemaal pientere wetenschappers. Als geen ander begrijpen jullie wat zo'n doctoraat inhoudt, waardoor dit ook vaak het gespreksonderwerp was. Ook jullie bedankt voor jullie steun doorheen de jaren!

Hier en daar pik je ook een hobby op, en maak je vrienden al gaande. En er is één eigenschap dat ze allemaal gemeenschappelijk hebben: hun liefde voor alcohol. Sure, ze zijn ook allemaal slim, fantastisch en emotioneel ontwikkeld, maar vooral drinken ze graag alcohol. Van Ciders in Kroatië met mijn badminton vrienden (Leen, Bernd, Ferre), rode wijn in Madrid of tijdens 'Ven A Comer!'-etentjes (Sam, Aline, Tom, Giel), cocktails tijdens wellnessuitjes en campingtrips (Ines, Sara, Christophe, Jens), tot schuimwijn op de Keizersberg drinken tot vlak voor de avondklok (Hannelore, Arwen, Anissa, Anne). Bedankt om mij steeds terug op te laden, zodat ik terug met volle moed naar het werk kon!

Een laatste paragraaf wil ik graag besteden aan mijn familie; mama en Peter, zusje en Iris, en ook mijn petekindje Sigge. Een opleiding is belangrijk, maar jullie hebben er voor gezorgd dat ik nieuwsgierig ben en jullie hebben me geleerd om door te zetten van jongs af aan. Twee kwaliteiten die onmisbaar zijn voor een wetenschapper. Mijn mama die 7 jaar oude Glenn oefeningen liet maken totdat hij het kon (één oefening fout, drie oefeningen erbij! Drie!), Peter die me de discriminant nog maar eens uitlegt op het whiteboard, Kim en Iris die de verdomd ingewikkelde chemische reacties of genetica uitleggen. Jullie hebben meer bijgedragen aan deze thesis dan jullie denken, en daarvoor dank.

List of abbreviations

ABC	ATP binding cassette
ADME(T)	Absorption, distribution, metabolism, excretion (and toxicity)
ALI	Air-liquid interface
API	Active pharmaceutical ingredient
ASBT	Apical sodium-dependent bile acid transporter
AUC	Area under the curve
BCRP	Breast cancer resistance protein
BCS	Biopharmaceutical classification system
BSEP	Bile salt export pump
CD	Crohn's disease
CES	Carboxylesterase
CHIM™	Cryopreserved human intestinal mucosa
C_{max}	Maximal drug concentration
COX	Cyclooxygenase
CRC	Colorectal cancer
CXB	Celecoxib
CXB-OH	Hydroxy celecoxib
CXB-COOH	Carboxy celecoxib
CYP	Cytochrome P450
DDI	Drug-drug interaction

DME	Drug metabolising enzyme
ECM	Extra cellular matrix
F_a	Human fraction absorbed
FaSSCoF	Fasted state simulated colonic fluid
FaSSGF	Fasted state simulated grastic fluid
FaSSIF	Fasted state simulated intestinal fluid
FeSSCoF	Fed state simulated colonic fluid
FeSSCoF-V2	Fed state simulated colonic fluid version 2
FeSSIF	Fed state simulated intestinal fluid
F_g	Human fraction escaping enterocyte metabolism
GLP	Glucagon-like peptide
FITC dextran 4	Fluorescein isothiocyanate dextran average molecular weight 4000
HIMEC	Primary intestinal microvasculature endothelial cells
HPLC	High pressure liquid chromatography
HT29-MTX	Human colorectal adenocarcinoma cell line differentiated into mature goblet cells using methotrexate
HV	Healthy volunteer
HuMix	Human-Microbial crosstalk
IBD	Inflammatory bowel disease
IC_{50}	The half maximal inhibitory concentration
IDE	Sulindac sulfide
iPS	Induced pluripotent stem cells
IS	Internal standard

LC	Liquid chromatography
LGFR5	Leucine-rich repeat-containing G-protein-coupled receptor 5
L-SHIME	Luminal Simulator of the Human Intestinal Microbial Ecosystem
MATE1	Multidrug and toxin extrusion 1
MCT	Monocarboxylate transporter protein
MMC	Migrating motor complex
MRI	Magnetic resonance imaging
MRP	Multidrug-resistance-associated protein
M-SHIME	Mucosal Simulator of the Human Intestinal Microbial Ecosystem
MUC	Mucin
NAD	5-hydroxy-L-tryptophan and 5-hydroxytryptamin
NSAID	Non-steroidal anti-inflammatory drug
NTCP	Sodium/taurocholate co- transporting polypeptide
OAT2	Organic anion transporting polypeptide 2
OATP	Organic anion transporting peptide
OCT	Organic cation transporter
ONE	Sulindac sulfone
Papp	Apparent permeability coefficient
PDMS	Permeable polydimethyl siloxane
PEPT1	Peptide transporter protein 1
P-gp	P-glycoprotein
qPCR	Quantitative Polymerase Chain Reaction

SCFA	Short chain fatty acid
SHIME	Simulator of the Human Intestinal Microbial Ecosystem
SIF_{ileum}	Simulating intestinal fluid
SIF_{ileum}-V2	Simulating intestinal fluid version 2
SLC	Solute carrier
SLCO	Solute carrier organic anion transporter
SUL	Sulindac
SULT	Sulfotransferase
TEER	Transepithelial electrical resistance
TIM	Tno gastro-intestinal model
Tim-agc	Tno gastro-intestinal model advanced gastric compartment
T_{max}	Time to reach maximal drug concentration
UC	Ulcerative colitis
UGT	Uridine 5'-diphospho-glucuronosyltransferases
ZO-1	Zonula occludens 1

Table of contents

Dankwoord ..... **ii**

List of abbreviations ..... **vi**

CHAPTER 1 - Introduction **5**

1.1 Drug barriers for colonic absorption 6
1.1.1 The colonic epithelium 7
1.1.2 Mucus 10
1.1.3 Microbiome 11
1.2 Colonic fluid characteristics 12
1.2.1 Colonic volume 12
1.2.2 Colonic pH 14
1.2.3 Colonic motility 14
1.2.4 Buffer capacity, osmolality, protein content and bile acids 15
1.3 *In vitro* evaluation tools for colonic drug disposition 17
1.3.1 Dissolution and degradation 17
1.3.2 Drug absorption and stability 20
1.4 Colonic drug disposition of NSAIDs 40

CHAPTER 2 - Objectives **43**

CHAPTER 3 – Colonic disposition of Celecoxib **45**

3.1 Abstract 45
3.2 Introduction 46
3.3 Material and methods 47
3.3.1 Chemicals 47
3.3.2 Media 48
3.3.3 Clinical studies 48
3.3.4 Processing of biological samples 51
3.3.5 LC analysis 52
3.3.6 Data presentation 53
3.4 Results and discussion 54
3.4.1 Optimizing enema administration and collection of colonic contents 54
3.4.2 Optimizing time and region to evaluate colonic celecoxib disposition 56
3.4.3 Time-dependent systemic and caecal dispostion of celecoxib 58
3.5 Conclusion 63
3.6 Acknowledgements 63

CHAPTER 4 - Colonic disposition of Sulindac **65**

4.1 Abstract 65

4.2 Introduction 66
4.3 Material and methods 69
4.3.1 Chemicals 69
4.3.2 Media 69
4.3.3 Clinical study 70
4.3.4 Three stage dissolution testing 71
4.3.5 In situ metabolism and excretion of sulindac in rats 72
4.3.6 Processing of biological samples 72
4.3.7 LC analysis 74
4.3.8 Data presentation 75
4.4 Results and discussion 76
4.4.1 Dissolution of sulindac in a three stage set-up 76
4.4.2 Time-dependent systemic and caecal disposition of sulindac 77
4.4.3 Intestinal disposition of sulindac and metabolites in rats 86
4.4.4 Mechanistic insights into the caecal disposition of sulindac and metabolites 86
4.5 Conclusion 89
4.6 Acknowledgements 89

CHAPTER 5 – In vitro accumulation assays 91

5.1 Abstract 91
5.2 Introduction 92
5.3 Materials and methods 94
5.3.1 Chemicals 94
5.3.2 Media 94
5.3.3 In situ metabolism and excretion of celecoxib and carboxy celecoxib in rat 95
5.3.4 In vitro drug disposition studies in Caco-2 cells 96
5.3.5 Ex vivo drug disposition studies in human colonic biopsies 98
5.3.6 Processing of biological samples 100
5.3.7 LC analysis 101
5.3.8 Data presentation 102
5.4 Results 102
5.4.1 In situ metabolism and excretion of celecoxib and carboxy celecoxib in rat 102
5.4.2 Colonic accumulation in in vitro/ex vivo intestinal models 103
5.5 Discussion 109
5.5.1 The intrinsic accumulation behaviour in colonic mucus and tissue 111
5.5.2 Simulating an in vivo relevant colonic disposition – suspensions 113
5.5.3 Remarks on performing accumulation assays 113
5.6 Conclusion 115

CHAPTER 6 – Concluding discussion 117

6.1 Understanding how high colonic concentrations are reached: gut versus systemic driven uptake 118
6.2 Implications for colon-targeting drugs 120
6.3 Implications for colonic drug disposition in pathophysiology 123

6.4 Implementation of in vitro accumulation assays in drug development tests 124

Supplementary Figure 129

English summary 131

Nederlandstalige samenvatting 135

Bibliography 139

Author contributions, scientific acknowledgements and conflict of interest 155

Author contributions 155
Scientific acknowledgements 156
Conflict of interest 156

Curriculum vitae 157

CHAPTER 1 - Introduction

This chapter is based on a review manuscript, which has been published in a slightly different form:

Drug disposition in the lower gastrointestinal tract: targeting and monitoring

Glenn Lemmens, Arno Van Camp, Stephanie Kourula, Tim Vanuytsel, and Patrick Augustijns

Pharmaceutics. 2021 Jan 26;13(2):161

Colorectal cancer is the third most abundant type of cancer with an estimated 1.8 million new cases in 2018 and the fourth most commonly diagnosed cancer, with incidence rising continuously, especially in developing countries [1]. Inflammation plays a key role in the development and progression of the disease. Therefore, non-steroidal anti-inflammatory drugs (NSAIDs) such as sulindac and celecoxib are suitable candidates for the treatment and/or prevention. For instance, after taking 400 mg of the COX-2 inhibitor celecoxib twice a day for three years, the incidence of recurrent adenomas was reduced by 45% [2]. Treatment of familial adenomatous polyposis patients with 150 mg sulindac twice a day for 9 months reduced the number of polyps with 44% and their size with 35% [3]. Even though multiple studies have shown the efficacy of these NSAIDs for the prevention of colorectal polyps and cancer, multiple hiatus remain about the colonic disposition of these drugs. For example, it is not known whether high colonic concentrations are reached through the systemic circulation after intestinal drug absorption, or by luminal and local exposure in the colon. This is affected by the release strategy, the physicochemical properties of the drug and the physiology of the gastro-intestinal tract. Firstly, we consider the selected release strategy: while drug delivery systems can be engineered towards physiological colonic triggers (ileal pH, extensive transit time, etc) to achieve local release in the colon, drugs that were formulated as immediate release can also arrive at the colon due to incomplete small intestinal absorption. Subsequently, the drug's physicochemical properties (i.e. pKa, solubility, logD, chemical stability) and the colonic fluid variables (i.e. composition, residual volumes, motility) underlie the dissolution behaviour. Prior to uptake, the drug will encounter various colonic barriers such as the gut microbiome, the thick

bilayered mucus, and ultimately the colonic mucosa that expresses uptake-, and efflux transporters and drug metabolising enzymes in a region dependent manner. To better understand the colonic drug disposition, and to also work towards a successful selection of clinical drug candidates, there is a need to better understand the interplay between the drug delivery system, the physicochemical properties of the drug, and physiological variables. In order to achieve this, techniques need to be established that can be used to assess the *in vivo* colonic disposition. Moreover, *in vitro* dissolution assays and media (biorelevant media, faecal slurries, etc.) need to allow physiologically relevant dissolution kinetics, and screening assays need to closely mimic intestinal function *in vitro* as to assess intestinal stability, permeation and accumulation. This introduction will first give a comprehensive overview of the colonic physiology in relation to drug absorption, including the various colonic barriers (epithelium, mucus, microbiome) and the colonic fluid variables (volume, pH, etc.). Then, the available *in vitro* tools that can be used to characterize GI drug disposition will be reviewed, covering dissolution, degradation, and absorption and stability models. Finally, we will address how we will evaluate the colonic disposition of celecoxib and sulindac, through both *in vivo* and *in vitro* studies.

1.1 Drug barriers for colonic absorption

The colonic mucosa is a highly differentiated structure that comprises multiple cell types, which are localized at the surface, or in the invaginations called crypts of Lieberkühn. The colonic crypts contain LGFR5 (leucine-rich repeat-containing G-protein-coupled receptor 5)-positive stem cells that give rise to transit-amplifying cells, which can rapidly proliferate, divide and differentiate into the different epithelial cell lineages [4]. The stem cells are often interspersed with CD24+ (CD = cluster differentiation) cells, and Paneth cells in the right hemicolon. CD24+ cells might represent Paneth cells, which secrete anti-microbial peptides [5,6]. Enteroendocrine L-cells, situated at the base of the crypt, produce hormones such as Glucagon-like peptide 1 and 2 (GLP-1/2) [7]. Differentiated colonocytes are mostly present at the surface of the crypt, and important for resorption, secretion and humoral immunity. Furthermore, M-cells function as specialized surface epithelial cells that cover the lymphoid follicles of Peyer's patches, and transport antigens and microorganisms to the underlying lamina propria, which is a connective tissue layer harbouring the immune cells [8]. The amount of epithelial goblet cells ranges from 4% in the duodenum to 16% in the distal colon [9,10]; they produce a thick two-layered mucous

intestinal lining, with the outermost layer colonized by a highly dense and diverse microbiome [11,12], and in contact with a complex luminal environment (presence of bile salts, lipid degradation products, etc.). The inner layer is more densely structured and largely devoid of bacteria [13].

1.1.1 The colonic epithelium

Intestinal models should represent the biochemical (metabolism, efflux, uptake) and physical (cell layer, mucus, unstirred water layer) barrier characteristics of the GI tract to enable an accurate prediction of intestinal absorption and metabolism. To this end, simulation models need to accurately capture the different transport mechanisms, both passive and active. Passive diffusion is gradient driven and can occur paracellularly for low molecular weight hydrophilic molecules. It is determined by tight junctions, which are the most apical part of the junctional complexes that connect neighbouring epithelial cells [14–16]. Paracellular transport is limited [17] as the available surface area is considerably lower (estimated at 1%) compared to transcellular transport. Not surprisingly, a substantial fraction of the commercially available drugs, 85% - 90%, permeate transcellularly [18], with lipophilic drugs generally partitioning into the cell membrane by passive diffusion. The absorption of drugs can also be facilitated by transporters or can undergo efflux out of the enterocytes. This process is often associated with drug-drug interactions (DDI) given its stereoisomer specific, saturable, and inhibitable nature [19]. Since the mucosa is functionally differentiated throughout the GI tract, drug absorption can differ along the intestinal region. The absorption in the colon is compromised by various factors in comparison to the small intestine. First, the absence of villi in the colon drastically reduces the available surface area (from 60 m^2 in the jejunum and ileum to 0.3 m^2 in the colon) for passive absorption [20]. Secondly, the electrical resistance of the colonic epithelium, a measure for paracellular permeability, is higher than in the small intestine [14–16] resulting in decreased paracellular passive absorption. Furthermore, in humans, the left hemicolon is more permeable than the right hemicolon [21]. The regional expression of claudins, cell-cell adhesion molecules of the tight junctions, is likely at the base of these absorption differences [22]. Lastly, transporters and metabolizing enzymes are expressed in a manner specific for the colonic region, affecting drug absorption and metabolism.

The absorption of a drug can be influenced by the activity of uptake and efflux transporters as well as metabolizing enzymes. Efflux transporters such as P-glycoprotein (P-gp; ATP binding cassette subfamily B member 1 (*ABCB1*)) have a higher affinity, especially for cationic lipophilic components to prevent a toxic build-up of harmful xenobiotics (e.g. alkaloids and flavonoids), while uptake transporters such as peptide transporter protein (PEPT1; Solute carrier family 15 member 1 (*SLC15A*)), monocarboxylate transporter protein (MCT1; *SLC16A*), and apical sodium-dependent bile acid transporter (ASBT; *SLC10A2*) take up hydrophilic compounds, e.g. dipeptides, monocarboxylic acids, and bile acids, respectively. These ionized and high molecular weight drugs generally cannot pass the epithelium transcellularly or paracellularly via passive diffusion. Although transporters have their respective role in regulating drug absorption, the expression pattern is not homogenous in the GI tract [23,24].

In the colon, the following protein ratios were determined through a proteomics approach [23]: MCT1 (55%) > multidrug-resistance-associated protein (MRP3; *ABCC3*) (14%) > MRP4 (*ABCC4*) (9%) > MRP2 (*ABCC2*) (8%) > P-gp (5%) > organic anion transporting peptide 2B1 (OATP2B1; Solute carrier organic anion transporter family member 1B1 (*SLCO2B1*)) (4%) > breast cancer resistance protein (BCRP; ABCG2) (3%) > PEPT1 (2%) > organic cation transporter 1 (OCT1; *SLC22A1*) (1%). MCT1 and MRP4 are represented highest in the colon, and MRP4 was homogenously present along the entire intestine. Some transporters displayed a gradient-like gene expression and protein abundance along the intestine. Efflux transporters P-gp and BCRP, and uptake transporter PEPT1 increased noticeably from the duodenum to distal jejunum and ileum, and substantially dropped in the colon. MRP2, MRP3 and OCT1 protein levels were the highest in the jejunum. Various other transporters such as MRP1, Bile salt export pump (BSEP; *ABCB11*), multidrug and toxin extrusion 1 (MATE1; *SLC47A1*), Sodium/taurocholate co-transporting polypeptide (NTCP; *SLC10A1*), organic anion transporting polypeptide 2 (OAT2; *SLC22A7*) OATP1A2 (*SLCO1A2*), OATP1B1 (*SLCO1B1*), OATP1B3 (*SLCO1B3*), and OCT3 (*SLC22A3*) could not be detected on protein level. Trace amounts of *ABCC1* (MRP1), *SLC22A3* (OCT3), *SLC22A7* (OAT2), and *SLC47A1* (MATE1), were only observed in the form of messenger RNA (mRNA) [23].

Similar to transporter proteins, there is evidence that drug metabolizing enzymes (DME) are expressed heterogeneously along the GI tract, with the highest expression levels in the proximal to mid small intestine, the main site of drug absorption and metabolism. Expression of

Cytochrome P450 Family 3 Subfamily A Member 5 (CYP3A5), CYP2B6, CYP2J2 and particularly CYP3A4 and CYP2C9 is high in the duodenum and jejunum, but significantly decreases in the ileum/colon when quantified using liquid chromatography/tandem mass spectrometry [25]. This observation could be extended towards all the investigated DMEs, although CYP2C19, CYP2B6, CYP3A5, and CYP2D6 were poorly expressed in all segments. In the colon, the mean contribution to intestinal gene expression is: CYP2B6, 9%; CYP2C9, 0.8%; CYP2C19, 1.1%, CYP2D6, 2.4%; CYP3A4, 0.3%; CYP3A5, 3%). Sulfotransferases 1A (SULT1A), uridine 5'-diphospho-Glucuronosyltransferases 1A (UGT1A) and UGT2B7 were expressed in a similar longitudinal pattern: an increase was observed from duodenum to jejunum, followed by a substantial decline in the ileum and the colon [24].

Several DMEs have been reported to work in tandem with transporter proteins, including CYP3A4 and P-gp, UGTs and MRP2/3 as well as SULTs and BCRP [24]. Interestingly, the increase in P-gp expression from the proximal to the distal region of the small intestine coincides with a decrease in CYP3A4 expression [26,27]. Due to the synergistic interplay of CYP3A and P-gp on dual substrates and the long intestinal transit time, drugs can undergo extensive pre-systemic intestinal metabolism. Nevertheless, expression or protein levels do not always accurately reflect activity [27].

Drozdzik et al. reported a good correlation between mRNA-protein levels of various transporters in jejunal tissue (i.e. P-gp and PEPT1, but not MRP3 and OATP2B1) [23]. Similarly, a study by Fritz et al. demonstrated good correlations between gene and protein expression for several DMEs (i.e. CYP3A4/5, CYP2C9/19, CYP2D6, UGT1A1/1A3 and UGT2B7) in small intestinal tissues, but not in hepatic tissue (i.e. CYP2E1, UGT1A3 and UGT2B7/15 and 46) [24]. However, overall gene expression data are not necessarily a good predictor for the encoded protein nor transporter capacity. Moreover, transporter capacity can be influenced by differences in surface area, blood flow, mode of action (pH–dependency of PEPT1 or ATP requirements of ABC transporters), and repeated cycles of metabolism [23]. Therefore, one should be careful to interpret mRNA/protein levels of transporters and enzymes in both *in vivo* and *in vitro* settings.

1.1.2 Mucus

The colonic epithelium is lined with a mucus layer, acting as a barrier to potential pathogens, but also to drug absorption [28]. Mucus is an aqueous matrix composed of water (95%), lipids, electrolytes and glycoproteins, with a thickness and composition that is region dependent. The number of goblet cells increases from 4% in the duodenum to 16% in the distal colon [9,10], resulting in a thin and loosely structured mucus layer in the small intestine that allows an efficient drug and nutrient absorption (10 µm in the ileum) [29,30]. In contrast, the colonic mucus is organized as a thick two-layer system [31,32], and consists of a dense inner mucus layer (± 100 µm in sigmoid human biopsies) which does not contain bacteria and is further remodelled by endogenous proteases into the thicker and more porous outer mucus layer (± 300 µm) to allow a symbiotic relationship with the microbiome [11,12], [27]. In contrast to the previous study that investigated mucus thickness solely in the sigmoid colon, Strugula et al. reported that thickness of the adherent layer varies throughout the colon, ranging from 10-30 µm in the caecum to 30-85 µm in the rectal region. Possible discrepancies in mucus thickness between laboratories might be due to non-standardized protocols [32]. The mucus properties, which include viscosity, mesh size, lipophilicity, and ionisation state can influence drug diffusion and permeability, and require consideration when evaluating drug disposition.

Diffusion through the mucus is dependent on the physicochemical properties of the drugs and mucins. Mucins are highly glycosylated and negatively charged molecules at small intestinal and colonic pH, due to the low pKa (between 1 and 2.6) of the sialic acid at the terminal part of the oligosaccharide chain. MUC 2 is the predominant secreted mucin [13]. Desai et al. reported that several positively charged drugs (NAD, 5-hydroxy-L-tryptophan and 5-hydroxytryptamin) diffuse more slowly through porcine mucus than uncharged drugs [34], while anionic drugs can get repulsed by glycoproteins [35]. Hydrophilic and net-neutrally charged drugs are therefore favoured for mucopenetration, as they will not form strong adhesive bonds with mucins. The group of Behrens compared the apparent permeability for a series of lipophilic drugs (including barbiturates and testosterone) between mucus-free Caco-2 cells and mucus producing HT29 cells, and reported a slower diffusion for drugs with logP > 1, e.g. up to 43% for testosterone [36]. Wikman-Lahred and colleagues came to a similar conclusion when using porcine intestinal mucus to investigate the diffusion of small molecules with logP values ranging from -3.1 to 3.3 [37]. The reduced diffusion of lipophilic drugs through mucus can be

due to non-specific binding to the lipidic non-glycosylated protein domains of the mucins [36,38]. Although hydrophilicity and charge-selectivity are important characteristics to achieve good mucus diffusion, hydrophobic drugs are more prone to partition into the lipid-dense cellular membranes.

Mucus is a randomly organized network of fibres, with a mesh size or diameter between 50 and 1800 nm in aqueous media. Common drugs with a size below 10 nm can freely diffuse through the mucus layer as the amount of steric interactions is limited. Even small capsid viruses (Norwalk virus, human papilloma virus, polio virus) can rapidly diffuse through human mucus, [35]. Desai and colleagues reported a consistent retarding effect of mucus on the diffusion of macromolecules between 126 and 186,000 Da [39]. As such, size only has a substantial effect for very large drugs. However, since colonic conditions (limited and scattered free water pockets) are unfavourable to dissolve a drug which arrives in the colon in particulate form, mucus penetration may be restricted. Furthermore, size-dependent diffusion might be more restricted towards the distal part of the colon since the thickness of the viscous, gelatine-like mucus increases along the GI-tract. When a drug is subjected to suboptimal diffusion, either through interaction or size-filtering, the intestinal mucin turnover time can pose a prominent problem for drugs to reach the epithelium. Mucus turnover and clearance varies from minutes to several hours and can prevent drug accumulation in tissue. Especially the outermost mucus layer in the colon needs to be traversed quickly as it is also rapidly cleared [40,41]. Lastly, mucus contains digestive enzymes (including exopeptidases, such as carboxypeptidases and aminopeptidases) that can consequently affect the diffusion through the mucus layer [35]. To summarize, mucus penetration is favoured by net-neutrality, an increase in hydrophilicity and decrease in size, and a good stability against mucus-located enzymes.

1.1.3 Microbiome

The human gut contains trillions of microbes, predominantly bacteria from hundreds of different species, with Bacteroidetes and Firmicutes being the most prevalent phyla, but also archaea, viruses and fungi. The microbiome exerts a crucial role in a range of physiological functions (food digestion, synthesis of essential vitamins, contributing to a functioning immune system, regulating intestinal functions, and others) and also produces organic compounds which fulfil an important physiological role (e.g. short chain fatty acids (SCFAs),

phosphatidylcholine, branched-chain amino acids, vitamin K, secondary bile acids and neurotransmitters such as serotonin). Not only is the composition of the microbiome highly individual (age, geographical location, diet, drugs, disease), the bacterial density and composition also varies along the GI tract. More than 400 species of bacteria are present, with high bacterial concentrations in the colon (10^{11} per gram content) compared to the proximal small intestine (10^{4} per gram) [42], which can be exploited for microbiome based colonic drug delivery. Moreover, most of the available studies have focused on the faecal, i.e. distal luminal microbiome, but this is different from the mucosa-adherent microbiome in the mucus layer or the lumen in the different regions of the GI tract which are more difficult to access [43,44]. For a detailed discussion of the microbiome diversity from multiple colonic mucosal sites and faeces, and how it differs from the mucosa-adherent microbiome, we refer to studies by Eckburg [45] and Zoetendal [44], respectively.

After oral intake, many drugs can be modified by the gut microorganisms in the small and large intestine. Zimmerman et al. reported microbiome-induced alterations of two thirds of the 271 investigated drugs. This can result in their activation (e.g. sulfasalazine), inactivation (e.g. digoxin) or toxification (e.g. sorivudine) [46]. Furthermore, the microbiome can indirectly influence drug bioavailability by modulating the local environment by secretion of SCFAs like butyrate, or by altering the solubility and ionisation state of drugs through fermentation products that result in pH fluctuations [32]. Also, dysbiosis in diseased states can be linked to an altered colonic transit, which impacts the extent of bacterial metabolism [47]. Lastly, an increase of the mucin-degrading bacterium *Ruminococcus gnavu* has been described, which can affect mucus diffusion [48]. For a more extensive study on human microbiome drug metabolism, we refer to [46].

1.2 Colonic fluid characteristics

1.2.1 Colonic volume

Drug dissolution and release in the colon is influenced by a range of physiological variables, including pH, bile salts, pressure, buffer capacity, and fluid volume. The ascending, transverse and descending colon contain an average of 561 ± 321 mL of biomass with 86% being water. Nevertheless, most of the water is bound to or contained inside the bacteria or biomass and not

freely available to allow drug dissolution [49]. An MRI study showed a total free water volume in the colon of only 13 mL (range 1- 44 mL) dispersed into small pockets [50].

However, the total free water volume is dependent on liquid and food intake. The group of Murray observed 11 ± 5 pockets of resting liquid with an average total volume of 2 ± 1 mL in the ascending colon in fasted state. Thirty minutes after administration of a glass of water, 17 ± 7 separate liquid pockets were observed that amounted to a total volume of 7 ± 4 mL. This increase in volume and number of pockets might be related to the gastro-colonic reflex, potentially transferring ileal contents into the ascending colon upon ingestion of water. An alternative explanation is that an initial fraction of the ingested liquid arrives in the colon [49]. Diakidou et al. compared the fluid volumes 5 hours after ingestion of either a reference meal or 240 mL of water. They reported that fluid volumes were higher after food than after water intake in the distal ileum, caecum and the ascending colon (e.g. 22.3 ± 7.7 mL after water vs. 29.9 ± 10.8 mL after the reference meal in the ascending colon) and that liquid fractions were generally higher in the fasted than in the fed state [51]. Additionally, the fluid volume in the ascending colon is 5.9 and 4.2 times bigger compared to the ileum in the fasted and fed ileal condition, respectively [51]. This is in agreement with a regional analysis of Murray and colleagues, who demonstrated that free water pockets were found primarily in the ascending colon, although they noticed a very high interindividual variability [49]. This difference in volume might be due to a longer residence time in the ascending colon and to a change in bacterial content.

It is evident that a restricted colonic fluid volume can hamper drug dissolution and absorption. The group of Tannergren reported regional absorption data of 42 drugs demonstrating that most BCS I drugs (high solubility and high permeability) were well absorbed, implying a sufficient dissolution and uptake, either through convective or diffusive transport. However, some BCS II drugs (low solubility and high permeability) were associated with a lower colonic absorption compared to oral dosing (F_{rel} Colon: $AUC_{colon,\ local\ solution}/AUC_{reference,\ oral\ administration}$), despite being administered to the colon as solutions, which suggests *in vivo* precipitation [52]. This indicates that (i) the low colonic fluid volume is an important aspect in early assessment of absorption potential for controlled release products (i.e. Tannergren and colleagues suggested the use of dose:solubility ratio of 50 mL for high solubility drugs) and (ii) that there is a need for a more relevant incubation method, e.g. suspensions or granules opposed to solutions.

Tannergren and colleagues showed that administering a suspension of dexloxiglumide (BCS II) to the colon resulted in a delayed maximal plasma concentration (T_{max}) compared to a solution, which also indicates a slow dissolution rate. When the same comparative analysis was applied to BCS I drugs, a high relative colonic absorption was achieved, which is consistent with the higher solubility [52].

1.2.2 Colonic pH

Upon arrival of carbohydrates in the caecum, the microbiome can transform undigested carbohydrates into SCFA including acetic, propionic, and butyric acid. The fermentation of carbohydrates is accompanied by an intraluminal pH drop in the proximal colon (caecum or ascending colon). The pH drop averages between 1.5 (to pH 5.8 – 6.8) and 1.2 units (to pH 6.1 – 7.1) in the fasted and fed state, respectively, indicating that the food status only marginally affects luminal pH in the distal GI tract [53]. A gradual pH increase is described along the colon, reaching 6.1-7.5 in the rectum [54–56]. This pH rise along the colon is likely due to decreasing intraluminal SCFA concentrations [55]. Moreover, the colonic mucosal surface pH (7.1 – 7.5) [57] is reported to be higher than the luminal pH [55].

Besides prandial state, the effect of non-environmental factors such as gender and age on the pH profile has recently been reviewed by Broesder et al. [53]. The pH in the lower GI tract of fasted healthy children (age 8 – 14) differed only slightly from the pH observed in adults, while the effect of aging (age group 62 – 83) was inconclusive. Furthermore, gender showed no significant effect on the pH profile in the ileum and colon, although this was only investigated in the fasted state.

1.2.3 Colonic motility

The smooth muscles of the gastric wall follow a cyclic iteration of three contractility phases, called the interdigestive migrating motor complex (MMC), which range from an absence of contractions (MMC phase 1) over irregular contraction patterns (MMC phase 2) to a short burst of contractions with maximal amplitude and frequency (MMC phase 3) that induce emptying of contents into the small bowel [58]. Segmental contractions start in the duodenum, become less spatiotemporally organized as activity propagates, and reach the terminal ileum in approximately 2 hours [59]. This results in a net overall distal movement of chyme, that slows

down substantially in the terminal ileum, resulting in a local temporary build up. The ileocolonic junction then regulates the passage to the caecum in a pulsatile contractive manner and is associated with propagating ileal contractions. Caloric intake can furthermore induce an ileocecal transfer. In total, a volume of 1-2 L reaches the caecum on a daily basis. The colon is characterized by rhythmic, phasic and tonic contractions that lead to both propulsion and mixing. Furthermore, high-amplitude propagating contractions induce mass movements and ultimately result in defecation [9]. The motility of the colon depends on many variables. For example, colonic transit is usually delayed during sleep, and motility increases significantly at awakening and with the intake of food. Also, a gender effect was observed, with healthy woman usually having a slower colonic transit (Maurer, 2016). Therefore, transit times are highly variable, e.g. Maurer et al. reported a colon arrival time of 3.25 to 8.20 h and a whole gut transit time of 10.01 to 59.39 h when using an IntelliCap® system (an electronic oral drug delivery and monitoring device) [60]. The prolongation of the colonic residence time as compared to the small intestine (4 h) [61] in healthy subjects can be relevant for the disposition of colon-targeted delivery systems. For a more in-depth characterisation of colonic transit, we refer to [60] and [62].

1.2.4 Buffer capacity, osmolality, protein content and bile acids

Human intestinal fluids contain bile salts, fatty acids, enzymes and other components that can impact the integrity of the mucosal barrier, as well as the dissolution and permeation rate of a drug. To this end, characterisation of colonic fluids can result in a better understanding of drug absorption. Reppas et al. analysed aspirated samples from the ileum, caecum and ascending colon, in both fed and fasted state. They reported that the pH and buffer capacity of caecal contents as compared to the ileum are lower and higher, respectively, which is the result of a higher concentration of total SCFA. Buffer capacity further increased towards the ascending colon. Prandial state did not influence SCFA levels in the ileal and caecal region but did in the ascending region. Furthermore, the osmolality of caecal and ascending colonic contents are lower compared to duodenal fluids; they are hypo-osmotic. While colonic protein contents are lower, total carbohydrate concentrations are higher in fed state conditions. Peptides and proteins are completely digested and the degradation products are largely absorbed along the proximal small intestine. This is not the case for carbohydrates, as the undigested fraction can reach the colon. The colonic concentrations of bile acids, which are largely reabsorbed in the distal ileum,

vary between 70µM and 500 µM in the fasted state. The composition is markedly different in the fed state. Consumption of a meal leads to a saturation of the metabolic capacity of the microbiome. Consequently, an increase in primary (cholic acid, chenodeoxycholic acid) over secondary (deoxycholic acid, lithocholic acid) bile acids is observed in the fed ascending colon. Free fatty acid concentrations are twice as high in the caecum and ascending colon compared to the ileum in both prandial states. An increased total concentration of phospholipids was observed from the distal ileum to caecum to ascending colon in the fasted state. In fed state conditions, the increase was only observed from the cecum to ascending colon. Cholesterol concentrations were not markedly different between the colonic regions, regardless of food intake [51,63,64].

The characterisation of the composition of aspirated samples can improve our understanding of the performance of active pharmaceutical ingredients and has also been used to develop biorelevant media. Although the use of Fasted or Fed State Simulated Colonic Fluids (FaSSCoF and FeSSCoF) is still limited, other simulated fluids have proven useful to study drug behaviour in *in vitro* models. The presence of bile acids in biorelevant media can positively influence dissolution and solubility of lipophilic drugs. However, the components present in the biorelevant media may affect the barrier function. For instance, Ingels and colleagues showed how compounds in FaSSIF can modulate the function of efflux carriers. An inhibitory effect on P-gp was seen especially for sodium taurocholate up to 3mM [65]. Mixed micelles, present in biorelevant media, may affect the extent of drug absorption. Hydrophobic drugs have been reported to partition into these mixed micelles, thereby reducing the amount of free drug as driving force for permeating the Caco-2 layer [66,67]. The pH of the intestinal media will also affect the degree of drug ionisation and permeation, i.e. weakly basic drugs such as propranolol and carvedilol can acquire a higher degree of ionization at pH 5 of FeSSIF, which could impair the permeation. Noteworthy is that biorelevant media are still an approximation of the complex *in vivo* fluid composition.

1.3 *In vitro* evaluation tools for colonic drug disposition

1.3.1 Dissolution and degradation

During drug development, *in vitro* release and dissolution setups continue to be essential tools, especially given the wide range of physiological variables (including pH, bile salts, pressure, buffer species, and fluid volume) that can affect colonic drug disposition. In this section, we discuss a selection of media that can be used in these dissolution studies to create relevant conditions, including biorelevant media, and media supplemented with rodent caecal contents as well as human faecal slurries.

1.3.1.1 Biorelevant media - Inclusion of relevant intestinal components

Since plain aqueous physiological buffers are not ideal for the prediction of the *in vivo* release of poorly soluble drugs (BCS class 2 and 4), biorelevant media have been developed, containing relevant bile components, and reflecting the physiological pH, osmolality, and surface tension. For the development of biorelevant media representative of the lower intestine, Reppas et al. analysed aspirated samples from the ileum, caecum and ascending colon, in both fed and fasted state [51,64]. The composition of these media simulating the distal ileum (simulating intestinal fluid, SIFileum), ascending colon in the fasted state (fasted state simulated colonic fluid, FaSSCoF) and in the fed state (fed state simulated colonic fluid, FeSSCoF) are listed in table 1.1. All these media differ in pH, buffer capacity, osmolality and bile salts. Vertzoni et al. used these media to determine the solubility of poorly soluble drugs (ketoconazole, danazol and felodipine) (FaSSCoF and FeSSCoF) in comparison to the solubility in plain buffers [68]. Georgaka et al. implemented the biorelevant media into dissolution tools. The dissolution was then evaluated in the distal ileum and the proximal colon (two-stage), under fasted and fed state conditions [69,70]. Briefly, in a first stage of the dissolution setup, SIFileum is added, and after a certain time (0 - 2 h) FaSSCoF or FeSSCoF is created (second stage; 2 – 6 h); Georgaka et al made use of SIFileum-V2 and FeSSCoF-V2. Furthermore, they described a two-stage single-compartment model making use of the mini-paddle apparatus; this two-stage *in vitro* evaluation simulates dissolution in the distal ileum and proximal colon, thus creating the possibility to evaluate low solubility drugs and pH dependent release formulations in two different media differing in bile salts composition and pH [69].

Table 1.1 Composition of simulating the distal ileum (SIFileum/SIFileum-V2), ascending colon in the fasted state (FaSSCoF) and in the fed state (FeSSCoF/FeSSCoF-V2).

	SIF_{ileum} [70]	SIF_{ileum}V2 [69]	FaSSCoF [69,70]	FeSSCoF [70]	FeSSCoF-V2 [69]
Sodium Cholate (mM)	0.8	-	0.15	0.6	0.6
Lechitin (mM)	0.2	-	0.3	0.5	0.5
Sodium oleate (mM)	-	-	0.1	0.2	0.2
Glucose (mg/mL)	-	-	-	14	4.8
Maleic acid (mM)	52.8	120	75.8	30.15	65
Tris (mM)	-	-	45.4	30.5	65
NaOH (mM)	105	240.6	120	16.5	16.5
Sodium chloride (mM)	30.1	-	-	34	-
pH	7.5	8	7.8	6.0	6.0

1.3.1.2 Rat caecal and faecal slurries

Since formulations and prodrugs intended for colonic delivery often make use of bacterial enzyme-mediated degradation, inclusion of colonic enzymes can be considered. Alternative approaches have been developed to better represent the colonic environment by using rat caecal slurries, human faecal slurries and multi-stage culture systems.

Rat caecal contents have been widely utilized in drug release and dissolution testing. Due to the anaerobic nature of the caecum, rat caecal contents are isolated and immediately diluted and transferred under anaerobic conditions to sealed glass vials. Its relevance has been reported by Hawksworth et al. [71] as similar amounts of the bacteria Bacteroides and Bifidobacteria were observed in human colonic contents as in rat caecum. Another advantage is that rat caecal contents are readily available and donor-dependent variability can be decreased by standardized housing conditions. The usefulness of this approach has been demonstrated in various studies: the presence of caecal contents resulted in increased drug release from a guar gum matrix (indomethacin [72]), calcium pectinate tablets (indomethacin [73], 5-fluorouracil [74]), chitosan tablets (Ibuprofen [75]), calcium pectinate microbeads (satranidazole [76]), and enteric coated guar gum microspheres (ornidazole [77]). Although the use of rat caecal contents has been valuable to explore enzyme-mediated colon drug delivery systems, the results obtained with rat caecal contents containing media may not always be extrapolated to humans due to

differences in the microbiome (e.g. lactobacilli in humans are present in a lower proportion compared to rodents).

Alternatively, faeces collected from humans can be used to prepare slurries. It should be noted that the microbiome and composition in the lower colon parts differ from the upper colon. Also, a large variation in composition of faecal samples from different individuals needs to be considered [78]. Different research groups have shown the applicability of faecal slurries for assessing the performance of colonic drug delivery systems that depend on the presence of the colonic microbiota. For instance, Milojevic et al. [79] tested the release of mesalazine from pellets coated with amylose/ethylcellulose while using human faecal slurries prepared from faeces of healthy volunteers. It was observed that mesalazine was completely released within 6h in the fermenter whereas negligible release was observed within 12h in simple buffer systems. The release occurred because of the degradation of amylose rather than the physical destruction of the coating. Faecal contents can be useful to evaluate microbiome based drug release from different donor groups (e.g. healthy and diseased), and is therefore also implemented in various multi-compartment models such as the three-stage compound continuous culture system [80,81], the Netherlands Organization for Applied Scientific Research (TNO) Gastro-Intestinal Model (TIM) and the Simulator of the Human Intestinal Microbial Ecosystem (SHIME®) (see section 1.3.2.3). Nevertheless, the complexity of the models limits throughput, and donor availability (right donor population depending on scientific question) as well as heterogeneity of the microbiome, remain challenges for the study design and data interpretation.

1.3.1.3 Drug degradation

In addition to prodrug activation or degradation of colon specific drug delivery systems, the colonic microbiome may also contribute to drug degradation, thereby decreasing the amount available for colonic absorption [52]. Faecal material can be used to asses *ex vivo* drug degradation [82,83]. Tannergren et al. [84] showed the *in vivo* relevance of using faecal homogenates from healthy human volunteers, dogs and rats in stability studies, using almokalant, budesonide and ximelagatran as model compounds. Metoprolol was used as negative control as it does not undergo bacterial degradation. The three model compounds underwent colonic degradation; *t*he *in vivo* relevance was demonstrated as a correlation

coefficient (R^2) of 0.90 was obtained between the percentage of drug remaining after 60 min of *in vitro* incubation and the f_a after colonic drug administration in humans. Similar as discussed before, faecal contents are not truly representative of the proximal colon. To circumvent this issue, Vertzoni et al. [85] performed the stability studies using contents collected from the ascending colon. The mean half-lives of metronidazole and olsalazine were determined using ascending colon contents and faecal contents collected from healthy adults [51,86]. These experiments revealed that degradation in ascending colon contents was significantly lower compared to degradation in faecal material. In view of the difficulties associated with the collection of colonic contents, the use of faecal material remains a valuable alternative.

1.3.2 Drug absorption and stability

For drug evaluation, intestinal setups need to represent the biochemical (metabolism, active transport mechanisms) and physical (surface area, cell-types, mucus production, unstirred water layer) characteristics of the GI tract to enable an accurate prediction of bioaccessibility (drug that is released from a matrix and becomes available for absorption), permeability, and stability. We will discuss different traditional as well as recently emerged novel intestinal *in vitro* tools and compare them concerning suitability to evaluate colonic drug behavior. Intestinal *in vitro* tools can be categorised into systems derived from (i) immortalized cells ("gold standard for permeation studies"; Caco-2), (ii) *ex vivo* (Ussing chamber) and (iii) primary systems (primary enterocytes, Cryopreserved human intestinal mucosa CHIM™)), (iv) stem cell derived models (intestinal organoids, scaffold-based models, and Gut-on-a-Chip), and (v) *in vitro* tools to study the role of the microbiome (TIM and SHIME®). Several of the stem-cell derived models discussed below are currently only available (or described in literature) as small intestinal models. However, the methodologies and platforms can likewise be applied to the colon and colonic models are often either in development, already available (but data concerning DMEs, transporters and functional characterisation are often still limited or not available in the public domain yet) or can be foreseen. A selection of currently available small and large intestinal models will be discussed. For more models, and a more comprehensive description we refer to our recently published review, [87].

1.3.2.1 Available as colonic models

Traditional immortalized cell-lines: Caco-2

One of the most routinely used *in vitro* set-ups for the prediction of human drug absorption is the Caco-2 cell culture model. The cell line, cultured as a monolayer, originates from colorectal carcinoma cells that spontaneously differentiate into columnar enterocytes, mainly representing the small intestinal epithelium, after having reached confluency on a porous membrane (Fig. 1.1) [88]. After three weeks (21 – 28 days), the cells resemble the human epithelium, which in terms of morphology (polarity, tight junctions, brush borders with microvilli) and functionality (passive and active transport mechanisms, limited metabolic capacity) is in many ways more representative of the small intestine than the colon. Also the lack of mucous producing goblet cells makes the monolayer more similar to the small intestine compared to the colon. The system has shown strong correlations between the human fraction absorbed (Fa) and the apparent permeability for a series of passive diffusion drugs with heterogeneous structures [89,90], allows classification into completely absorbed and poorly absorbed drugs [91], and can do so in a high throughput and reproducible manner. Tannergren et al. were able to establish a sigmoidal relationship ($R^2 = 0.74$) between the apparent permeability coefficients (Papp) of 18 drugs and their corresponding colonic absorption in humans, expressed as F_{rel} (see 1.2.1.) [52], likely due to its colonic origin. This validates the value of using Caco-2 in the early assessment of colonic absorption potential for controlled release drugs. Nevertheless, there are several shortcomings: Caco-2 cell monolayers have a physiologically high tightness (tight junction pore radius smaller than native tissue) [92], the enterocytes lack the main intestinal metabolising enzymes (i.e. CYP3A4), and drug transporter expression levels are not always reflective of the *in vivo* levels, which partially explains why a poor correlation exists for drugs that are transported via carrier-mediated mechanisms [89].

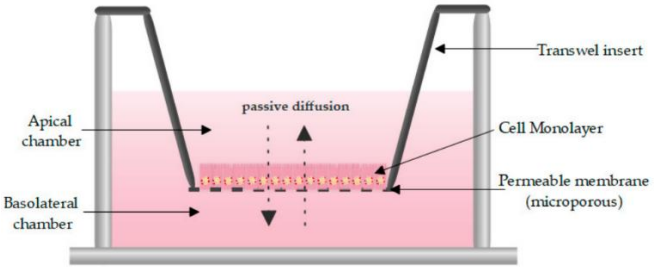

Fig. 1.1: Schematic overview of Caco-2 monolayer on a transwell insert. Adopted from [93].

Although DMEs such as UGTs are present, several metabolizing enzymes are missing or not expressed at physiologically relevant levels. For example, carboxylesterases-1 (CES) is overexpressed while CES-2 is underexpressed in Caco-2 cells compared to the small intestine. In particular the lack of CYP3A4, which accounts for 80% of total CYP in human small intestine, is disadvantageous when the drug of interest is susceptible to CYP-mediated metabolism during absorption. [94]. Englund et al. explored how the expression and activity of transport proteins of the SLC (PEPT1, MCT1, OATPB, OCT1, OCTN2) and ABC family (P-gp, BCRP, MRP2 and MRP3) is expressed in Caco-2 cells in relation to different intestinal regions. Overall, the *in vivo – in vitro* expression level of transporters was distinctly different, but often highly dependent on a single transporter. For example, expression levels of BCRP were noticeably lower, and MRP2 and OATPB were higher in Caco-2 compared to duodenum, ileum and colon. For the colon, a substantial difference was also observed for PEPT1. The same group also described how the culturing time can affect the transcript levels; the mRNA level of PEPT1 and OATPB more than doubled between day 4 and day 21, and expression of P-gp was even four-fold higher [95]. Noteworthy is that there is a large inter- and intra-laboratory, clone and passage dependent variability in metabolizing and transporter proteins [94]. For example, the expression level and functionality of BCRP varies greatly between labs, which might be due to a different origin of the Caco-2 cells [96], and non-standardized culture conditions [97,98]. Lastly, the thickness of the unstirred water layer in the caco-2 system (2000 µm) can deviate from the *in vivo* state (< 100 µm) [99], and there is no mucous lining although this can be circumvented by pipetting porcine mucin on top of the Caco-2 monolayer or by using a coculture system such as HT29-MTX [100].

Ex vivo: Ussing chambers

A more complex translational model is the Ussing chamber technique that comprises tissue, a biopsy (only mucus and mucosa is present), or an epithelial cell monolayer placed between two half chambers, which can be filled with a physiologically relevant solution (Fig. 1.2). The intestinal tissue provides a better representation of the *in vivo* morphology and physiology (multiple cell types, mucus layer, acid microclimate, surface area), and approximates the *in vivo* expression levels of enzymes and transporters more closely than several immortalized cell lines [101–106], but is donor dependent. Thus, it is well suited to study both passively and actively transported drugs [107]. The Ussing chamber system has a strong record in predicting the human F_a and does so in a robust and reliable manner [103,108,109]. Moreover, the model lends itself to use various preclinical species, including rats, rabbits, dogs, or monkeys, which can support the interpretation of preclinical *in vivo* studies [110], but species difference in permeability and metabolic capability can be a restricting factor for human extrapolation [111],[112].

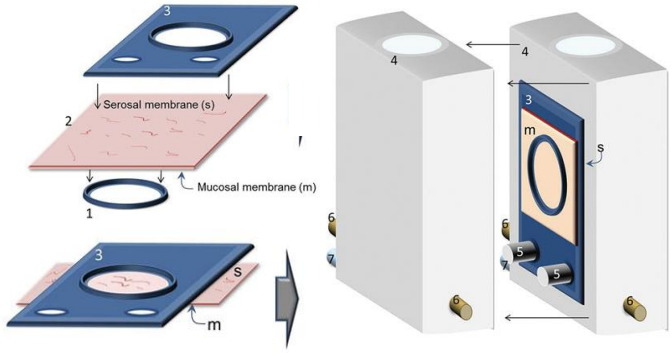

Fig. 1.2: Schematic view of tissue fixation in the Ussing chamber. After removal of muscle layer, fat, and sub-mucosa, the tissue clamp is pushed carefully under the intestinal segment . The mucosal side (m) faces the bottom and the serosal membrane (s) faces the top. Then, the tissue holder is pressed down onto the tissue, fixing the tissue in-between the tissue holder and the tissue clamp. After removal of overlapping tissue, the tissue holder is mounted into the Ussing chamber (4) by fixing it onto the bars (5). The mucosal side can face the left or the right chamber half (here the mucosal side faces the left). 6 = connectors for agar-salt bridges; 7 = connectors for carbogen. Adopted from [113].

When considering colonic uptake of drugs, the Ussing chamber technique allows to evaluate candidate drugs that are intended for extended release, which can prevent attrition in the later stages of drug development. The group of Sjoberg and Tannergren showed a clear sigmoidal relationship between the apparent permeability of human colonic tissue mounted in the Ussing chambers system and the human colonic F_a, respectively, with both curves being in agreement with one another [52,108]. The group of Sjöberg was also able to report regional differences in drug absorption of passively transported drugs: polar drugs (atenolol, creatinine, mannitol, ximelagatran, rosuvastatin) had the lowest permeability coefficients in the colon (jejunum > ileum ≥ colon), while the reverse was observed for non-polar and more permeable drugs (antipyrine, oxprenolol, metoprolol and propranolol) for which the highest values were recorded in the colon (jejunum < ileum ≤ colon) [108]. The exact underlying mechanism is unclear, which is why the authors refer to the general physiological differences. Important to remark is that Pgp-substrates can show higher apparent permeability values in the colon compared to other intestinal regions, which is likely due to its lower expression in colonic tissue (see section 1.1.1) [114]. Lastly, one should keep in mind that when human tissue is used for permeability assessments, the different medical history, type of surgery of the donor and age of the patients can affect the integrity and viability of the resected tissue, and consequently absorption [108].

Lastly, two separate studies [103,112] have shown how including possible drug accumulation in tissue (respectively coined 'Papp, Total' and 'Transport Index'), which is not covered by the conventional apparent permeability, can improve the prediction of the human Fa. Rozehnal showed that correlation between Papp, total and human Fa was only marginally better than Papp, except for metoprolol, ibuprofen, and pravastatin, drugs which significantly accumulated in the mucosa. Miyake showed that the rank order of a 4kDa labelled dextran, atenolol and metoprolol coincided with Fa in humans, but only when tissue accumulation was considered. Not factoring in the accumulated drug fraction, which can contribute to absorption at a later stage, would lead to an underestimation of drug permeability. Furthermore, assessing colonic accumulation can be of value since colon-targeted delivery systems aim at local accumulation for an efficacious treatment, while also minimising systemic absorption. Although the low-through-put nature of this technique restricts its application in early stages of drug discovery given the scarcity of human intestinal tissue, it can ameliorate the prediction of drug absorption

in a late discovery or early development stage and contribute to the optimization of the lead compounds.

Organoids

The establishment of intestinal organoids derived from LGFR5-positive stem cells for long-term culturing and expanding in the presence of growth factors (WNT, R-Spondin and Noggin, all providing the essential stem cell signalling) has been described originally for mouse small intestine [115], later on for mouse colon, human small intestine and colon [116] (Fig. 1.3). The culture conditions can be modified for enrichment with major epithelial intestinal cells with physiological relevance to biological readouts [117,118]. Those intestinal organoids are grown as 3D cultures embedded in extracellular matrix (Matrigel).

Mizutani et al. [119], looked at expression of transporters and identified the apical presence of P-gp in 3D small intestinal organoids created from adult mice, and confirmed its functionality by incubating the organoids with a P-gp substrate (e.g. rhodamine123), and inhibitor (e.g. verapamil). These 3D organoids were reported to be lined by a differentiated epithelial monolayer with the apical membranes facing the luminal space inside. Similarly, Zhang et al. [120] reported functionality of BCRP on the apical membrane of 3D organoids from mouse small intestine, and reported a comparable expression to the small intestinal epithelium of mice. Onozato et al. [121] used human induced pluripotent (iPS) stem cells that were differentiated to functional organoids presenting microvilli structures and tight junctions. Several intestinal cell types like enterocytes, intestinal stem cells, goblet cells, enteroendocrine cells, Paneth cells, and supporting cell types like smooth muscle cells and fibroblasts were also identified. Under these differentiated organoid conditions, the authors demonstrated activity of efflux transporters P-gp and BCRP and the activity of DMEs like CYP3A4. Besides efflux transporters, the expression of the uptake transporter PEPT1 was determined by immunofluorescence staining. Other CYP enzymes were not tested for their activity but the mRNA levels of CYP3A4, 2C9, 2C19 and 2D6 were determined and described to be similar to those in the small intestine of men. However, it should be noted that all mRNA expression data of functional cell markers, several metabolising enzymes, and transporters were lower than in intestinal tissue. However, the expression and functionality may differ depending on differentiation protocols and might reflect species (e.g. mice and human) and regional differences (e.g. small intestine and colon)

as organoids from different species and regions can be generated and compared. This makes the organoid model an attractive model for drug disposition studies not only under “generic” conditions but also to study drug disposition under specific circumstances as organoids can be generated from any donor e.g. healthy, diseased, geriatric, paediatric, neonatal etc. thereby moving closer to individualised medicine.

To perform drug disposition studies, drug exposure to the apical and basolateral side is essential. Since traditional 3D organoid culturing techniques only enable direct drug exposure to the basolateral side of the organoid (apical side is facing the inside of the organoid) 2D transwell culturing are essential. Transwell culturing conditions have been first described for mouse colonic organoids [122], and Subsequently by VanDussen et al. [123] for human rectal and ileal organoids. One week after seeding of organoid-derived stem cells on Matrigel-coated transwell inserts, a single layer of intestinal epithelial cells with MUC2-expressing goblet cells and tight junction proteins (ZO-1 and claudin 3) was obtained. The observed mucus layer in this study with a thickness of 36 µm for the rectal monolayer and 26 µm for the ileal monolayer This model may become an interesting tool to evaluate colonic permeability and to explore underlying transport mechanisms similar to the Caco-2 system. One should keep in mind however that although transwell culturing of organoids has been described, so far, no data related to the expression nor activity of transporters in transwell cultured colonic organoids have been reported.

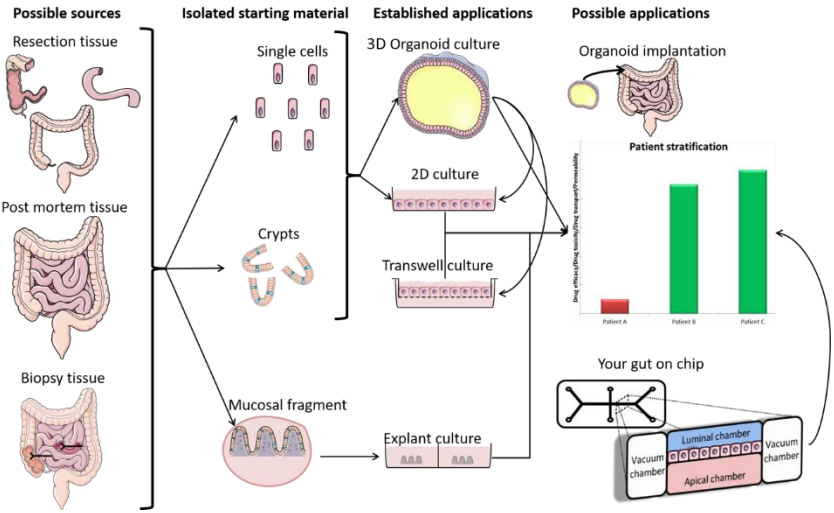

Fig. 1.3: A representation of the generation of 2D and 3D organoids, and their application. Resection-, post mortem-, and biopsy tissue can be used to acquire crypts or single stem cells, which can then be cultured as organoids under the right conditions. 3D Organoids can be exposed to microbes and drugs by micro-injection, while the transwell culture (2D) allows both luminal and basolateral exposure. Possible applications are discussed in the text and depicted on the right panel. Adopted from [124].

Organoids are a promising model since it also provides the possibility to generate, study and compare region-, disease-, and age-specific models which might enable the assessment of drug disposition in specific target populations e.g. IBD patients, paediatric, geriatric patients and others. Also, preclinical models can be generated which allow the comparison of preclinical *in vivo* to *in vitro* data to further validate the model. However, the characterisation of intestinal organoids as a drug disposition model still needs further evaluation.

Colon chip

In the past years, a number of organ-on-a-chip intestinal models have been described (Fig. 1.4). Especially the first emerging models used Caco-2 as the epithelial cell source [125–127]. Organ-on-a-chip separates itself from other systems by incorporating microvasculature, mechanical forces of fluid flow (shear stress) and intestinal peristalsis, though it can be

questioned whether this will result in improved absorption and metabolism properties compared to traditional models. Depending on the provider those chips typically consist of two layers of microfluidic channels separated by either a thin porous membrane (polydimethylsiloxane (PDMS)) coated with extracellular matrix (ECM) on top of which Caco-2 cell are plated [125,126,128] or by ECM only on which Caco-2 cells are seeded in one lateral line forming a polarized epithelial tube [127]. The culture medium is then perfused through both channels and thus, the apical and basal side is accessible for drug exposure.

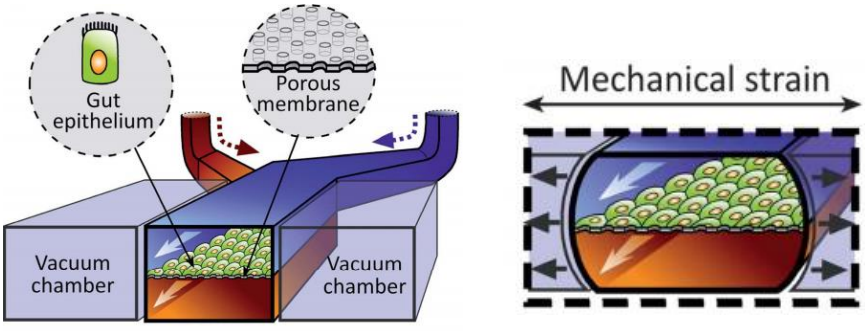

Fig. 1.4: Organ-on-a-chip. Left panel: The central microchannel comprises a flexible porous ECM-coated membrane lined by gut epithelial cells, positioned between two vacuum chambers. Right panel: Mechanical strain is applied on the gut intestinal monolayers by suction from the vacuum chambers. Adopted from [125].

The use of shear stress (flow) demonstrated some advantages over traditionally used transwell culturing especially regarding differentiation and polarisation, which is achieved in Caco-2 chips as early as 3 – 4 days after cell seeding in comparison to 21 days of culturing needed for traditional transwell monolayers [127–129]. Applying shear stress not only decreased the differentiation time tremendously but also increased the cell size and polarisation status (epithelial cells 6-fold taller in size vs. transwell culturing with clear basal nuclei) compared to static transwell Caco-2 cells presenting rather flattened, almost squamous epithelial cells [125,126]. Especially the addition of mechanical stress (cyclic mechanical strain mimicking peristalsis) enabled the spontaneous formation of undulations and folds exhibiting the morphology of intestinal villi, and intestinal differentiation. However, similar to the traditional static monolayer, the cells are somewhat more representative of the small intestine concerning

the observed cell types (enterocytes, goblet cells, enteroendocrine cells, and Paneth cells) [125,126]. But, in contrast to static cultures, the goblet cells present in the Caco-2 chip have been shown to produce MUC-2. Despite those interesting observations, it was not clearly shown that main drawbacks of the Caco-2 system like the lack of CYP3A4 expression (increased activity shown by Kim et al [128] but very limited data set), deviating expression of uptake and efflux transporters from human intestinal tissue, large clone- and passage-dependent variance, and increased monolayer integrity compared to the *in vivo* situation, could be overcome by incorporating Caco-2 cells in a more physiological environment [125–128].

Recently, a colon-chip using colonic organoids from the sigmoid and ascending region as the epithelial cell source has also been described [130], with specific focus on mucus production. The authors demonstrated that maturation and differentiation to goblet cells in the colon-chip occurred spontaneously under stem cell expansion conditions. This is not observed in "traditionally-cultured" organoids in Matrigel or on transwell inserts, which require differentiation medium, depleting the stem cells [116,123,131]. Similarly, to the Caco-2 chip, when using colonic organoids, a polarized columnar epithelium with undulating structures was formed (only shear stress no mechanical stress), and the appearance of ZO-1 containing tight junctions and F-actin rich brush boarders was confirmed. Most striking, high levels of MUC2 producing goblet cells, similar in morphology and number (approximately 15% of all cell types) to those seen in histological human colon sections (approximately 10 – 30% dependent on donor) were observed in the colon organoid chip. Moreover, those functional and differentiated goblet cells produced a mucus layer that was comparable to *in vivo* colonic bi-layered mucus concerning thickness and structural organization into a penetrable (for bacteria) outer and impenetrable (for bacteria) inner layer. The colonic organoid chip model appears as a very promising tool for colonic drug permeation studies due to its physiological representation of the bi-layered mucus

1.3.2.2 Available small intestinal models

EpiIntestinal™ (MatTek)

EpiIntestinal™ (MatTek, Slovak Republic) is a novel organotypic 3D microtissue, which is currently available as a small intestinal model, derived from the ileum of a 19-year old female donor. Having this microtissue platform developed for other intestinal regions holds a great promise for colonic drug delivery research in the future. EpiIntestinal™ can be used in two different setups, either as an epithelial layer only (EpiIntestinal™) or in co-culture with human fibroblasts, which are commercially purchased and thus derived from a different donor (EpiIntestinal-FT™). The epithelial cell layer is cultured at the air-liquid interface (ALI) on a transwell insert thus creating a bicompartmental setup with an apical and a basolateral side (Fig. 1.5). Several reports have been published recently describing EpiIntestinal™ as a model to asses intestinal drug disposition [94,132] and safety [133]. Ayehunie et al. [132] performed a comprehensive characterisation of EpiIntestinal™, zooming in on structural features, drug transporters and metabolizing enzyme expression, and functional evaluation of the bidirectional transport of 11 test drugs. TEER values measured with EpiIntestinal™ ($152.5 \pm 39\ \Omega*cm^2$) are in close proximation to human intestinal *ex vivo* tissue ($50 - 100\ \Omega*cm^2$) indicating that structural features may more closely mimic small intestinal tissue than Caco-2 cell monolayers with TEER values ranging from $250 – 2400\ \Omega*cm^2$ [134]. This is further underpinned by microscopic imaging demonstrating a crypt-villi architecture, positive cytokeratin-19 (epithelial differentiation marker), villin (enterocytes marker), and vimentin (fibroblast marker) staining as well as transmission electron micrographs confirming brush boarder membranes and tight junctions in EpiIntesintal™ tissue. Given the crypt-villus architecture and the presence of microvilli, the surface area might be enlarged compared to traditional 2D cell culture models. Functional characterisation was performed, using 11 reference drugs (BCS I – III, with the majority of drugs being BCS III), by determining P*app* and comparing those values to Caco-2-derived data as well as to the known human oral bioavailability of those drugs. For EpiIntestinal™, P*app* values correlated more closely with known human absorption ($R^2 = 0.91$) than for those obtained with the Caco-2 model ($R^2 = 0.71$), most likely due to the closer *in vivo*-like structure, barrier function, and transporter expression as suggested by the authors. EpiIntestinal™ appears also suitable to study transporter-dependent permeation. qPCR data confirmed the expression of ABCG2, ABCC1, ABCC2, and ABCB1 encoding BCRP, MRP1,

MRP2, and P-gp, respectively. Unfortunately, a direct comparison to the explant tissue as given for expression data of metabolising enzymes is lacking. However, functional transporter activity was confirmed using P-gp, BCRP, and MRP2 substrates and transporter specific inhibitors. Efflux ratios > 2 were reached for all transporter substrates and efflux decreased substantially in the presence of a transporter-specific inhibitor. The expression level and functional activity of several important uptake transporters (including OCT1, OATPs, and PEPT1) was not evaluated, and requires further investigation. Finally, also expression and functional activity of intestinal CYP450 DMEs (CYP3A4, CYP3A5, CYP2C9, CYP2C19) was confirmed by Ayehunie et al. [132] and was further investigated by Cui et al. [94]. The study described by Cui and co-workers, mainly focused on characterising EpiIntestinal™ as an *in vitro* tool to predict the human GI first pass availability of drugs (F_a x F_g) because both, absorption and metabolism can be determined using EpiIntesintal™. They convincingly show that GI first pass availability determined with EpiIntestinal™ is in good correlation with F_a x F_g in humans for 12 reference drugs (range of low, medium and high bioavailability, mainly metabolized by CYP3A4) used in the study. Moreover, they provide metabolic activity data for CYP3A4, CYP2B6, CYP2C8, CYP2C9, CYP2C19, CYP2D6, CYP2J2, UGTs, SULTs, and Carboxylesterase 1 and 2 (CES 1 and 2). Given the results of the above-described studies, it seems evident since e.g. metabolite-mediated toxicities, or transporter-mediated drug-drug interactions (DDI) could potentially be identified with EpiIntestinal™. Peters and co-workers [133] have also shown that the EpiIntestinal™ could be used to evaluate intestinal safety of drugs, by employing a validation set of 39 drugs with known diarrhea responses in humans.

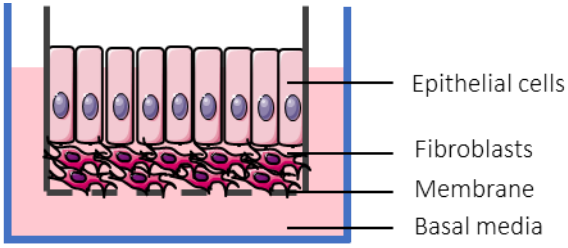

Fig. 1.5: EpiIntestinal full thickness tissue cultured at the air-liquid interface. Adopted from [133].

Small intestinal chip

Here, we focus on reviewing the duodenal chip commercialised by Emulate for which basic characterisation as an ADME tool has been performed [135]. The duodenal chip consists of epithelial cells derived from adult intestinal stem cells (crypts) that were acquired by the enzymatic dissociation of organoids and then seeded into the microtube, and primary intestinal microvasculature endothelial cells (HIMECs, different donor) seeded into the "vascular" channel of the duodenal chip (Fig. 1.6). Medium flow was applied to both channels and once confluency was reached, cyclic mechanical strain was applied in order to mimic intestinal peristalsis. This setup resulted in accelerated polarisation (in 72 hours), the formation of villus-like structures, and apical microvilli. Shear stress in comparison to static cell culture conditions boosted cell maturation and differentiation into enterocytes, goblet cells, enteroendocrine cells and Paneth cells with cell ratios closely reflecting *in vivo* ratios. The authors further characterised the chip by applying differential gene expression analysis to intestine-chips generated from intestinal organoids and comparing those data to the intestinal tissue and organoid source. Both, duodenal organoids and intestine chip used for differential gene expression analysis were first expanded for 6 days followed by 2 days of differentiation. Interestingly, although duodenal organoids and duodenal chip derived from the same tissue source, 472 genes were identified with significantly different expression levels. Moreover, 305 genes, associated with digestion, transport of nutrients and ions, extracellular matrix organisation, wound healing, metabolism, and tissue development, were expressed similarly in the duodenal chip and the tissue of origin but were differently expressed in the organoid cultures. While those data strongly suggest that the duodenal chip transcriptome more closely resembles the human adult duodenum, it should be taken into consideration that the differentiation and maturation in the chip is enhanced and therefore when comparing to 2-day differentiated organoids, the organoid culture might not yet be fully matured. Further evaluation of the duodenal chip confirmed apical expression of MDR1, BCRP1, and PEPT1 gene expression comparable to the tissue of origin and functional activity of MDR1, demonstrated by increasing Rhodamine 123 cell accumulation in the presence of the MDR1 inhibitor vinblastine. Finally, CYP3A4 metabolism using testosterone as a substrate, and CYP3A4 induction by rifampicin and 1,25 – dihydroxyvitamin D3 could also be demonstrated.

The duodenal chip (organoids from adult donor) described by Kasendra et al. is a follow-up of their previously described duodenal chip using paediatric donors [135]. The authors convincingly show that the addition of a microvascular channel, shear stress, and mechanical strain mimicking peristalsis create an intestinal microenvironment which appears to closely resemble the *in vivo* situation, especially demonstrated with gene expression data, imaging techniques, and some functional data.

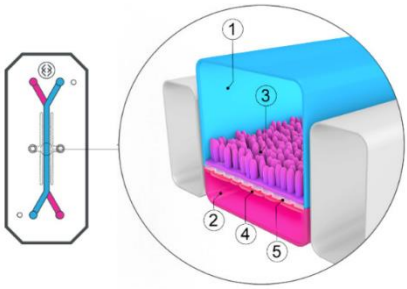

Fig. 1.6: Organ-on-a-chip. Duodenum Intestine-Chip from Emulate, including its top view (left) and vertical section (right) showing: the epithelial (1; blue) and vascular (2; pink) cell culture microchannels populated by intestinal epithelial cells (3) and endothelial cells (4), respectively, and separated by a flexible, porous, ECM-coated polydimethylsiloxane (PDMS) membrane (5). Adopted from [135].

1.3.2.3 Colonic microbiome based in vitro tools

The use of single enzymes or a combination of enzymes, as well as the inclusion of faecal or caecal material in incubation media to explore colonic drug and formulation behaviour have been mentioned in section 1.3.1.2. In several multicompartmental *in vitro* tools, which mimic the GI tract or GI tract fluids, the microbiome is included which allows studying the interaction between the drug and the human gut microbiome in isolation. Gut microbiome models include the Netherlands Organization for Applied Scientific Research (TNO) dynamic model of the human large intestine (TIM-2) [136], and Simulator of the Human Intestinal Microbial Ecosystem (SHIME®) [137]. However, these models do not permit communication between bacteria and intestinal epithelium. Based on microbiome studies, new comprehensive approaches in which the interplay between the microbiome or a microbiome component and the epithelial lining is included are emerging. Therefore, the microfluidics based model HuMix

(human–microbial crosstalk) and the microbiome intestine-chip [138] will also be discussed in this section.

TIM

The TNO Intestinal Model (TIM) could be used to simulate intraluminal drug behaviour in a dynamic setting, as various parameters (mixing, meal transit, secretions, variable pH, contents of GI fluids, the variable amounts of digestive compounds, and water) can be remotely adjusted and controlled to represent different species, age, pathologies and meals. So far, one model named TIM-2, has been developed that simulates the colonic conditions and uses faecal incubations. The set-up of the system is illustrated in figure 1.7. Briefly, the set-up consists of four interconnected glass compartments equipped with a flexible membrane. It contains a level sensor to control the volume and makes use of nitrogen to create anaerobic conditions. Samples can be collected through the sampling-port or from the dialysate. Formed gas can escape through the bubbling-vial. The 'ileal efflux' container is a syringe through which the microbiome is fed into the system; it contains a simulated ileal efflux medium, which mimics the luminal composition of the ileal-caecal region [139–141].

The TIM-2 has several unique features: In between the glass jacket and the membrane there is water of body temperature, which allows peristaltic movements. Furthermore, the system can be kept at a pH of 5.8, mimicking the pH in the proximal colon (pH 5.8 – 6.8 fasted status [53]) or can be programmed as a gradient over time: a pH of 5.8, 6.4 and 7.0 can be used representative for the proximal colon, transverse colon and distal colon, respectively (see section 1.2.2.). 1M NaOH is secreted to neutralize acids produced by the microbiome, which can be maintained active for 3 weeks. Also, since faecal incubations are used, the model can assess interindividual profiles (various faecal donors, or pooled), demographics (age, paediatric and geriatric population) and healthy or diseased state (IBD) [136]. Advantages also include the presence of a dialysis system and the possibility to test multiple parameters in parallel (e.g. pH and microbiome activity), to monitor one single parameter. The main disadvantages of the TIM system is its complexity and low throughput.

TIM-2 is mostly used to explore food effects, or to investigate kinetics of production of microbial metabolites, which is made possible by frequent sampling, and to make an almost

complete mass balance. It has the potential to evaluate colonic drug solubility, dissolution, and bacterial degradation using either large microbiome pools or individualized microbiome (diet, healthy, diseased state, different age groups, etc.), but few studies have been performed on this topic.

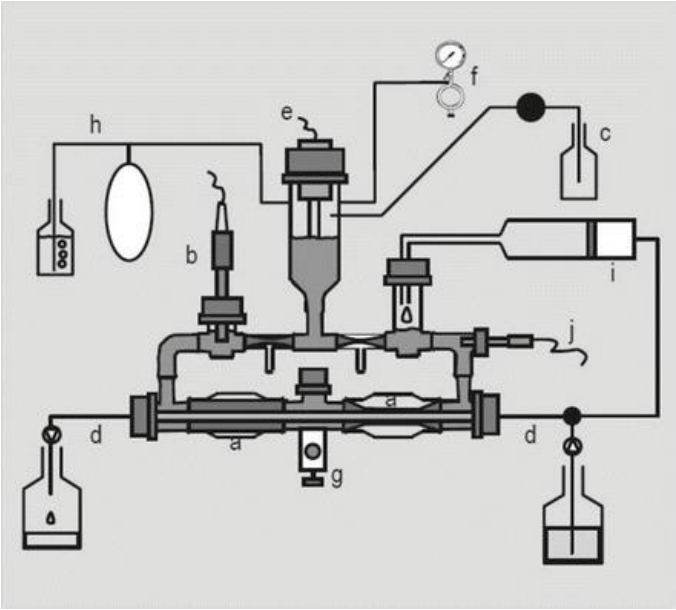

Fig. 1.7: Schematic overview of the TNO *in vitro* model of the colon (TIM-2). (a) peristaltic compartments containing faecal matter; (b) pH electrode; (c) alkali pump; (d) dialysis liquid circuit with hollow fibre membrane; (e) level sensor; (f) N_2 gas inlet; (g) sampling port; (h) gas outlet; (i) 'ileal efflux' container; (j) temperature sensor. Adopted from [136].

SHIME

SHIME® (Simulator of the Human Intestinal Microbial Ecosystem) [142] consists of five compartments (stomach, small intestine, ascending colon, transverse colon and descending colon) (Fig. 1.8) that are interconnected with peristaltic pumps. This multi-compartment dynamic simulator was created once it was established that faecal microbiome used in single-stage models differ from the *in vivo* colon microbiome in terms of pH, redox potential, available nutrients and microbial contents. As these environmental parameters change dynamically, it is impossible to simulate a representative bacterial culture in one compartment.

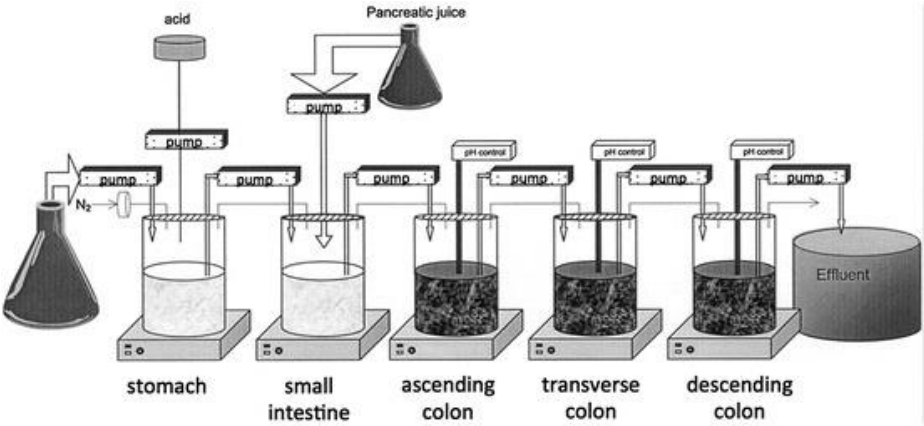

Fig. 1.8: Schematic overview of SHIME®. Adopted from [137].

The setup is extensively discussed by Van de Wiele et al. [137]. Briefly all double-jacketed glass vessels operate at 37°C and are kept anaerobic using N_2 gas or a 90/10 % N_2/CO_2 gas mixture during the total length of an experiment (up to several days). Subsequently, defined nutritional medium and bile liquid are added by a fill-and-draw principle to the first (stomach) and second (small intestine) compartment, respectively. This medium is composed of a mix of carbohydrate, protein sources, mucins, minerals and vitamins [142]. Upon digestion in the first two compartments, the slurry is pumped into the third (ascending colon) compartment where colon digestion is initiated. This slurry is constantly mixed with magnetic stir bars. The three colon compartments (ascending colon, transverse colon and descending colon) are monitored

for constant volume and pH control. Retention times for the upper GI-tract and lower GI-tract compartments are modulated by flow rates and compartment volumes, respectively. The SHIME® set-up is completely computer controlled, therefore different pH profiles can be established. The pH of the gastric and small intestinal compartment is typically fixed at a pH of 2.0 and a slightly acidic to neutral pH, respectively. The following three colon compartments are fixed at a pH of 5.6-5.9, 6.1-6.4 and 6.6-6.9.

Relevance and validation of the model have also been tested. Metabolism of the prodrug sulfasalazine by intestinal bacteria to the active metabolites sulfapyridine and mesalazine (5-aminosalicylic acid) was tested and was consistent with *in vivo* data gathered by Peppercorn and Goldman [143]: no conversion into the active drug 5-aminosalicylic acid was detected in the gastric compartment, limited conversion in the small intestine compartment and full conversion in the colon compartments.

The SHIME® model consists of different features [137]. An important feature of the SHIME® model is its flexibility by adding or removing compartments depending on the kind of study to be performed. Another important feature is the possibility to change the target group: adult vs. infant, healthy vs. diseased, as well as preclinical species (pig, dog). In that case the following will be adapted: microbial inoculum (individual or pooled), residence time, contents of gastric juices, pH, feed, feeding regimes and temperature.

The inoculum used in the SHIME® model consists of faecal microbiome as the different parts of the human colon region are difficult to access. The mucosal microbiome is known to differ in composition from the luminal microbiome and to be responsible for the colonization of the mucus overlying the gut epithelium. Due to its proximity to the epithelial cells, the mucosal microbiome is thought to play an important role in the modulation of gut health [144]. To this end, Van den Abbeele et al. [145] developed mucosal SHIME (M-SHIME®) to obtain a better understanding of the importance of a possible host-microbe interactome in a gut simulator model. This first feature was achieved optimizing SHIME® by enabling colonization of the mucosal microbiome using microcosms submerged in mucin agar and combined in a polyethylene ring, added to each colon unit and followed by inoculation with fresh stools (Fig. 1.9) [145].

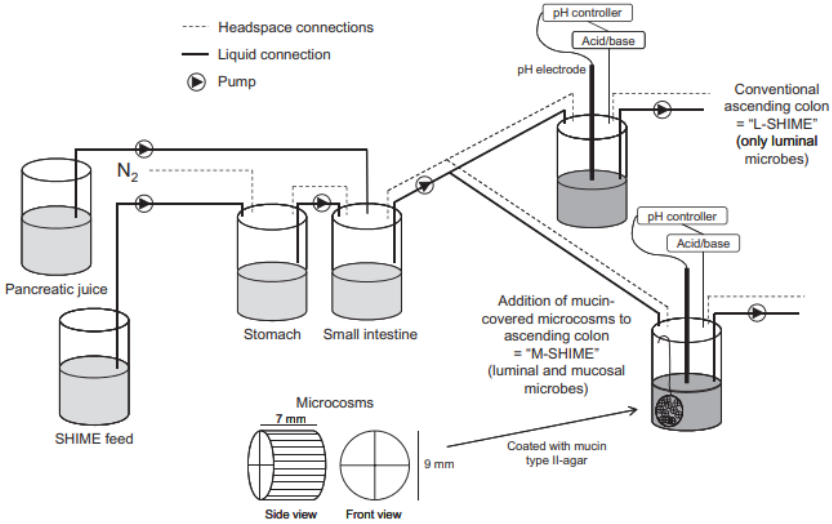

Fig. 1.9: A schematic overview of the implementation of a new second unit modified by incorporating a mucosal compartment (= mucosal SHIME or M-SHIME), which contained 100 mucin-covered microcosms per 500 ml suspension. The general experimental design composed of several double-jacketed vessels, simulating the stomach, small intestine and three main colon regions. In this experiment, only the first colon compartment (ascending colon) was used and inoculated with a human faecal microbiome. The first ascending colon unit consisted of the conventional set-up that only harbours luminal microbes (= luminal SHIME or L-SHIME), whereas the second unit is the M-SHIME. Adopted from [145].

Van den Abbeele et al. [145] also showed a higher abundance of butyrate producing Clostridium clusters IV and XIVa in the microspheres of M-SHIME®, responsible for the delivery of butyrate as primary energy source to the colonocytes and strengthening of the tight junctions, crucial to maintain gut barrier integrity *in vivo*. In addition to the use of individual inocula, Van den Abbeele et al. [145] determined that M-SHIME® was able to maintain the mucosal composition of an individual and revealed that a high variability in the microbial dataset due to *in vivo/in vitro* transition and difference between the luminal and mucosal contents was obtained. Van den Abbeele et al. also proved that the addition of a mucosal environment allowed the colonization of specific microbes (e.g. *Lactobacillus mucosae* and *Lactobacillus rhamnosus GG*) which is in correspondence with the *in vivo* situation.

The M-SHIME® model can be used to investigate the effect of therapeutic treatments or diseased state on the functionality or composition of the microbiome. For example, Vermeiren et al. [146] reported a depletion in butyrate producing microbial communities in both luminal and mucosal samples from UC patients compared to healthy volunteers. However, no data are available in the public domain concerning the effect of the *in vitro* microbiome on the stability of colon targeted drug delivery systems, although the set-up seems to have the interesting potential to do so.

Intestine-chip with microbiome

Besides small and large intestinal chips, several chips have been established that enable simultaneous aerobic and anaerobic culturing conditions. These chips can incorporate a microbiome component with either Caco-2 cells or small intestinal organoids. However, they are currently not characterised with respect to drug disposition [125,147,148].

Extended co-culturing of aerobic and anaerobic commensal bacteria with intestinal epithelial cells using chip technology is described by Jalili-Firoozinezhad and co-workers [147]. A transluminal hypoxia gradient is set in place in a microfluidic intestine-on-a-chip that achieves low oxygen-concentration (< 0.5%) by using an oxygen-sensing, dual channel chip. The chip comprises epithelial cells that are grown on a PDMS polymer that face an anaerobic chamber on the top and are supported by an oxygen and medium containing flow-channel on the bottom, which is lined by endothelial cells (Fig. 1.10). The intestinal chip has been developed with increments in physiological complexity. Initially Caco-2 cells were used as an epithelial source, and co-cultured with one anaerobic strain, *Bacteroides fragilis* [125]. One of the last models are intestinal organoids isolated from the non-diseased regions of surgical ileal biopsies from a 15-year-old UC patient were co-cultured with commensal bacterial from faecal samples from preterm infants (born before 32 weeks of gestation). The co-culture could be sustained for at least 5 days. The primary epithelial cells formed a polarised epithelium with villin-containing brush boarders and MUC2 producing cells, and the presence of the microbiome did not negatively impact the viability of the epithelial cells in this *in vitro* setting, It is striking that the presence of commensal bacteria consistently leads to increased barrier integrity, as demonstrated by either an increase in TEER and/or a decrease in the Papp value of high molecular integrity markers [125,147,148].

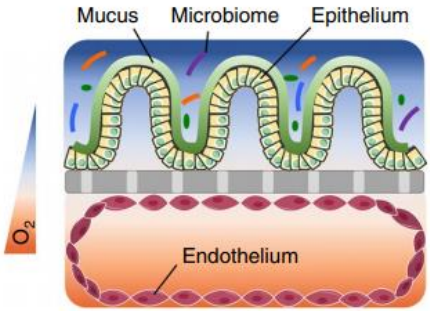

Fig. 1.10: A representation of the microfluidic intestine chip with microbiome, under the presence of an oxygen gradient (colour scale). The human intestinal epithelium is overlaid with its own mucus layer and complex gut biota and positioned over an extracellular matrix-coated porous membrane (grey). Below the porous membrane lies the vascular endothelium. Adopted from [147].

The physiological chip described by Jalili-Firoozinezhad and co-workers with built-in oxygen gradient holds great potential to assess drug disposition under colon-emulating (currently the chip is from the derived from the ileum) conditions but seem to require a complex experimental setup (controlling different chip conditions) and can only be used at low throughput rate.

1.4 Colonic drug disposition of NSAIDs

In this thesis, we will elucidate the colonic drug disposition of celecoxib and sulindac, two NSAIDs with preventative effects on the development of colorectal cancer. Celecoxib is lipophilic (LogP = 3.5), and weakly acidic (pKa = 11.1) [149], and has been reported as a high permeability drug [150]. Celecoxib is extensively metabolized in the human liver by CYP2C9 to form hydroxy celecoxib, which can then be oxidized to carboxy celecoxib by cytosolic alcohol dehydrogenases ADH1 and ADH2. Sulindac is a lipophilic (LogP = 2.93), acidic (pKa = 4.09), and moderately to highly permeable [151] prodrug of sulindac sulfide, and has a solubility that strongly depends on the pH of the gastrointestinal region. Upon absorption of sulindac, it can be biotransformed into the COX-inhibiting sulindac sulfide by hepatic

metabolism, and is furthermore prone to oxidation by flavin-containing monooxygenase subtype 3 (FMO3) into the sulindac sulfone metabolite [152].

After oral administration, these NSAIDs are absorbed in the systemic circulation and as such, distributed across the body, including the colon. However, relatively high concentrations are needed to demonstrate anti-carcinogenic effects in *in vitro* cell cultures for both celecoxib and sulindac. For example, Grösch et al. (2006) reported that concentrations of celecoxib between 10 µM and 100 µM are generally used in cell culture experiments to get anti-carcinogenic effects, which are not reached in plasma by administering a single 200 mg dose. Therefore, it can be questioned whether direct uptake from the gut lumen into the colonic tissue might be required, even though neither of the NSAIDs have been formulated as a colon-targeting delivery system. Studying the colonic disposition of celecoxib and sulindac could therefore provide much needed insight, both from a pharmacokinetic and therapeutic point of view..

So far only a limited amount of techniques are available to study the *in vivo* colonic disposition. For example, Edsbäcker et al. used gamma-scintigraphy to assess budesonide release from the orally taken controlled release capsule Entocort® and relied on blood concentration data to estimate the dissolution by deconvolution-based methods [153,154]. Other groups rely on faecal samples to estimate colonic drug release and concentrations, e.g. Yu et al. determined mesalazine concentrations in faecal contents after administration of locally acting formulations [155]. However, the approaches mentioned so far only give an indirect idea of drug and formulation behaviour in the colon. It would be more relevant to be able to determine local *in vivo* concentrations in the colon. The collection of colonic contents during endoscopy has been shown to be feasible, and has already contributed to the characterisation of these aspirates in terms of pH, lipids, bile salts, buffer capacity, etc. [51,64] and has been used to facilitate the development of biorelevant media [68]. Collected colonic fluids were also used to measure drug solubility post-collection [51,64,68]. In chapter 3, we established our own colon preparation technique that uses rectal enemas, enabling us to simultaneously collect biopsies and colonic contents. This technique was then used to study the colonic disposition, and more specifically, to evaluate whether local drug accumulation is gut-driven and/or systemically driven, for both celecoxib (chapter 3) and the more soluble sulindac (chapter 4).

As indicated by chapter 1.3.2, many *in vitro* models are available that can simulate the colonic environment. Of these models, the Caco-2 cell line and the Ussing chamber technique are routinely used as in vitro permeation screening tools, correlating well with the fraction absorbed (Fa) in humans at a small intestinal level [89,90,103,109,112,156], but also at a colonic level [52,108]. However, these systems can also provide much needed insight into the accumulation of drugs, in particular for colon-targeting drugs that exert their therapeutic effect in a local manner. To this end, the Caco-2 and Ussing chamber system were selected to provide insight into the local accumulation behaviour (chapter 5).

CHAPTER 2 – Objectives

Multiple studies have shown the efficacy of celecoxib and sulindac for the prevention of colorectal polyps and cancer, yet multiple hiatus remain about the disposition of these drugs, especially at the level of the colon. Most notably, it is unclear how therapeutic concentration in colonic tissue are reached: either the drug dissolves in the intraluminal fluids, crosses the intestinal mucosa and is delivered to colonic tissue through the systemic circulation, and/or an undissolved intestinal fraction reaches the colon through the transit. The increasing amount of new chemical entities that are highly lipophilic and thus poorly soluble in the aqueous environment of the stomach and intestine, makes the second option probable. For this purpose, several small-scale clinical studies with healthy human volunteers were performed to elucidate the colonic disposition:

- To determine local *in vivo* drug concentrations in the colon, a protocol that allowed simultaneous sampling of colonic contents and biopsies needed to be established (chapter 3).

- To better understand the colonic disposition of celecoxib, and whether colonic accumulation of celecoxib is gut or systemic driven, healthy and fasted volunteers were administered an immediate release formulation, Celebrex® (Chapter 3).

- To study whether colonic accumulation of sulindac, a weakly acidic and relatively better soluble compound, is gut or systemic driven, healthy and fasted volunteers were administered an immediate release formulation, Arthrocine® (Chapter 4).

The acquired *in vivo* data with respect to the disposition of the compounds in the colon and the systemic circulation can be used as reference data to optimize predictive *in vitro* (Caco-2) and *ex vivo* (Ussing) absorption models. Currently these tools and models are not adapted to predict colonic disposition in humans, and are barely used to evaluate drug accumulation, even though colon-targeting drugs target the epithelium or immune cells in a local manner. To this end accumulation of celecoxib of sulindac was evaluated in both the Caco-2 system and the Ussing chamber model (chapter 5).

CHAPTER 3 – Colonic disposition of Celecoxib

Insight into the colonic disposition of celecoxib in humans

Glenn Lemmens, Joachim Brouwers, Jan Snoeys, Patrick Augustijns, and Tim Vanuytsel

European journal of pharmaceutical sciences 2020 Mar 30;145:105242.

3.1 Abstract

Although the effect of NSAIDs such as celecoxib on the progression of colorectal polyps has been established, it is currently unknown how sufficiently high concentrations of celecoxib are reached in colonic tissue. Indeed, the lipophilic and poorly soluble celecoxib is orally dosed as an immediate release capsule without any colon-targeting delivery strategy. In the present study, we aimed to distinguish between plasma and gut driven caecal tissue accumulation of celecoxib in healthy volunteers. After developing a protocol to reliably collect colonic biopsies and contents, the disposition of celecoxib was assessed in plasma, caecal tissue and caecal contents collected after intake of a celecoxib capsule (200 mg; Celebrex®) with 240 mL of tap water. During a first colonoscopy (1.0-2.5 h after drug intake), plasma concentrations of celecoxib and its carboxy metabolite were increasing, while caecal tissue concentrations were relatively low. As no celecoxib was present in caecal contents, tissue accumulation was clearly plasma driven. During a second colonoscopy (6.0-7.5 h after drug intake), tissue concentrations of the drug and its metabolite were substantially higher despite decreasing plasma concentrations. As a high amount of celecoxib was found in the caecal contents, the increased tissue accumulation most likely resulted from direct uptake of celecoxib from the gut. These data demonstrate that incomplete small intestinal absorption of the poorly soluble drug celecoxib enables gut driven drug accumulation in caecal tissue, which is, most likely, critical for the role of this NSAID in the prevention of colorectal cancer.

3.2 Introduction

Colorectal cancer is the third most abundant type of cancer, with an estimated 1.8 million new cases in 2018 [157]. Inflammation plays a key role in the development and progression of the disease; therefore, non-steroidal anti-inflammatory drugs (NSAIDs) such as sulindac, aspirin, and celecoxib are eligible candidates for the treatment and/or prevention of precursor lesions of colorectal cancer; i.e. polyps. NSAIDs inhibit the cyclooxygenase (COX) pathway, in addition to many COX-independent pathways. In humans, two important isoforms of COX exist: COX-1 is expressed constitutively and is important for maintaining the physiological functions of the gastrointestinal tract, while COX-2 is an inducible isoform that becomes overexpressed in states of inflammation and carcinogenesis [158]. The effect of NSAIDs in colorectal cancer treatment and prevention has been reported in several epidemiological studies. For instance, after taking 400 mg of the COX-2 inhibitor celecoxib twice a day for three years, the incidence of recurrent adenomas was reduced by 45% [2]. Treatment of familial adenomatous polyposis patients with 150 mg sulindac twice a day for 9 months reduced the number of polyps with 44% and their size with 35% [3]. Also for the COX-1 inhibitor aspirin, the Melbourne Control Case Study showed a 42% reduction in the risk of colorectal cancer [159]. However, COX-2 inhibitors such as celecoxib are generally preferred over COX-1 inhibitors as upregulation of COX-2 happens in the early stages of carcinogenesis, and as they are associated with less severe side effects [160].

To exert their effect on colorectal cancer progression, the NSAIDs need to be present at sufficiently high concentrations in the colon. To date, however, the disposition of these NSAIDs in the human colon has not been evaluated yet. In this respect, it is currently unknown how these compounds reach the colon. After oral administration, the NSAIDs are absorbed in the systemic circulation and, as such, distributed across the body, including the colon. However, relatively high concentrations are needed to demonstrate anti-carcinogenic effects in *in vitro* cell cultures. Indeed, Grösch et al. (2006) reported that concentrations of celecoxib between 10 µM and 100 µM are generally used in cell culture experiments to get anti-carcinogenic effects, which are not reached in plasma by administering a single 200 mg dose. Therefore, it can be questioned whether direct uptake from the gut lumen into the colonic tissue might be required, even though neither of the NSAIDs have been formulated as a colon-targeting delivery system. In the present study, we aim to shed light on the colonic disposition of the COX-2 inhibitor

celecoxib after oral administration of its dosage form Celebrex® (immediate release capsule, 200 mg)

Celecoxib (CXB) is a lipophilic (LogP = 3.5), and weakly acidic drug (pKa = 11.1) [149]. It has been reported as a high permeability drug [150], explaining why the compound is rapidly absorbed (t_{max} = 1h) in dogs when administered orally as a solution. When dosing celecoxib as a solid, however, absorption is delayed with 1 to 2 hours, which indicates its low solubility in the aqueous gastrointestinal environment [150]. Increasing the orally administered dose in rats resulted in a higher fraction of celecoxib that could be retrieved in the faeces [161]. As celecoxib is extensively metabolized in the human liver by CYP2C9 to form hydroxy celecoxib (CXB–OH), which can then be oxidized to carboxy celecoxib (CXB-COOH) by cytosolic alcohol dehydrogenases ADH1 and ADH2 [158], the appearance of celecoxib in the faeces implies that this poorly soluble drug does not get completely absorbed in the upper gastrointestinal tract [161]. With respect to celecoxib's effect on colorectal polyps and cancer, this observation further implies that direct uptake of celecoxib from the colonic lumen into the colonic tissue is possible, even though it should be noted that the low and scattered water content in the colon hinders drug dissolution and that the comparably smaller surface area of the colonic mucosa makes it less optimal for drug uptake than the small intestinal mucosa.

To evaluate the pharmacokinetic disposition of celecoxib at the level of the colon, the present study focused on two main goals: (i) to develop a protocol through which biopsies and colonic contents can be reliably collected, and (ii) to simultaneously assess celecoxib and its major metabolites in the systemic circulation, in the colonic lumen and in colonic tissue, allowing an improved insight into the underlying mechanisms.

3.3 Material and methods

3.3.1 Chemicals

Celecoxib was acquired via TCI Europe N.V. (Zwijndrecht, Belgium). Hydroxy celecoxib and carboxy celecoxib were provided to us by Toronto Research Chemicals (Toronto, Canada). Propyl-p-hydroxybenzoate was provided by Sigma-Aldrich (St. Louis, Missouri, USA). Chem-Lab (Zedelgem, Belgium) and Biosolve (Valkenswaard, The Netherlands) supplied acetic acid and formic acid, respectively. Methanol (HPLC grade) and glucose were ordered from Acros

Organics (HPLC grade; Geel, Belgium). Purified water for analytical purposes was obtained using a Maxima system (Elga Ltd., High Wycombe Bucks, UK). Hanks' Balanced Salt Solution without phenol red (HBSS) and 4-(2-hydroxyetheyl)-1-piperazineethanesulfonic acid (HEPES) were obtained from Lonza (Verviers, Belgium), while sodium hydroxide (NaOH) pellets were purchased from Merck (Darmstadt, Germany).

3.3.2 Media

Medium (HBSS+) was prepared by dissolving 25 mM glucose in 500 mL HBSS, buffered with 10 mM HEPES and adjusted to pH 7.4 with 2 M of NaOH.

3.3.3 Clinical studies

3.3.3.1 Study medication

Celebrex® capsules (200 mg celecoxib; Pfizer, Brussel, Belgium) were ordered via the hospital pharmacy of the University Hospitals Leuven (UZ Leuven, Belgium).

3.3.3.2 Ethics

Clinical trials followed the tenets of the Declaration of Helsinki and were approved by the Federal Agency for Medicines and Health Products (FAMHP; EudraCT reference numbers 2017-000131-13, 2017-001194-16) and the Ethics Committee Research UZ/KU Leuven (reference numbers S60240, S60302, S60322). All volunteers provided written informed consent prior to participation. Volunteers with hepatitis B/C and/or HIV infection were excluded to guarantee the safety of the study personnel. Illness at the time of the study, allergy for NSAIDs, medication use, a history of acute/chronic gastrointestinal disease(s), (possible) pregnancy, and/or frequent exposure to radiation during the previous year were criteria for exclusion.

3.3.3.3 Study protocol

In all studies, volunteers were asked to follow a three-day low-fibre diet (e.g. white bread or pasta, canned fruit in heavy syrup or juice, no vegetables, clear drinks…) and to eat a last meal at 8 pm on the day before the study. To ensure fasted state conditions, volunteers could only

drink water 12h to 2h prior to the colonoscopy. All studies were schematically summarized in figure 3.1.

Study 1: Optimizing enema application and collection of colonic contents

Upon arrival at the endoscopy unit, the volunteers (aged between 23 and 30 years; 2 men and 3 women) were positioned on their left side and a varying volume of enema (250 mL or 500 mL of tap water) was administered rectally. Next, a sigmoidoscopy was performed to validate whether the left hemicolon was cleansed without spill over to the right hemicolon. Once this condition was achieved, the volunteer was brought under conscious sedation (midazolam 1-5 mg and pethidine 25-50 mg i.v.) in order to perform a full colonoscopy and to reliably sample colonic contents from the right hemicolon. To collect colonic contents, several approaches were evaluated: (i) collection with a polyCatch Retrieval Device (Endo-Flex, Germany), (ii) aspiration with a Faucher catheter (PVC, Fr 27 x 150 cm; Vygon, Brussels, Belgium) or a weighted duodenal tube (PVC, Fr 16 x 125 cm; Vygon, Brussels, Belgium), which were attached during the colonoscopy to the mucosa of the ascending colon with hemostatic clips (Boston Scientific, US), (iii) sampling as much caecal contents as possible through the suction channel of the colonoscope (a stiff brush was pulled through the entirety of the suction channel to collect the contents of the suction channel into a falcon tube).

Study 2: Region- and time-dependent accumulation in colonic tissue

In a preliminary study, one female volunteer (aged 23 years) was asked to take a Celebrex® capsule (200 mg celecoxib) with 240 mL of tap water either 2 h, 4 h, 6 h or 8 h prior to the colonoscopy. The time factor was evaluated on different test days. Upon arrival at the endoscopy unit, the volunteer was positioned on her left side and 250 mL of tap water was administered rectally. Next, the volunteer was brought under conscious sedation (midazolam 1-5 mg and pethidine 10-50 mg i.v.). During the colonoscopy, four biopsies were taken with a standard biopsy forceps (Radial Jaw™3 with needle; outside diameter 2.2 mm; Boston Scientific) at each of the following regions: caecum, hepatic flexure, splenic flexure and sigmoid. The participant was not allowed to drink or consume food during the colonoscopy.

Study 3: Systemic versus gut-driven tissue accumulation

After colonic preparation with an enema as previously described, a colonoscopy was performed to obtain two blank biopsies. Next, a Celebrex® capsule (200 mg celecoxib) was orally administered with 240 mL of tap water to the volunteers (5 men, aged between 20 and 23 years). Between 1 and 2.5 h after drug intake, two caecal biopsies were taken every 15 min with a standard biopsy forceps (Radial Jaw™3 with needle; outside diameter 2.2mm; Boston Scientific). After 2.5 h, as much colonic contents as possible (± 2 mL) were sampled through the suction channel of the colonoscope and collected into a falcon tube by pulling a stiff brush through the entirety of the suction channel. A few hours later, the colonoscope was positioned again in order to sample caecal biopsies every 15 min between 6 and 7.5 h after drug intake. After 7.5 h, colonic contents were collected once again. During the colonoscopies, volunteers were not sedated, as sedation might influence gastrointestinal motility and thus the pharmacokinetic disposition of celecoxib. Venous blood samples were collected on ice in heparinized tubes (BD Vacutainer systems, Plymouth, U.K.) at predetermined time points, i.e., 0, 5, 15, 30, 60, 90, 120, 180, 240, 360, 480, and 1440 min after drug intake. Participants were not allowed to drink or consume food for the first 4 h after drug intake. After 4 h, participants were allowed to drink and/or eat ad libitum.

Study 4: Plasma concentration-time profile of celecoxib

Upon arrival at the endoscopy unit, volunteers (aged between 20 and 25 years; 3 men and 4 women) were asked to take a Celebrex® capsule (200 mg celecoxib) with 240 mL of tap water. Venous blood samples were collected in heparinized tubes (BD Vacutainer systems, Plymouth, U.K.) on ice at predetermined time points, i.e., 0, 5, 15, 30, 60, 90, 120, 180, 240, 360, 480, and 1440 min after drug intake. Participants were not allowed to drink or consume food for the first 4 h after drug intake. After 4 h, participants were allowed to drink and/or eat ad libitum.

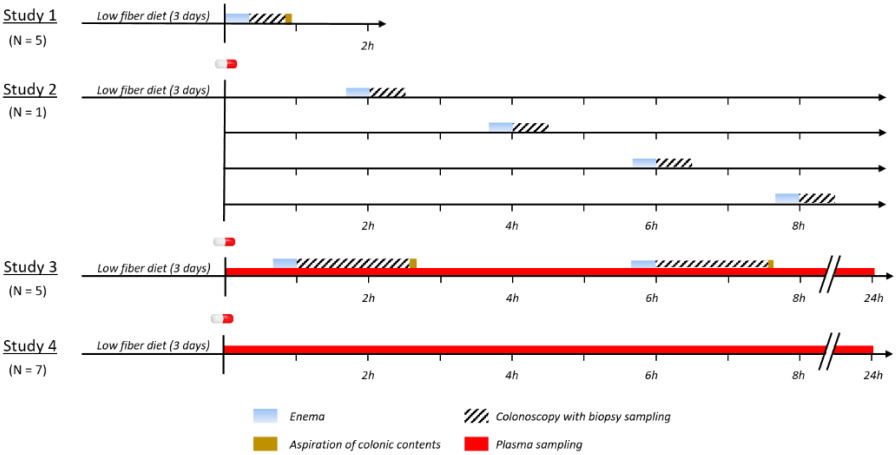

Fig. 3.1: Schematic representation of the clinical studies (study 1: optimizing enema application and collection of colonic contents; study 2: region- and time-dependent accumulation in colonic tissue; study 3: systemic versus gut-driven tissue accumulation; study 4: plasma concentration-time profile of celecoxib).

3.3.4 Processing of biological samples

Biopsies

Upon sampling, biopsies were rinsed threefold with HBSS+, excess liquid was removed with a paper tissue, and biopsies were stored in 1 mL of methanol. Prior to further processing, samples were stored at 4°C. To quantify drug concentrations in biopsies, 10 µL of DMSO containing an internal standard (10 µM propyl-p-hydroxybenzoate) was added. Biopsies were then air dried for 1 h, weighed, placed back into the methanol and homogenized with a TissueLyser II (3 x 4 min, 1/30 s; Qiagen, Hilden, Germany). Subsequently, samples were centrifuged (20817 x g, 1 min, 4°C; Centrifuge 5417R; Eppendorf, Hamburg, Germany) and the supernatant was evaporated under a continuous air flow before being reconstituted in 100 µL of methanol:water (50:50, v/v).

Colonic contents

Colonic contents were processed on the day of the experiment to determine the total and dissolved concentrations of celecoxib and its metabolites. After vortexing (Vortex Genie,

Scientific industries, New York, USA) the contents for 1 min, the total drug concentration was measured by directly diluting 10 µL of the colonic contents with 990 µL methanol:acetate buffer pH 4.5 (45:55, v/v), which was then immediately centrifuged (20817 x g, 5 min; Microcentrifuge 5424, VWR International); the supernatant was collected for liquid chromatography (LC) analysis. The dissolved drug concentration was measured by first centrifuging (20817 x g, 5 min; Microcentrifuge 5424, VWR International) a fraction of the colonic contents after being vortexed for 1 min. Next, 10 µL of the supernatant was diluted in 990 µL methanol:acetate buffer pH 4.5 (45:55, v/v) and centrifuged (20817 x g, 5 min; Microcentrifuge 5424, VWR International) once more; the supernatant was collected for LC analysis.

Venous blood samples

Immediately after collection, blood samples were stored on ice; at the end of the day of the experiment, they were centrifuged (1699 x g, 15 min, 4°C; Centrifuge 5804R; Eppendorf, Hamburg, Germany) to collect plasma samples, which were stored at -26°C until analysis. To quantify drug concentrations in plasma, 10 µL of DMSO containing an internal standard (500 µM propyl-p-hydroxybenzoate) was added to 1 mL plasma. After adding 4 mL methanol, the mixture was thoroughly vortexed and subsequently shaken for 1 min. The samples were then centrifuged (1699 x g, 15 min, 4°C; Centrifuge 5804R; Eppendorf, Hamburg, Germany) and the supernatant was collected for LC analysis.

3.3.5 LC analysis

Processed biopsy samples were analysed with LC-MS/MS, using an Acquity H-class UPLC system coupled to a Xevo TQ-S micro triplequadrupole analyser equipped with an ESI source (Waters, Milford, MA, USA). Separation was achieved using a Kinetex C18 column (2.6 µm, 50 x 2.1 mm, Phenomenex, Utrecht, The Netherlands) with methanol (solvent A) and water acidified with 0.1% formic acid (solvent B). The elution gradient was as follows: 0–0.8 min, 50% A; 0.81 – 1.8 min, 80% A; 1.81 – 3.0 min, 90% A; 3.01 – 4.50 min, 50%. The flow rate was 0.5 ml/min for the first 4 min, and 2 mL/min for the last 30 s of the run. Column temperature was held at 35°C, and the injection volume was 1 µL. The mass spectrometer was set to positive ionization MS/MS mode for celecoxib and its metabolites, and to negative ionization MS/MS

mode for the internal standard with the following parameters: source temperature 150°C, capillary voltage 0.80 kV, cone voltage 30 V, cone gas flow 40 L/h, desolvation gas flow 1000 L/h and desolvation temperature 600°C. The mass transitions (m/z) followed were 381.8 –361.9 (celecoxib), 397.8–377.9 (hydroxy celecoxib), 411.8–391.9 (carboxy celecoxib) and 178.8–91.8 (propyl-p-hydroxybenzoate). Stock solutions of celecoxib, hydroxy celecoxib, carboxy celecoxib, and the internal standard were prepared in DMSO at a concentration of 10 mM, and calibration curves were made by serial dilution in methanol/water (50:50, v/v), containing 1 µM internal standard. Linearity was observed between 4000 nM and 0.15, 0.07, 0.15 nM for celecoxib, hydroxy celecoxib and carboxy celecoxib, respectively. For validation purposes, control samples were prepared containing 10 µM, 1 µM and 100 nM of celecoxib and metabolites. Concentrations of celecoxib and metabolites could be precisely (intraday variability RSD ≤ 15.07 % and interday variability RSD ≤ 11.81 %) and accurately (range: 81.93 – 99.91 %) determined in samples.

Processed plasma and colonic fluid samples were analysed using HPLC with UV detection (252 nm). Separations were performed on a Novapak C18 column under radial compression (pore size 60 Å, particle size 4 µm, 8 mm i.d. x 100 mm, Waters, Milford, MA, USA). 100 µL sample was injected and eluted with a gradient of 25 mM sodium acetate buffer pH 4.5 (solvent A) and methanol (solvent B) at a flow rate of 1.0 mL/min for 18.5 min. The elution gradient was as follows: 0.0 - 1.5 min, 55% A; 2.5 – 7.0 min, 30% A; 8.0 – 13.5 min, 22% A; and 14.5 – 18.5 min, 55% A for reconditioning. Carboxy celecoxib, hydroxy celecoxib, the internal standard and celecoxib eluted at 6.6 min, 7.9 min, 8.6 min, and 12.5 min, respectively. Linearity was observed in a range from 20 µM to 10 nM. For validation purposes, control samples were prepared containing 10 µM, 1 µM and 100 nM. Concentrations of celecoxib and metabolites could be precisely (intraday variability RSD ≤ 4.04% and interday variability RSD ≤ 7.00%) and accurately (range: 89.95 – 99.89%) determined in samples. Chromatograms were integrated with Waters Empower 2 software (Milford, MA, USA).

3.3.6 Data presentation

This mechanistic study was designed as exploratory, i.e. without the intention to formally test hypothesis. As such, the data obtained are descriptive in nature and do not allow statistical comparison.

Plasma concentrations are represented as the amount of celecoxib or metabolite per volume of plasma (µg/mL). Concentrations in colonic contents are represented in amount of celecoxib or metabolite per volume of colonic content (µg/mL). The accumulation in colonic biopsies was normalized for the weight of the tissue, and represented as the amount of celecoxib or metabolite per amount of tissue (ng/mg). Data in text are presented as mean + SD, unless stated otherwise.

3.4 Results and discussion

Documentation regarding the sampling of colonic contents and the gastrointestinal behaviour of low solubility compounds at the level of the colon is limited. The present study pursued to evaluate the colonic disposition of celecoxib in human volunteers, and to explore whether the accumulation into colonic tissue is either plasma or gut driven. To this end, we first needed to develop a protocol that allowed us to collect relevant luminal and tissue samples from the colon.

3.4.1 Optimizing enema administration and collection of colonic contents

To sample colonic tissue and contents in a reliable way, i.e. without affecting the disposition of celecoxib, the colonoscopy and the required preparation procedure should disturb the normal physiology of the colon as little as possible (e.g. by diluting the colonic contents). To our knowledge, only one group has attempted to sample proximal colonic fluid in the framework of drug disposition studies. Diakidou et al. (2009) collected the contents from the ileum and caecum following the administration of 10 mg of bisacodyl, a stimulant laxative, 50 h and 44 h prior to the colonoscopy in combination with a strict dietary regimen of liquefied food (e.g. fish/chicken/rice soups, fruit juices) to allow visual control. In the present study, however, we preferred not to use a laxative in order to avoid the risk of disturbing the physiological state of the proximal colon at the time of sampling. After the volunteers followed a three-day low-fibre diet, enemas were administered to cleanse only the left hemicolon and enable the safe passage of the colonoscope. Midazolam was used as sedation while performing the colonoscopy and could be a potential disturbing factor. By varying the frequency and volume of the enemas, we observed that a one-time enema of 250 mL of water appeared sufficient to cleanse the left

hemicolon while avoiding spill over to the right hemicolon where then physiologically relevant samples could be taken (Fig. 3.2).

Next, multiple sample techniques were evaluated to collect proximal colonic contents. First, a polyCatch Retrieval Device (Endo-Flex, Germany) was inserted through the colonoscope into the caecum, where the retrieval pouch was used to collect colonic contents. This method was not optimal as fluids slipped out of the PolyCatch Retrieval Device after retraction. A second option was the use of aspiration catheters: a 27 Fr Faucher tube or a 16 Fr Gastro-duodenal feeding tube (Vygon, Belgium). The tubes were inserted through the colonoscope and attached to the mucosa of the ascending colon with hemostatic clips (Boston Scientific, US), after which we attempted to aspirate colonic contents regularly over a period of 4 hours. Due to the high viscosity of the contents, however, the volume of the aspirated samples was limited and it appeared not possible to collect samples in a time-dependent way. Finally, using the suction canal of the colonoscope turned out to be the most reliable way to collect the contents from the proximal colon. Immediately after collecting colonic contents, a hard brush was inserted into the colonoscope and contents (± 2 mL) were pulled out and collected in a falcon tube. While this method allowed us to collect physiologically relevant samples, it is limited to one sample per colonoscopy.

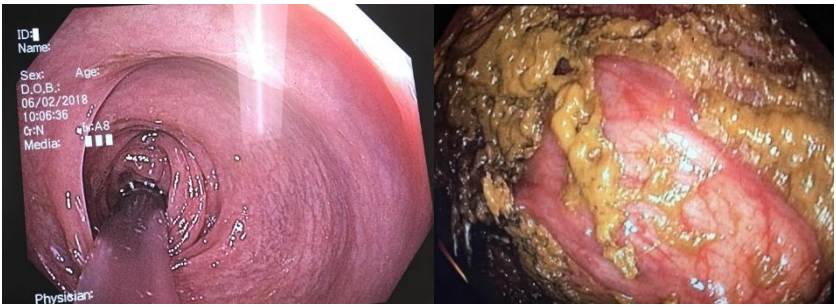

Fig. 3.2: Visualization of the cleansed left hemicolon (left) and the maintained physiological state of the right hemicolon (right) after a 250 mL enema.

3.4.2 Optimizing time and region to evaluate colonic celecoxib disposition

To assess the optimal time and colonic region to sample tissue for the evaluation of the disposition of celecoxib, we determined, in a preliminary experiment, the concentration-time profile of celecoxib in colonic tissue collected from four regions (Fig 3.3). Following a low-fibre diet for 3 days, one volunteer took one tablet of Celebrex® (200 mg of celecoxib) with 240 mL of tap water. After cleansing the left hemicolon with the above-mentioned enema, a colonoscopy was performed under conscious sedation, and four biopsies were taken from each of the following regions: the caecum, the hepatic flexure, the splenic flexure, and the sigmoid. The sampling of the biopsies was performed either 2, 4, 6, or 8 h after intake of Celebrex® on different test days. In Figure 3.3, we see that the concentration (ng/mg) of celecoxib in the tissue decreased from 2 to 4 h and increased from 4 to 8 h after intake of the drug in all sampled regions except for the hepatic flexure where the highest accumulation was seen at 6 h. Similar to celecoxib, accumulation of the metabolite carboxy celecoxib was the highest 8 h after intake, but concentrations were about 30-fold lower in comparison with celecoxib. Tissue concentrations of celecoxib were the highest in the caecum in comparison with other regions. Based on these data, it was decided to further evaluate the disposition of celecoxib and its main metabolite only at the level of the caecum.

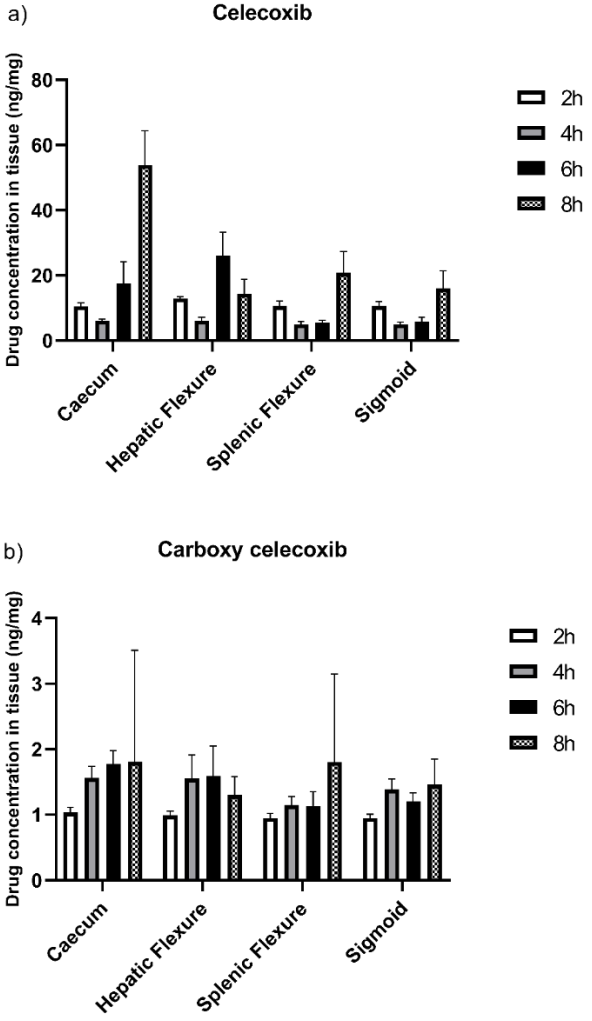

Fig. 3.3: Region- and time-dependent accumulation of celecoxib (a) and its metabolite carboxy celecoxib (b) in biopsies collected from one healthy volunteer after oral intake of one tablet of Celebrex (200 mg celecoxib) with 240 mL of tap water under fasted state conditions. Bars represent mean (+ SD) drug accumulation in biopsies (n = 4) from the caecum, hepatic flexure, splenic flexure and sigmoid, which were collected either 2 h (white bars), 4 h (grey bars), 6 h (black bars) or 8 h (speckled bars) after oral intake.

3.4.3 Time-dependent systemic and caecal dispostion of celecoxib

First, we determined the concentration-time profile of celecoxib in the systemic circulation, without performing a colonoscopy. To match the colonic disposition studies, volunteers followed the same dietary regimen (a three-day low fibre diet), and were asked to take Celebrex (200 mg celecoxib) with 240 mL of tap water. The mean plasma T_{max} was 2.5 ± 0.87 h in healthy volunteers (Fig. 3.4), which is in agreement with the study performed by the group of Werner et al. (2002), who observed a mean T_{max} of 2.9 ± 1.2 h under fasted conditions [162]. After reaching the T_{max}, the decrease in plasma concentrations is initially reflected in the decrease in colonic tissue concentrations of celecoxib from 2 to 4 h in figure 3.3. However, there is a discrepancy between the plasma T_{max} (2.5 h) and the above-mentioned T_{max} in caecal tissue (8 h, Fig. 3.3). This suggests that colonic tissue concentrations are not driven solely by plasma levels, but also by direct uptake from the gut.

To further distinguish between plasma and possibly gut driven caecal tissue accumulation of celecoxib, a study was performed involving colonoscopies after intake of a Celebrex® tablet (200 mg celecoxib) with 240 mL of tap water. One hour after drug intake, biopsies were taken from the caecum every 15 min for 90 min (see Fig. S1 for an overview of sampling sites), after which caecal contents were aspirated (first colonoscopy, phase 1). Based on the systemic concentration-time profile in figure 3.4, plasma levels are expected to increase in this first phase (between 1 and 2.5 h post drug intake) and drive caecal tissue accumulation. Six hours after drug intake, caecal biopsies were collected again every 15 min for 90 min, after which caecal contents were aspirated (second colonoscopy, phase 2). In this second phase (between 6 and 7.5 h post drug intake), plasma levels of celecoxib are expected to decrease. Tissue concentrations could be plasma driven (in which case they would decrease as well), but also gut driven if celecoxib arrived at the caecal lumen through transit.

The plasma concentration-time profile of celecoxib, shown in figure 3.4, indicates a substantially higher plasma T_{max} for celecoxib (4.4 h ± 0.9 h) in this colonic disposition study as compared to the T_{max} observed in the above-mentioned study without colonoscopy. We assume that the difference in T_{max} is due to rectal distention by the colonoscope, delaying gastric emptying [163]. Also, volunteers generally experience higher stress levels during the colonoscopy, which is known to modulate gastrointestinal motility [164,165]. Despite the

longer T_{max}, it is still in-between the first and second colonoscopy, which is critical for our study design.

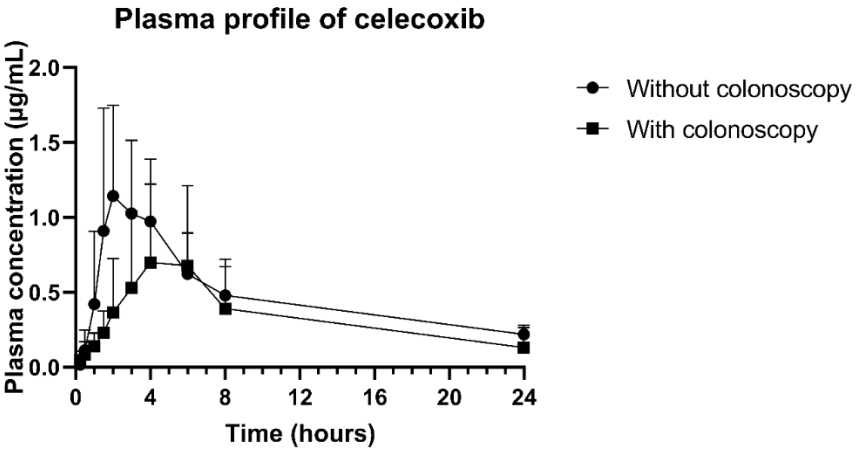

Fig. 3.4: Mean (+ SD) plasma concentration – time profiles in healthy volunteers after oral intake of one tablet of Celebrex (200 mg celecoxib) with 240 mL of water under fasted conditions. Studies were performed either without performing a colonoscopy (n = 7) (●) or with performing a colonoscopy (n = 5)(■).

Figure 3.5 depicts the mean concentrations of celecoxib and its main metabolite carboxy celecoxib in caecal tissue during the two colonoscopies (phase 1 and phase 2), in comparison with the systemic concentration-time profiles. As expected, the plasma concentration of celecoxib and its carboxy metabolite increased during phase 1. However, caecal tissue concentrations remained relatively low. No celecoxib could be detected in the luminal contents of the caecum, collected after 2.5 h (< 100 nM, limit of detection). The lack of celecoxib in the luminal contents is in line with the median gastric and small intestinal transit time of 56 and 255 min, respectively [166]. Tissue accumulation is thus clearly plasma driven during phase 1.

During phase 2, tissue concentrations of the drug and its main metabolite were substantially higher than in phase 1, despite decreasing plasma concentrations. For instance, at 405 min after drug intake (phase 2), tissue concentrations of celecoxib and carboxy celecoxib were

respectively 39- and 228-fold higher than after 105 min (phase 1). The level of carboxy celecoxib was 109-fold lower than the level of celecoxib. At the same time, relatively high levels of celecoxib and carboxy celecoxib were observed in the luminal contents, collected from the caecum after 7.5 h; total concentrations amounted to 614.37 ± 614.45 µg/mL and 63.79 ± 72.19 µg/mL, respectively (Fig. 3.6). These data clearly indicate that accumulation of celecoxib in caecal tissue is predominantly gut driven once the drug reaches the caecal lumen.

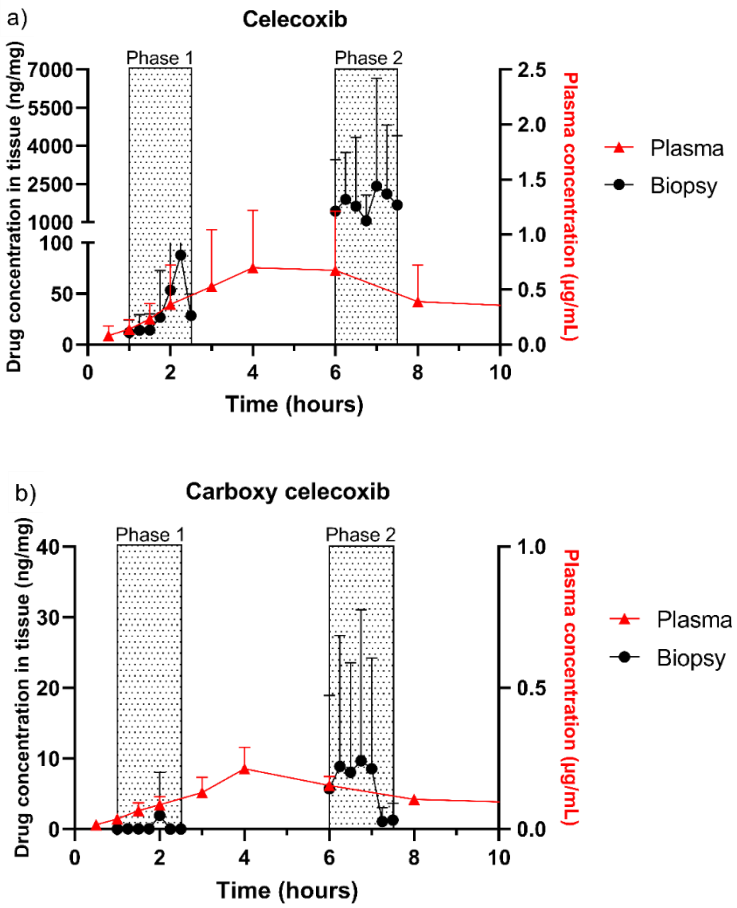

Fig. 3.5: Mean (+ SD) concentration – time profiles of celecoxib (a) and carboxy celecoxib (b) in plasma samples (▲) and caecal biopsies (●), collected from healthy volunteers (n = 5) after oral intake of one tablet of Celebrex (200 mg celecoxib) with 240 mL of water under fasted conditions.

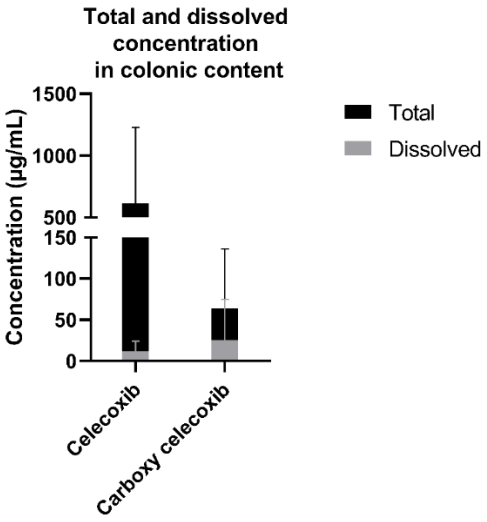

Fig. 3.6: Mean (+ SD) total and dissolved concentration of celecoxib and carboxy celecoxib in colonic contents sampled from healthy volunteers (N = 4) 7.5 h after oral intake of one tablet of Celebrex (200 mg celecoxib) with 240 mL of water under fasted conditions.

Our data in human volunteers corroborate earlier findings by the group of Paulson (2000) in rats: in the caecum or colon, the highest tissue concentration of celecoxib was found 8 h after oral administration, in contrast to the majority of other tissues, where maximum levels were seen after 1 h. Knowing that celecoxib is predominantly eliminated in faeces after oral administration, the group of Paulson varied oral doses from 20 to 400 mg/kg in male rats, and observed that a higher dose leads to a higher recovery of celecoxib in faeces, which implies a higher fraction of unabsorbed drug. Paulson's group also reported that only 2% of intravenously administered celecoxib was recovered in urine or faeces as the parent compound. Thus, the high level of celecoxib in colonic contents, observed in our study, most likely resulted from incomplete absorption in the upper gastrointestinal tract, and not from biliary excretion. In contrast, extensive hepatic metabolization of absorbed celecoxib followed by biliary excretion likely contributes to the presence of carboxy celecoxib in colonic contents during phase 2 of the present study, even though intestinal secretion or colonic metabolization cannot be excluded.

Analysis of the luminal aspirates collected from the caecum in phase 2 of our study (7.5 h after drug intake) showed a difference between total (i.e., celecoxib as solid and solute; 614.37 ± 614.45 µg/mL) and dissolved (I.e., celecoxib as solute; 11.65 ± 12.51 µg/mL) drug concentrations, implying that celecoxib is mainly present in the solid state in the caecum. The mean solid fraction of celecoxib and carboxy celecoxib amounted to 0.91 ± 0.09 and 0.51 ± 0.32, respectively, which also indicates that the (probably) bile secreted carboxy celecoxib precipitates in the lumen. Although the total concentration of carboxy celecoxib (63.79 ± 72.19 µg/mL) was 8.9 times lower than celecoxib in colonic aspirates, the dissolved drug concentration of carboxy celecoxib is higher (25.40 ± 49.32 µg/mL). The large solid fraction of celecoxib reflects the low solubility of the compound in combination with the suboptimal dissolution conditions in the colonic lumen due to the scarce and scattered pockets (median 2 mL) of colonic fluid and the increase in viscosity from the proximal to distal lumen [50]. This may also explain why the highest tissue concentrations of celecoxib (Fig. 3.3) were observed in the caecum compared to the more distal regions, where dissolution probably becomes even harder. In addition to other factors, including gastrointestinal residence time, the poor dissolution conditions may also contribute to the highly variable drug concentrations that were observed in colonic aspirates and tissue.

When considering therapeutic efficacy, our *in vivo* studies reported a systemic Cmax of 3.1 ± 2.0 µM in healthy volunteers, which is considerably higher than the IC50 (0.040 µM) of celecoxib for COX-2 [167]. However, recent research indicates that the antineoplastic effect cannot be ascribed solely to COX-inhibition, but that many COX-independent pathways are involved, i.e. by repressing the PI3-K/PDPK1/Akt and Wnt/β-catenin oncogenic pathways [168]. The group of Egashira even reported that celecoxib can inhibit proliferation and induce apoptosis in HCT-116 cells independent of its action on COX-2 but by inducing TCF7L2 degradation [169]. It is noteworthy that the concentrations of celecoxib that are required to get an anti-carcinogenic effect in cell culture experiments are generally between 10 µM and 100 µM [170], which are not reached in plasma by administering a single 200 mg dose. In this respect, the relatively high levels of celecoxib in the colonic lumen and the resulting accumulation in colonic tissue, which were demonstrated in the present study, seem essential to obtain the reported anti-carcinogenic effects.

3.5 Conclusion

By developing a protocol to reliably collect colonic tissue and contents, we were able to gain insight into the colonic disposition of the NSAID celecoxib. Intake of the oral dosage form Celebrex® initially results in limited plasma driven tissue accumulation in the colon. Several hours after drug intake, however, a substantial amount of celecoxib arrives at the colon due to incomplete absorption of this poorly soluble drug in the small intestine. Gut driven uptake then causes increased accumulation of celecoxib in colonic tissue, most likely enabling its inhibitory effect on the progression of colorectal cancer. As such, these data demonstrate the possible importance of colonic uptake of orally administered low solubility drugs, even without using a colon-targeted delivery strategy.

3.6 Acknowledgements

This work has received support from Flanders Innovation & Entrepreneurship (Vlaio) (Grant No. 155042). The authors have no conflicts of interest to declare.

CHAPTER 4 - Colonic disposition of Sulindac

Insight into the colonic disposition of sulindac in humans

Glenn Lemmens, Joachim Brouwers, Jan Snoeys, Patrick Augustijns, and Tim Vanuytsel

Journal of Pharmaceutical Sciences. 2021 Jan;110(1):259-267.

4.1 Abstract

NSAIDs such as celecoxib and sulindac play a critical role in the treatment of colorectal cancer, yet it is not understood how sufficiently high concentrations are reached in colonic tissue. We previously demonstrated that an incomplete small intestinal absorption of celecoxib enables gut driven drug accumulation in caecal tissue, which is most likely needed for inducing remission. However, a multistage dissolution experiment suggested a more extensive absorption of sulindac relative to celecoxib, though still incomplete. To study whether caecal accumulation of sulindac is solely plasma driven or also gut driven, we performed an exploratory clinical study in healthy volunteers. After intake of a tablet of sulindac (200 mg; Arthrocine), two colonoscopies (1.0-2.5 h, and 6.0-7.5 h after drug intake) were performed to assess concentrations of sulindac and metabolites in plasma, caecal tissue and caecal contents. We observed that sulindac, even without the use of a colon-targeted delivery strategy, can arrive at the colonic lumen due to incomplete absorption and biliary excretion, and that the microbiota can catalyse the production of sulindac sulfide, which then accumulates in a high and local manner in the colonic tissue. These data can be relevant for drug development in the treatment of colorectal adenomas and cancer.

4.2 Introduction

An estimated 1.8 million new cases of colorectal cancer are reported on a yearly basis, making it the third most abundant type of cancer [157]. Non-steroidal anti-inflammatory drugs (NSAIDs) such as sulindac and celecoxib exhibit anti-carcinogenic properties via inhibition of cyclooxygenase-1 or -2 (COX), but also COX-independent pathways play an important role [171–173]. The incidence of recurrent adenomas was reduced 45% by celecoxib 400 mg bid for three years [2]. Sulindac 150 mg bid for 9 months lowered the number of polyps with 44% and their size with 35% in patients with familial adenomatous polyposis [3].

In vitro testing suggests that relatively high local concentrations of NSAIDs are required in the colon to exert an effect on colorectal adenoma or carcinoma progression. However, no colon-targeting dosage forms are available for NSAIDs. For celecoxib, we recently demonstrated that effective concentrations, which should be between 10 µM and 100 µM according to various *in vitro* cell culture experiments [170], cannot be reached through the systemic circulation after oral intake of a 200 mg immediate release formulation. However, our in-depth assessment of the colonic disposition of celecoxib revealed that its limited aqueous solubility results in incomplete absorption from the small intestine and a substantial undissolved fraction that reaches the colon by the intestinal transit. This fraction exposes the colonic tissue to a high concentration of celecoxib, which is probably critical to exert its anti-carcinogenic effect. For sulindac sulfide, *ex vivo* IC_{50} values for COX-enzymes (COX-1: 0.017 µM; COX-2: 0.55 µM) [174] can be reached through systemic exposure after oral intake of a single 200 mg tablet of the prodrug sulindac. However, this is not the case for therapeutic concentrations that have been reported for non-COX targets, ranging between 10 µM and 600 µM in intestinal models (Table 4.1) [171,172,175–178]. Therefore, direct uptake from the colonic lumen may also be necessary for the anti-carcinogenic effect of sulindac and its metabolites. As compared to celecoxib, however, the physicochemical properties of sulindac suggest a different behaviour in the gastrointestinal tract.

Sulindac is a lipophilic (LogP = 2.93), acidic (pKa = 4.09), and moderately to highly permeable [151] prodrug of sulindac sulfide, and has a solubility that strongly depends on the pH of the gastrointestinal region. The solubility of sulindac is limited (0.099 mg/mL, ADMET Predictor 9.5) in the stomach, but increases noticeably upon arrival in the small intestine (0.511 mg/mL,

ADMET Predictor 9.5), where it is negatively charged. In comparison to celecoxib, which is poorly soluble across the entire physiological pH range, it can be expected that sulindac dissolves faster in the small intestine, possibly resulting in more extensive absorption before reaching the colon.

Upon absorption of sulindac, it can be biotransformed into the COX-inhibiting sulindac sulfide by hepatic metabolism, and is furthermore prone to oxidation by flavin-containing monooxygenase subtype 3 (FMO3) into the sulindac sulfone metabolite [152]. The group of Dobrinska reported that the prodrug and metabolites can be biliary excreted into the intestine, but observed that clearance is considerably lower for the sulfide metabolite [179]. Nevertheless, in faeces, sulindac only constitutes 1% of the dose, while equal quantities of the sulfide and sulfone metabolites make up 19% of the dose [152]. This indicates that a second metabolic pathway biotransforms sulindac to sulindac sulfide in the colonic region. Indeed, it has been shown that the metabolic capacity of the colonic microflora can explain the high percentage of sulindac sulfide in the faeces [180]. In addition to the behaviour of sulindac in the stomach and small intestine, the hepatic metabolism and biliary excretion are thus key to understand how sulindac and its metabolites may accumulate in the colon.

The aim of the present study was to investigate the colonic disposition of sulindac as to clarify if and how orally administered sulindac can accumulate in the colon to prevent the development of colorectal polyps. To this end, we first evaluated the pH-dependent dissolution behaviour of sulindac in the upper gastrointestinal tract by using a multistage dissolution setup. Secondly, we assessed sulindac and its major metabolites in the systemic circulation, in the colonic lumen and in colonic tissue of human volunteers after intake of a 200 mg sulindac tablet, using a protocol that allowed us to distinguish between plasma- and gut-driven colonic tissue accumulation. Finally, we obtained additional data on the hepatic metabolism and biliary excretion of sulindac and sulindac sulfide in rats to allow an improved insight into the underlying mechanisms of their colonic disposition.

Reference	Compound	Concentration	Model	Effect
Li (2015)	Sulfide	100 µM	RKO and SW480 colon cancer cells	Downregulation of Sp1; includes survivin, bcl-2, EGFR, cyclin D1, P65 subunit of NF-kB and VEGF
Lawson (2000)	Sulfide Sulfone Sulindac	120 µM 600 µM 400 µM	Caco-2 cells transfected with an activated K-ras oncogene	Reduction of colony formation by 50% in parental and K-ras transfected clones
Taylor (2000)	Sulfide Sulfone Sulindac	120 µM 600 µM 400 µM	Caco-2 cells transfected with an activated K-ras oncogene	Sulfoxide inhibited PGE2 production in K-ras-activated cells. Similar effects for sulindac sulfide and sulfone. Sulindac sulfone inhibited COX-2 protein and mRNA
Piazza (1997)	Sulfone Sulindac	250/475/ >10000 µM 380/ >550/>10000 µM	HT-29 cells	Growth inhibition/apoptosis/COX inhibition
Liggett (2014)	Sulfide	30 µM	HCT-116, HT-29, LoVo but not SW480 cells	Down regulation of EpCAM (independent of COX activity)
Liggett (2014)	Sulfide	30 µM	HCT-116 cells	Down regulation of Nesprin-2
Bottone (2003)	Sulfide	10 µM	SW-480 cells	Altered expression of 65 genes
Giuliano (1999)	Sulfide Sulindac	/ /	Human platelets and A549 cells	*Ex vivo*: IC_{50} for sulfoxide (COX-1: 13.85 µM; COX-2: 196 µM) and sulfide (COX-1: 0.017 µM; COX-2: 0.55 µM)
Williams (1999)	Sulfide Sulfone	< 50 µM 50 µM	HCA-7 and HCT-116 cells	Reduction of colony formation by 50%

Table 4.1: Concentrations of sulindac, sulindac sulfide and sulindac sulfone used in *in vitro* experiments to induce anti-carcinogenic effects. Sp1 = specificity protein transcription factor 1 ; bcl-2 = B-cell lymphoma 2 ; EGFR = epidermal growth factor receptor; NF-kB = nuclear factor κB; VEGF = vascular endothelial growth factor; PGE2 = Prostaglandin E2; EpCAM = Epithelial cell adhesion molecule.

4.3 Material and methods

4.3.1 Chemicals

Celecoxib was acquired via TCI Europe N.V. (Zwijndrecht, Belgium), and sulindac was ordered from Sanbio (Uden, Netherlands). Sulindac sulfide and sulindac sulfone were kindly provided by Janssen Pharmaceutica (Beerse, Belgium). Chem-Lab (Zedelgem, Belgium) supplied acetic acid and disodium phosphate, while sodium acetate trihydrate was purchased from VWR (Leuven, Belgium). Acetonitrile (ACN, HPLC grade), ammonium acetate ($CH_3COO{-}NH_4^+$), and NaCl were purchased from Fisher Scientific (Leicestershire, UK). Methanol (MeOH, HPLC grade), glucose, and dimethyl sulfoxide (DMSO) were ordered from Acros Organics (HPLC grade; Geel, Belgium). Purified water for analytical purposes was obtained using a Maxima system (Elga Ltd., High Wycombe Bucks, UK). Hanks' Balanced Salt Solution without phenol red (HBSS) and 4-(2-hydroxyetheyl)-1-piperazineethanesulfonic acid (HEPES) were obtained from Lonza (Verviers, Belgium), while sodium hydroxide (NaOH) pellets were purchased from Merck (Darmstadt, Germany). BHD Laboratory Supplies (Poole, UK) supplied HCl. Fasted State Simulated Intestinal Fluid (FaSSIF)/Fasted Sate Simulated Gastric Fluid (FaSSGF) powder was obtained from Biorelevant (Crydon, UK).

4.3.2 Media

The HBSS+ medium consisted of HBSS buffered with 10 mM HEPES and adjusted to pH 7.4 with 2 M of NaOH.

Fasted state simulated gastric fluid (FaSSGF) was prepared by dissolving 60 mg of SIF powder per liter FaSSGF buffer (NaCl 34 mM, pH 1.6). To simulate the gastrointestinal transfer, 100 mL of FaSSGF was decanted into 100 mL of double concentrated FaSSIF at pH 7.5 (2-fold transfer dilution) to obtain standard concentrations of FaSSIF at pH 6.5 after transfer. One liter of double concentrated FaSSIF was prepared by dissolving 1.12 g NaOH (21 mM), 10.54 g $NaH_2PO_4H_2O$ (56 mM) and 16.5 g NaCl (212 mM) in 0.9 l purified water. Subsequently, 5.98 g SIF powder was added. The pH was adjusted to 7.5 by using 2 M NaOH and, subsequently, the volume was adjusted to 1 L. To simulate transfer to colonic conditions, the pH of the FaSSIF medium was adjusted to pH 6.0 by using 2 M HCl.

4.3.3 Clinical study

4.3.3.1 Study medication

Arthrocine tablets (200 mg sulindac; Laboratoire AJC pharma, Chateauneuf-sur-Charent, France) and Celebrex capsules (200 mg celecoxib; Pfizer, Brussel, Belgium) were ordered via the hospital pharmacy of the University Hospitals Leuven (UZ Leuven, Belgium).

4.3.3.2 Ethics

The collection of human colonic biopsies, colonic contents and plasma followed the tenets of the Declaration of Helsinki and were approved by the Federal Agency for Medicines and Health Products (FAMHP; EudraCT reference study number 2019-001496-36) and the Ethics Committee Research UZ/KU Leuven (reference number S62732). All volunteers provided written informed consent prior to participation. Volunteers with hepatitis B/C and/or HIV infection were excluded to guarantee the safety of the study personnel. Illness at the time of the study, allergy for sulindac or NSAIDs in general, medication use (excluding contraceptives), a history of acute/chronic gastrointestinal disease(s), and a (possible) pregnancy were criteria for exclusion.

4.3.3.3 Colonic disposition of sulindac in human volunteers

Volunteers were asked to follow a three-day low-fibre diet (e.g. white bread or pasta, canned fruit in heavy syrup or juice, no vegetables…) and to eat a last meal at 8 pm on the day before the study. To ensure fasted state conditions, volunteers could only drink water 12 h to 2 h prior to the first colonoscopy. Upon arrival at the endoscopy unit, the volunteers (aged between 20 and 25 years; 3 men and 2 women) were positioned on their left side and an enema (250 mL of tap water) was administered rectally to rinse the left hemicolon while retaining the physiological state of the right hemicolon. A colonoscopy was then performed by a single experienced endoscopist (TV) to obtain two blank biopsies. Next, an Arthrocine tablet (200 mg sulindac) was orally administered with 240 mL of tap water to the volunteers. The colonoscope was left untouched and the light source was turned off to minimize thermal damage. Between 1 and 2.5 h after drug intake, two caecal biopsies were taken every 15 min with a standard biopsy forceps (Radial Jaw™3 with needle; outside diameter 2.2 mm; Boston Scientific). After 2.5 h, colonic contents (± 2 mL) were sampled through the suction channel of the colonoscope.

After retracting the colonoscope, the contents were collected into a falcon tube by pulling a stiff brush through the entirety of the suction channel. The contents were stored on ice, and briefly centrifuged as to allow a reliable pH measurement. Three hours later, and after rinsing the left hemicolon with an enema (250 mL of tap water), the colonoscope was positioned again in order to sample caecal biopsies every 15 min between 6 and 7.5 h after drug intake. After 7.5 h, colonic contents were collected once again, stored on ice, and pH was measured after a brief centrifugation step. During the colonoscopies, volunteers were not sedated, as sedation might influence gastrointestinal motility and thus the pharmacokinetic disposition of sulindac. Venous blood samples were collected on ice in heparinized tubes (BD Vacutainer systems, Plymouth, U.K.) at predetermined time points, i.e. 0, 15, 30, 60, 90, 120, 180, 240, 360, 480, and 1440 min after drug intake. Participants were not allowed to drink or consume food for the first 4 h after drug intake. After 4 h, participants were allowed to drink and/or eat ad libitum.

4.3.3.4 pH

The pH of the samples was measured using a BioTrode instrument (Hamilton, Bonaduz, Switzerland) calibrated prior to use. The pH of buffers and simulated intestinal fluids was measured with a SensION + pH 3 instrument (Hach-Lange GmbH, Düsseldorf, Germany).

4.3.4 Three stage dissolution testing

To assess the dissolution kinetics for Arthrocine and Celebrex as a function of pH, a three-step dissolution experiment was performed. In a first step, either 1 tablet Arthrocine (200 mg sulindac) or 1 capsule Celebrex (200 mg celecoxib) was added to 100 ml of FaSSGF in a beaker. After 30 min, the entire contents of the vessel were transferred to 100 ml of double concentrated FaSSIF (2-fold dilution, final composition: FaSSIF). The initial volume of FaSSGF was chosen as an average gastric fluid volume during the first 30 min after intake of a drug with 240 mL of water, based on the magnetic resonance imaging data of [181]; the 2-fold dilution to simulate the gastrointestinal transfer was in line with a standardized protocol for biorelevant dissolution testing as proposed by the OrBiTo (Oral Biopharmaceutics Tools) project, a public-private partnership that was funded by the European Union [182]. After 210 min, the pH of the medium was changed to pH 6.0 to represent caecal pH values. During the dissolution test, the contents of the vessels were magnetically stirred (300 rpm, 37°C). Samples were taken after 5, 10, 20,

30, 40, 50, 60, 75, 90, 120, 150, 180, 210, 220, 230, 240, and 255 min. The samples were centrifuged immediately, and supernatant was diluted and injected for HPLC analysis.

4.3.5 In situ metabolism and excretion of sulindac in rats

Purpose-bred, male Sprague–Dawley rats (Janvier, Le Genest Saint-Isle, France) were used for *in situ* experiments. The rats were housed according to the Belgian and European laws, guidelines and policies for animal experiments, housing and care in the Central Animal Facilities of the University. Approval for this project was granted by the Institutional Ethics Committee for Animal Experimentation.

Rats of approximately 350 g were anaesthetized using a mixture of ketamine (87.5 mg/kg) and xylazine (0.875 mg/kg). For blood sampling, a cannula was inserted into the right external carotid, secured with a suture and connected to a piece of silastic tubing (o.d. 1.19 mm, i.d. 0.64 mm; Helix Medical, USA). To administer the drug, the right jugular vein was cannulated with a heparinized (50 IU/ml) polyethylene cannula (o.d. 1.02 mm; Portex, Kent, UK). A laparotomy was performed in rats to isolate the bile duct, which was then cut to collect bile throughout the experiment. A bolus of either sulindac or sulindac sulfide (1 mg/kg) dissolved in DMSO (100 µL/kg) was then administered via the right jugular vein. Blood and bile samples were taken every 15 min for a duration of 90 min and 60 min, respectively. Samples were stored at 4°C before analysis of sulindac and metabolites.

4.3.6 Processing of biological samples

Biopsies

Upon sampling, biopsies were rinsed threefold with HBSS+, excess liquid was removed with a paper tissue, and biopsies were stored in 1 mL of methanol. Prior to further processing, samples were stored at 4°C. To quantify drug concentrations in biopsies, 10 µL of DMSO containing an internal standard (10 µM celecoxib) was added. Biopsies were then air dried for 1 h, weighed, placed back into the methanol and homogenized with a TissueLyser II (3 x 4 min, 1/30 s; Qiagen, Hilden, Germany). Subsequently, samples were centrifuged (20817 x g, 1 min, 4°C; Centrifuge 5417R; Eppendorf, Hamburg, Germany) and the supernatant was evaporated under

a continuous air flow before being reconstituted in 335 µL of acetonitrile:ammonium acetate buffer (20:80, v/v).

Colonic contents

Colonic contents were processed on the day of the experiment to determine the total and dissolved concentrations of sulindac and its metabolites. After vortexing (Vortex Genie, Scientific industries, New York, USA) the contents for 1 min, the total drug and metabolite concentrations were measured by directly diluting 10 µL of the colonic contents with 990 µL acetonitrile:ammonium acetate buffer pH 3.8 (20:80, v/v), which was then immediately centrifuged (20817 x g, 5 min; Microcentrifuge 5424, VWR International); the supernatant was collected for liquid chromatography (LC) analysis. The dissolved drug and metabolite concentrations were measured by first centrifuging (20817 x g, 5 min; Microcentrifuge 5424, VWR International) a fraction of the colonic contents after being vortexed for 1 min. Next, 10 µL of the supernatant was diluted in 990 µL acetonitrile:ammonium acetate buffer pH 3.8 (20:80, v/v) and centrifuged (20817 x g, 5 min; Microcentrifuge 5424, VWR International) once more; the supernatant was collected for LC analysis.

Venous blood samples

Immediately after collection, blood samples were stored on ice. At the end of the day of the experiment, samples were centrifuged (human: 1699 x g, 15 min, 4°C; rat: 2000 x g, 5 min, 21°C, Centrifuge 5804R; Eppendorf, Hamburg, Germany) to collect plasma samples, which were stored at -4°C until analysis. To quantify drug and metabolite concentrations in plasma, 10 µL of DMSO containing an internal standard (celecoxib) was added to plasma (1 mL for human plasma, 200 µL for rat plasma). After adding methanol to the plasma in a 4:1 ratio, the mixture was thoroughly vortexed and subsequently shaken manually for 1 min. The samples were then centrifuged (1699 x g, 15 min, 4°C; Centrifuge 5804R; Eppendorf, Hamburg, Germany) and the supernatant was collected for LC analysis.

Bile from rats

Upon collection, the sampled bile was weighed. The sample was then thoroughly vortexed for 1 min, and diluted 10 or 100 times in acetonitrile:ammonium acetate buffer (20:80, v/v), before being injected for LC analysis.

Dissolution samples

Immediately after collection, samples were centrifuged (20817 x g, 5 min; Microcentrifuge 5424, VWR International). For samples containing sulindac, the supernatants were diluted with acetonitrile:ammonium acetate buffer (20:80, v/v) as follows (sampling times: dilution factor): 5 – 30 min: 5; 40 – 50 min: 10; 60 – 255 min: 20. For samples containing celecoxib, the supernatants were diluted with methanol:sodium acetate buffer (55:45, v/v) as follows (sampling times: dilution factor): 5 – 75 min: 5; 90 – 210 min: 10; 220 – 255 min: 20. The diluted samples were then injected for HPLC analysis.

4.3.7 LC analysis

Celecoxib

Samples with celecoxib as test compound were analysed using HPLC with UV detection (252 nm). Separations were performed on a Novapak C18 column under radial compression (4 µm, 8 x 100 mm, Waters, Milford, MA, USA). A 100 µL sample was injected and eluted with a gradient of 25 mM sodium acetate buffer pH 4.5 (solvent A) and methanol (solvent B) at a flow rate of 1.0 mL/min for 18.5 min. The elution gradient was as follows: 0.0 - 1.5 min, 55% A; 2.5 – 7.0 min, 30% A; 8.0 – 13.5 min, 22% A; and 14.5 – 18.5 min, 55% A for reconditioning. Celecoxib eluted at 12.5 min. Linearity for celecoxib was observed in a range from 20 µM to 10 nM. For validation purposes, control samples were prepared containing 10 µM, 1 µM and 100 nM. Concentrations of celecoxib could be precisely (intraday variability RSD $\leq$ 4.04% and interday variability RSD $\leq$ 7.00%) and accurately (range: 89.95 – 99.89%) determined in samples. Chromatograms were integrated with Waters Empower 2 software (Milford, MA, USA).

Sulindac

Samples with sulindac as test compound were analysed using HPLC with UV detection (252 and 340 nm). Separations were performed on a Novapak C18 column under radial compression (4 µm, 8 x 100 mm, Waters, Milford, MA, USA). A 100 µL sample was injected and eluted with a gradient of 25 mM ammonium acetate buffer pH 3.8 (solvent A) and acetonitrile (solvent B) at a flow rate of 1.0 mL/min for 16 min. The elution gradient was as follows: 0.0 - 1.5 min, 80% A; 3.5 – 6.0 min, 38% A; 7.0 – 11.0 min, 15% A; and 13.0 – 16.0 min, 80% A for reconditioning. Sulindac, sulindac sulfone, celecoxib (internal standard), and sulindac sulfide eluted at 7.1 min, 7.8 min, 10.3 min, and 11.2 min, respectively. Linearity was observed in a range from 20 µM to 100 nM for sulindac and metabolites. For validation purposes, control samples were prepared containing 10 µM, 1 µM and 100 nM. Concentrations of sulindac and metabolites could be precisely (intraday variability RSD ≤ 6.29% and interday variability RSD ≤ 12.54%) and accurately (range: 86.76 – 96.54%) determined in samples. Chromatograms were integrated with Waters Empower 2 software (Milford, MA, USA).

4.3.8 Data presentation

This mechanistic study was designed as exploratory, i.e. without the intention to formally test hypotheses. As such, the data obtained are descriptive in nature and do not allow statistical comparison.

Plasma concentrations are represented as the amount of sulindac or metabolite per volume of plasma (µg/mL). Concentrations in colonic contents are represented as amount of sulindac or metabolite per volume of colonic content (µg/mL). The accumulation in colonic biopsies was normalized for the weight of the tissue and represented as the amount of sulindac or metabolite per amount of tissue (ng/mg).

The results of the *in vitro* dissolution experiments are expressed as the percentage dissolved drug compared to the total dose (%).

Data are presented as mean + SD, unless stated otherwise.

4.4 Results and discussion

Following oral intake of immediate release dosage forms, the NSAIDs celecoxib and sulindac need to reach sufficiently high concentrations in colonic tissue to exert an anti-carcinogenic effect. We recently reported that a substantial undissolved fraction of celecoxib can reach the colon by transit, exposing the colonic tissue to considerably higher local drug levels than can be achieved by purely systemically driven accumulation [183]. While the poor solubility of celecoxib along the entire length of the gastrointestinal tract can explain its incomplete absorption from the small intestine, the solubility of the weakly acidic sulindac (pKa 4.09, ChemAxon) is pH dependent and substantially higher in the intestinal region. Prior to evaluating the colonic disposition of sulindac and its metabolites, we therefore determined the pH dependent dissolution of sulindac in comparison to celecoxib.

4.4.1 Dissolution of sulindac in a three stage set-up

A three-step dissolution experiment was performed to compare the pH dependent dissolution kinetics for Arthrocine (200 mg sulindac, tablet) and Celebrex (200 mg celecoxib, capsule). The set-up included a gastric, small intestinal, and colonic step, represented by 100 mL FaSSGF, 200 mL FaSSIF pH 6.5, and 200 mL FaSSIF pH 6.0 and residence times of 30 min, 210 min, and 45 min, respectively.

The percentage dissolution of sulindac and celecoxib as a function of time is depicted in figure 4.1. When 1 Arthrocine tablet or 1 Celebrex capsule was exposed to gastric conditions, drug release from both formulations was negligible. Upon decanting the vessel into 100 mL double concentrated FaSSIF, the dissolution rate of both celecoxib and sulindac increased. Though incomplete for both, the extent of dissolution was much higher for sulindac: after 210 min, 75% of sulindac was dissolved as compared to only 3% of celecoxib (Fig. 4.1). Adapting to a slightly lower colonic pH did not change the percentage of drug in solution.

Although both compounds are weak acids, celecoxib has a pKa value of 11.0 [149] which translates to a net-zero charge over the entire physiological pH range. In contrast, sulindac has a pKa of 4.09 [184], and will be largely negatively charged in the intestinal medium. While the slightly improved dissolution of celecoxib in FaSSIF compared to FaSSGF is probably only

linked to the presence of solubilizing micelles, the much faster dissolution of sulindac in intestinal conditions can be explained by its altered ionisation state and, consequently, increased solubility. Considering that sulindac is a moderate to high permeability drug [151], this dissolution experiment hints at a higher uptake of sulindac from the small intestine in comparison to celecoxib. As such, it seems less evident that a substantial amount of sulindac reaches the colon by transit to allow a gut driven accumulation into colonic tissue, as was observed for celecoxib.

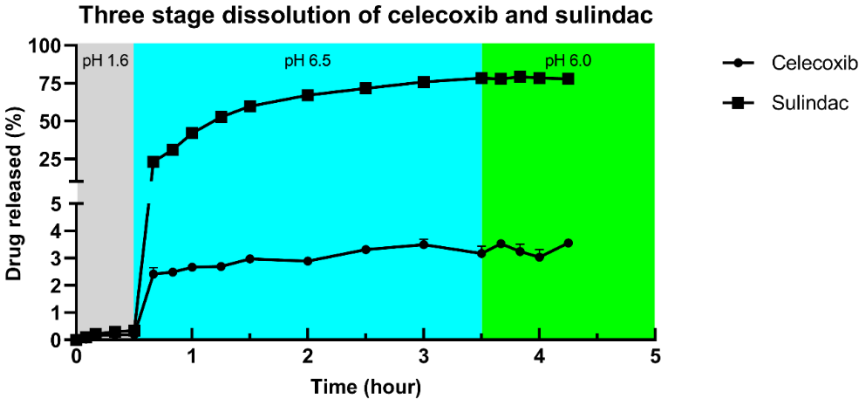

Fig. 4.1: Three-stage dissolution profiles of (●) Celebrex (capsule, 200 mg celecoxib) and (■) Arthrocine (tablet, 200 mg sulindac) in FaSSGF pH 1.6 (100 ml) (gastric conditions, grey area), FaSSIF pH 6.5 (200 mL) (small intestinal conditions, blue area), and FaSSIF pH 6.0 (200 mL) (caecal conditions, green area) for 30 min, 180 min, and 45 min, respectively (mean + S.D., n = 3).

4.4.2 Time-dependent systemic and caecal disposition of sulindac

To shed light on the disposition of sulindac and its metabolites in the human colon, we monitored their concentrations in the systemic circulation, the caecal lumen and caecal tissue following oral intake of an Arthrocine tablet (200 mg sulindac). To distinguish between plasma and possibly gut driven caecal tissue accumulation, the study involved two colonoscopies. One hour after drug intake, biopsies were taken from the caecum every 15 min for 90 min, after which caecal contents were aspirated (first colonoscopy, phase 1). Based on the systemic concentration-time profile of sulindac reported by the group of Reid (T_{max} of 2.5 h ± 1.4 h in

fasted human volunteers after oral intake of a 150 mg tablet) [185], plasma levels were expected to increase in this first phase (between 1 and 2.5 h post drug intake) and drive drug accumulation in the caecal tissue. Six hours after drug intake, caecal biopsies were collected again every 15 min for 90 min, after which caecal contents were aspirated (second colonoscopy, phase 2). In this second phase (between 6 and 7.5 h post drug intake), plasma levels of sulindac were expected to decrease. Tissue concentrations during the second phase of the experiment could be plasma driven (in which case they would decrease as well), but could also be gut driven if a sufficient amount of sulindac arrived at the caecal lumen through intestinal transit; an intermediate scenario might occur as well.

The study setup was designed for the systemic T_{max} to drop in-between the two colonoscopy phases, as to distinguish plasma- from gut-driven tissue accumulation. However, we observed substantial variation in the systemic T_{max}: for 3 out of 5 volunteers, a T_{max} higher than 4 h was observed (4.67 ± 0.58 h), while the two remaining volunteers had a relative early T_{max} of 2.0 h. This variability is likely linked to differences in gastric emptying, since our *in vitro* transfer experiment (Fig. 4.1) suggests that transfer to intestinal conditions is needed to substantially improve the dissolution of sulindac. A longer gastric residence will thus be associated with a delayed onset of absorption and late systemic T_{max}. Various factors can impact gastric emptying, and we assume that the colonoscopy and its effect on gastric motility can explain most of the variability. Indeed, a delayed gastric emptying can be caused by rectal/colonic distention by CO_2 insufflation during a colonoscopy, affecting systemic T_{max} [163]. This was also assumed to be the underlying cause for the delayed systemic absorption of celecoxib, using the same study setup [183]. Additionally, volunteers may experience higher stress levels during the colonoscopy, which is known to modulate gastrointestinal motility [164,165]. Another factor that influences systemic absorption is the time of tablet intake relative to the occurrence of gastric contractions [186]. When strong and frequent gastric contractions (migrating motor complex phase 3) onset shortly after the formulation reaches the stomach, sulindac might quickly transfer to the small intestine where a better dissolution and subsequently absorption is enabled (Fig. 4.1). As the variability in systemic T_{max} of sulindac implies a different gastrointestinal behaviour and interpretation of the results, we discuss the obtained data in two groups: (1) volunteers in which a delayed plasma T_{max} was observed, and (2) volunteers in which an early T_{max} was observed. The intestinal concentrations (biopsies) are grouped

accordingly (Fig. 4.2 and 4.4), as individual profiles were mostly similar within each group. If not, the individual differences are clarified, and discussed in accordance with the luminal concentrations (Fig. 4.3 and 4.5).

Group 1 – Delayed plasma T_{max} (n = 3)

The mean caecal tissue concentrations of sulindac and its main metabolite sulindac sulfide during two colonoscopies (phase 1 and phase 2) are compared with the systemic concentration-time profiles in Figure 4.2. Luminal concentrations observed at the end of phase 1 and phase 2 are depicted in Figure 4.3. As expected, the plasma concentrations of sulindac increased during phase 1 but caecal tissue concentrations remained relatively low (Fig. 4.2a). For two healthy volunteers (HV1 and HV3), we could not detect any sulindac or metabolites in the luminal contents that were collected 2.5 h after drug intake (Fig. 4.3a), which is in line with reported median gastric and small intestinal transit times of 56 and 255 min, respectively [166]. Therefore, initial drug accumulation in the tissue seems to be plasma driven during phase 1. However, in the luminal aspirations of one volunteer (HV2), we were able to detect a limited amount of sulindac 2.5 h after drug intake, which suggests that a fraction of the drug underwent a fast transit. This coincided with a 10.7-fold increase in drug accumulation in the biopsies that were taken at the same time (2.5 h) relative to the biopsies taken 15 min earlier (individual data not shown). This seems to indicate that, if sulindac is present in the caecal lumen, gut-driven uptake may substantially increase its accumulation in tissue.

During phase 2 of the experiment, tissue concentrations of sulindac were substantially higher than in phase 1, despite similar plasma concentrations in both phases (Fig. 4.2a). For instance, at 6.75 h after drug intake (phase 2), tissue concentrations of sulindac were 29.1-fold higher than after 1.75 h (phase 1). The increased tissue concentrations observed in phase 2 may be the result of gut-driven uptake, as relatively high levels of sulindac were observed in the caecal contents after 7.5 h (Fig. 4.3b). An exception are the luminal and tissue concentrations of HV3, which were low at the end of phase 2. It is remarkable that tissue accumulation in HV3 decreased gradually, yet substantially, during phase 2 and accumulated drug concentrations at the end of the experiment (7.5 h after intake) were 20-fold lower relative to the biopsies taken 90 minutes earlier (individual data not shown). Again, this specific observation seems to

confirm the link between the presence of sulindac in the caecal lumen and the extent of accumulation in caecal tissue.

In phase 2, the metabolite sulindac sulfide, which could not be detected in either plasma, lumen, or tissue during phase 1, reached similar tissue concentrations to those found for sulindac (Fig. 4.2b). As luminal concentrations of sulindac sulfide were relatively high in phase 2 (Fig. 4.3b), direct uptake from the gut may have contributed to the accumulation in the caecal tissue.

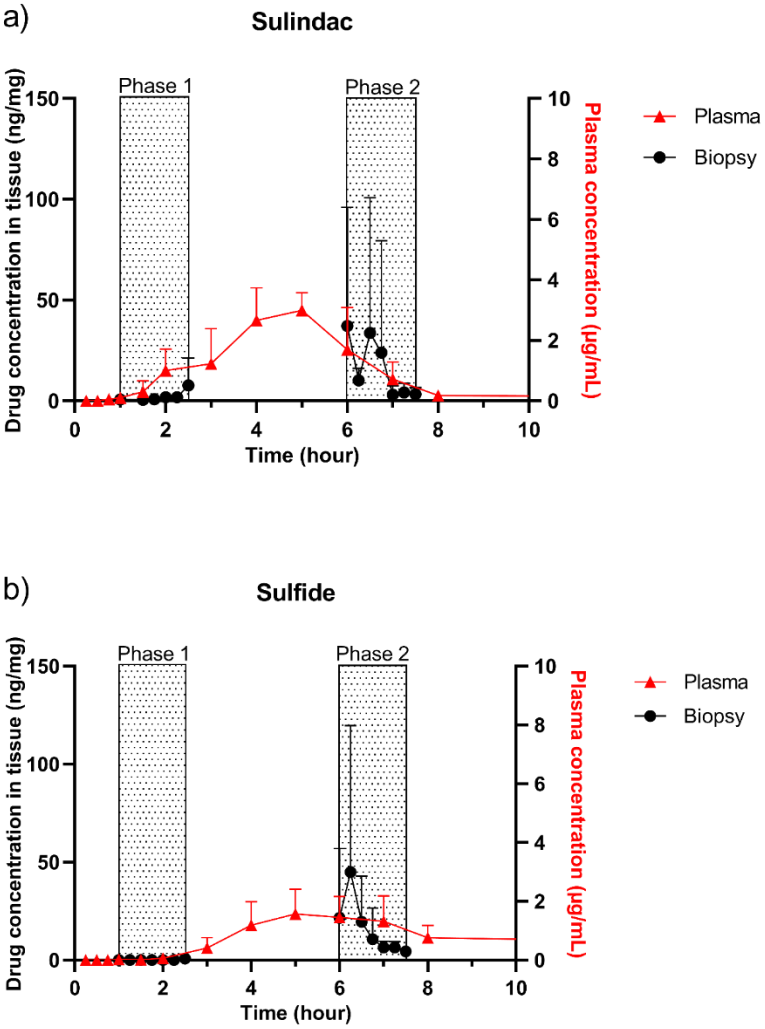

Fig. 4.2: Mean (+ SD) concentration – time profiles of sulindac (a) and sulindac sulfide (b) in plasma samples (▲) and caecal biopsies (●), collected from healthy volunteers (HV1, HV2 and HV3) with a delayed Tmax after oral intake of one tablet of Arthrocine (200 mg sulinac) with 240 mL of water under fasted conditions.

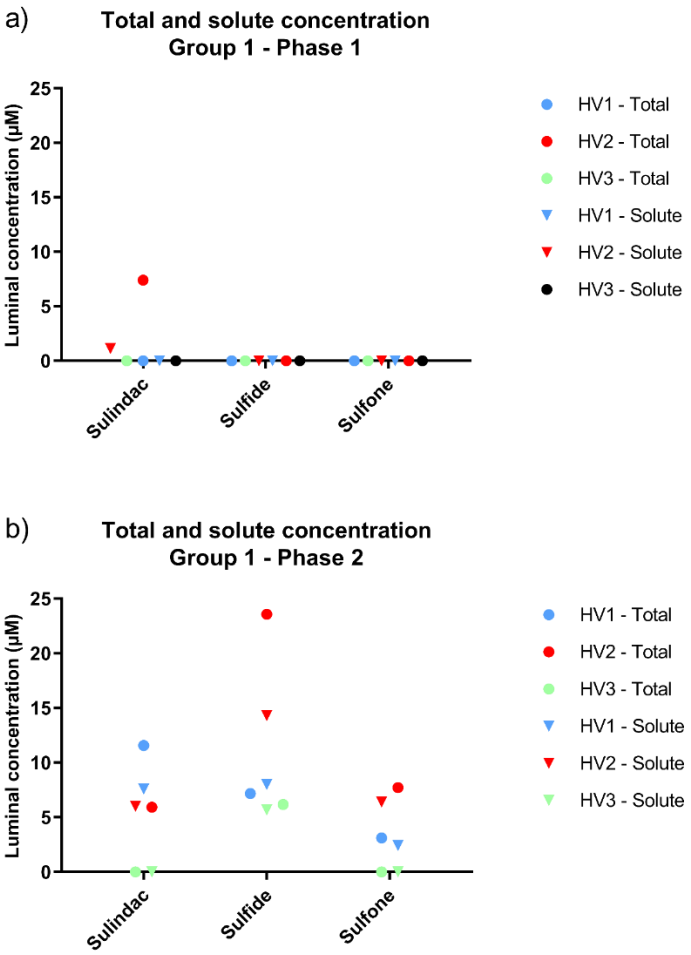

Fig. 4.3: Total and dissolved concentration of sulindac, sulindac sulfide, and sulindac sulfone in colonic contents sampled from healthy volunteers with a delayed Tmax (HV1, HV2 and HV3) 2.5 h (phase 1, a) and 7.5 h (phase 2, b) after oral intake of one tablet of Arthrocine (200 mg sulindac) with 240 mL of water under fasted conditions

Group 2: early plasma T_{max} (n = 2)

In two volunteers (HV4 and HV5), we observed an early plasma T_{max} for sulindac (Fig. 4.4a), 2 h after drug intake, likely resulting from a faster gastric emptying, as discussed above. Despite that the systemic profiles for sulindac were similar in the two volunteers (high and increasing concentrations in phase 1, low and decreasing concentrations in phase 2), the luminal (Fig. 4.5) and tissue accumulation profiles were not. For HV4, we observed high concentrations of sulindac in the caecal tissues and luminal aspirations of phase 1 but not phase 2, while the opposite was true for HV5. High tissue concentrations of sulindac thus seem to occur concomitantly with high luminal concentrations, independent of the systemic profile. The large variability in orocaecal and proximal colonic transit times likely underlie the differing luminal profiles. The group of Vertzoni et al. (2019) described for example how proximal colonic transit times are considerably longer and more variable compared to the small intestine; a mean value of 11 h with a standard deviation of 4 h has been reported [187]. In the case of HV5, a fraction of sulindac might have reached the caecum shortly after the end of phase 1 (absence of sulindac in phase 1), and resided there for an extended time period (presence of sulindac in phase 2), driving tissue accumulation. For HV4, the fraction of sulindac that reached the caecum (presence of sulindac in phase 1) might have undergone a relatively fast caecal transit (absence of sulindac in phase 2).

The luminal (Fig. 4.5) and tissue accumulation (Fig. 4.4b) profiles of the metabolites were similar for both volunteers (HV4 and HV5). In phase 1, concentrations were low or undetectable while systemic concentrations increased. During phase 2, concentrations were relatively higher despite decreasing systemic concentrations. To understand and clarify how sulindac and metabolites arrive at the caecal lumen, we performed *in situ* experiments in rats.

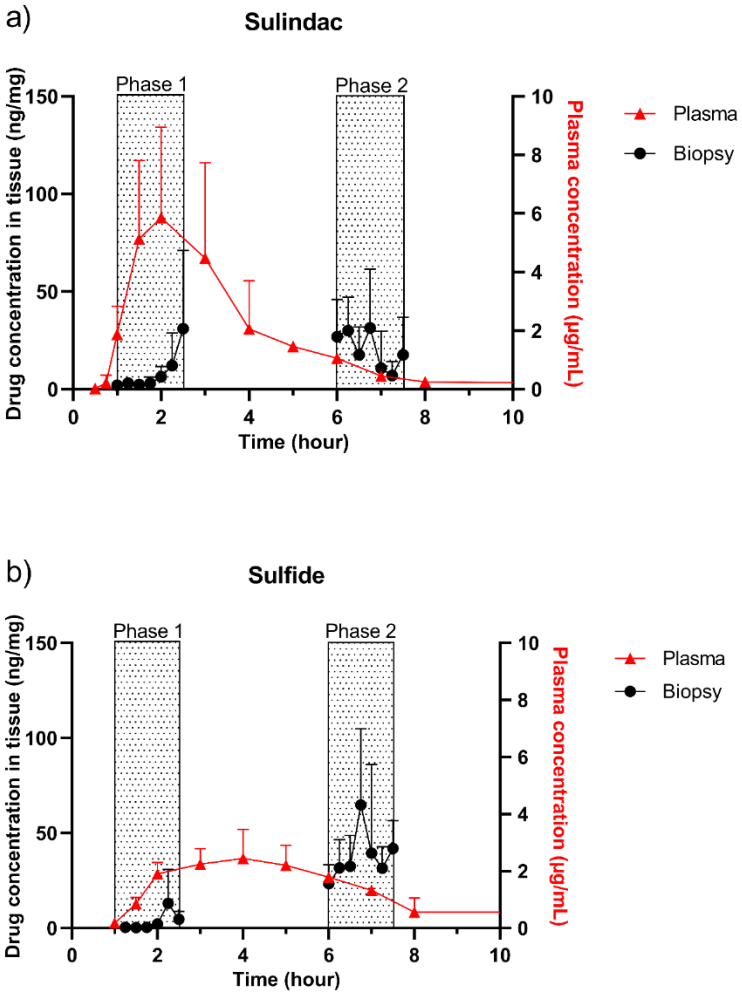

Fig. 4.4: Mean (+ SD) concentration – time profiles of sulindac (a) and sulindac sulfide (b) in plasma samples (▲) and caecal biopsies (●), collected from healthy volunteers with an early Tmax (HV4 and HV5) after oral intake of one tablet of Arthrocine (200 mg sulinac) with 240 mL of water under fasted conditions.

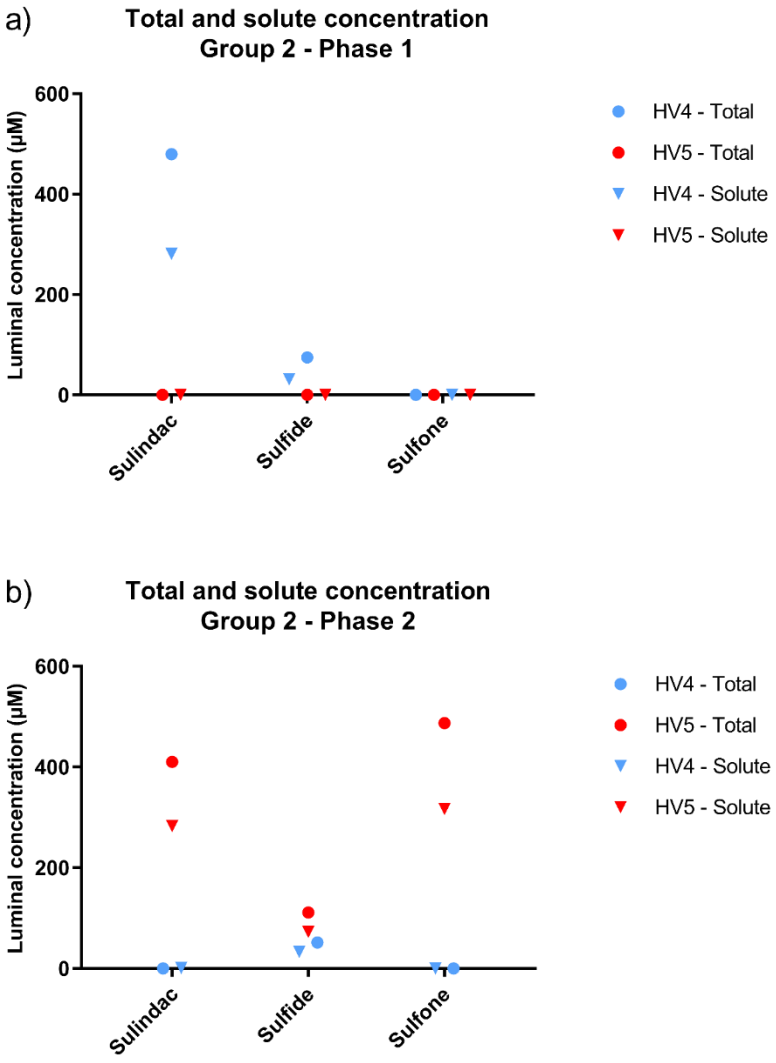

Fig. 4.5: Total and dissolved concentration of sulindac, sulindac sulfide, and sulindac sulfone in colonic contents sampled from healthy volunteers (HV4 and HV5) 2.5 h (phase 1, a) and 7.5 h (phase 2, b) after oral intake of one tablet of Arthrocine (200 mg sulindac) with 240 mL of water under fasted conditions.

4.4.3 Intestinal disposition of sulindac and metabolites in rats

The caecal contents from healthy volunteers aspirated during phase 1 predominantly contained sulindac (Fig. 4.3a and 4.5a), while phase 2 contents consisted mostly of metabolites (Fig. 4.3b and 4.5b). To clarify the origin of sulindac and metabolites in the caecal contents, we performed *in situ* rat experiments in which the metabolism and biliary excretion of said compounds was studied. Hereto, a bolus of 1 mg/kg of sulindac or sulindac sulfide was given intravenously to rats, after which bile was continuously collected over 15-minute intervals for a duration of 60 minutes; systemic blood samples were taken every 15 minutes.

One hour after the intravenous administration of sulindac, both sulindac (relative fraction of 0.89) and its active metabolite sulindac sulfide (0.11) were present in the systemic circulation (Fig. 4.6a). Also following intravenous administration of sulindac sulfide, both sulindac (relative fraction of 0.29) and sulindac sulfide (0.71) were present in the systemic circulation (Fig. 4.6b), confirming that the conversion between sulindac and sulindac sulfide is a reversible metabolic process [188]. This reductive metabolism process can occur in hepatic microsomes [189], since the liver is one of three major bioactivation sites; the kidney and gut microbiota being the other two. Sulindac sulfone concentrations were mostly undetectable, indicating that it is only a minor systemic metabolite.

In situ rat experiments also showed that biliary excretion of the sulfide metabolite was non-existent or limited (fraction of 0.025) after *intravenous* injection of a bolus of sulindac or sulindac sulfide (Fig. 4.7), respectively. This suggests that predominantly sulindac, and not the metabolites, can reach the caecum via the transit.

4.4.4 Mechanistic insights into the caecal disposition of sulindac and metabolites

The fraction of sulindac that reaches the caecum of healthy volunteers following oral administration (Fig. 4.3 and 4.5) likely results from (i) incomplete small intestinal dissolution (Fig. 4.1; 75%) in combination with a moderate permeability [151] and (ii) biliary excretion (Fig. 4.7). The different origin of sulindac and metabolites was reflected in the clinical study: when sulindac was already detected in caecal contents (Fig. 4.3a and 4.5a) or tissue (Fig. 4.2a and 4.4a) collected in phase 1 (i.e. after 2.5 h, HV2 and HV4), no or only minimal metabolite

concentrations were measured. Remarkably, the fraction of metabolites in phase 2 aspirations (i.e., after 7.5 h) (Fig. 4.3b and 4.5b) and tissue (Fig. 4.2b and 4.4b) was higher or comparable to the fraction of the parent compound. This shift in drug composition over time is most likely caused by colonic microbial metabolism that gradually converts sulindac into sulindac sulfide by sulfoxide reduction of the thioethers [180]. Sulindac can also be irreversibly oxidized to the sulfone metabolite [190], but it has not been reported whether this occurs by microbial biotransformation. Moreover, analysis of human faecal samples by the group of Duggan showed that sulindac only makes up 5% of the total dose in faeces [152]. These results suggest that the fraction of sulindac sulfide depends on the colonic residence time in the presence of microflora.

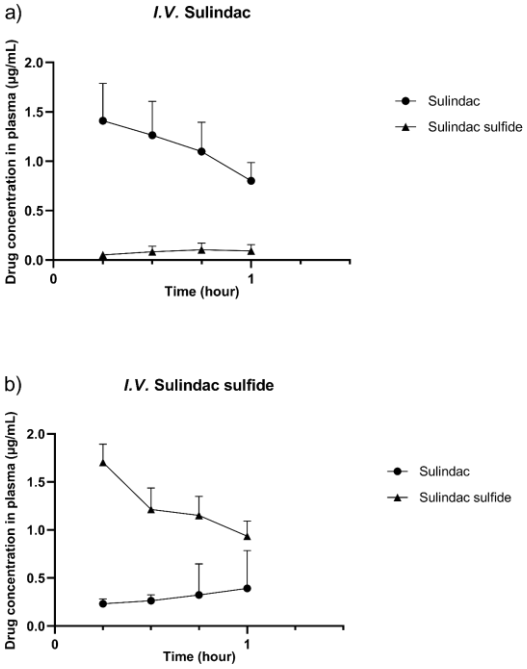

Fig. 4.6: Drug concentration of sulindac and sulindac sulfide in plasma after administering an intravenous bolus of 1mg/kg sulindac (a) or sulindac sulfide (b) in rats. Values represent mean + SD (n = 3).

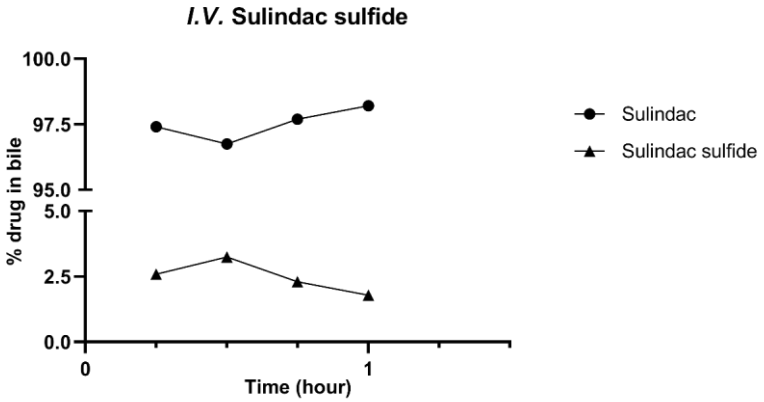

Fig. 4.7: Relative amount of sulindac and sulindac sulfide recovered in bile after administering an intravenous bolus of 1mg/kg of sulindac sulfide in rats. Values represent mean + SD (n = 3).

The analysis of the luminal aspirates collected from the caecum of the healthy volunteers further illustrated that sulindac and its metabolites were not always fully dissolved (Fig. 4.3 and 4.5). The solid fractions of sulindac, sulindac sulfide, and sulindac sulfone ranged between 0% - 84.64%, 0% – 57.83%, and 17.06% - 34.96%, respectively. The presence of undissolved and/or precipitated drug is remarkable considering that sulindac, sulindac sulfide and sulindac sulfone are all weak acids (pKa 4.09, 4.25, 3.97, respectively) that are in a predominantly ionized state in the colonic lumen (pH 6.44 ± 0.59). The presence of solid material most likely illustrates that colonic conditions, including the limited volume of colonic fluids in scarce and scattered pockets (median 2 mL) [50] and their relatively high viscosity are not ideal to keep drugs and metabolites in solution, which may affect the subsequent absorption.

To clarify how solubility affects colonic disposition, we made a comparative analysis between the *in vivo* studies for sulindac and celecoxib. We observed that celecoxib, which is characterised as lipophilic and poorly soluble throughout the gastrointestinal tract, reached about 75-fold higher total concentrations in the caecal lumen than sulindac. This is in agreement with our *in vitro* transfer experiment, which already hinted at a more complete uptake of sulindac from the small intestine (Fig. 4.1). Though a relatively smaller amount of sulindac reaches the colon, it is necessary to also account for the mean solid fractions in the caecum.

Celecoxib has a mean solid fraction of 0.91 ± 0.09 [183], which is about 3-fold higher than the solid fraction observed for sulindac. This implies that while low intestinal solubility enables a larger fraction of the compound to reach the caecum, it also hampers colonic dissolution and, consequently, absorption.

When considering therapeutic efficiency, concentrations of sulindac or metabolites in *in vitro* models ranged between 10 µM and 600 µM [171,172,175–177] to induce anti-carcinogenic effects through non-COX targets. Such concentrations cannot be reached in the systemic circulation after oral intake of a 200 mg immediate release formulation, but are likely to be present in colonic fluids, driving colonic accumulation. However, upon arrival of an undissolved fraction of sulindac to the colon, a time window has to be taken into account for microbial formation of sulindac sulfide. Furthermore, more distal contents will likely contain a higher fraction of sulindac sulfide, although it should be noted that the water content decreases along the colon, which hinders drug dissolution and uptake.

4.5 Conclusion

This study showed that sulindac, a compound with a higher intestinal solubility in comparison to celecoxib, can arrive at the colon several hours after intake, due to incomplete absorption and biliary excretion. Upon reaching the colon, the microbiota catalyses the production of the active sulindac sulfide, which then accumulates in a sufficiently high and local manner in colonic tissue. Compared to systemic exposure, the gut-driven accumulated fraction of sulindac and its metabolites in colonic tissue is high and most likely improves its inhibitory effect on the progression of colorectal polyps and cancer. As such, these data demonstrate how a drug without a colon-targeted delivery strategy can achieve sufficient concentrations in colonic tissue which is relevant for future drug development in the prevention of colorectal adenomas and cancer.

4.6 Acknowledgements

This work has received support from Flanders Innovation & Entrepreneurship (Vlaio) (Grant No. 155042) and KU Leuven Internal Funds (C24/17/076). We would like to thank Raf Mols

for performing the *in situ* rat experiments, and Lucas Wauters for assisting with the colonoscopies. The authors have no conflicts of interest to declare.

CHAPTER 5 – In vitro accumulation assays

In vitro assessment of colonic accumulation of NSAIDs used to treat colon cancer

Glenn Lemmens, Joachim Brouwers, Jan Snoeys, Ricard Farré, Patrick Augustijns, and Tim Vanuytsel

Pharmaceutics. 2021 – in preparation

5.1 Abstract

We recently reported that the anti-carcinogenic effect of celecoxib and sulindac is likely enabled by gut-driven uptake following transit of a substantial fraction of the drugs to the colon, emphasising the importance of evaluating the absorption and accumulation of such drugs in the colon. This is specifically crucial for colon-targeted drugs since they often aim to directly target the epithelium or immune cells of the lamina propria and are less desired to enter the blood stream. However, *in vitro* systems that address the accumulation behaviour are scarce, and mostly focus on stability and permeability assessment. In the present study, we made a comparative analysis of the accumulation behaviour of celecoxib and sulindac in two relevant non-clinical absorption models such as the Caco-2 cell line or the Ussing chambers setup with intestinal tissue. We observed more extensive accumulation of celecoxib compared to sulindac in both models, which can be attributed to their distinct physicochemical properties (ionisation state, lipophilicity). Higher accumulation was consistently found in human tissue for both compounds which is likely due to the different physiology of the epithelial layer; i.e. the larger absorptive area of human tissue over Caco-2, and the thicker mucus layer of human tissue that can serve as a depot for sustained drug release. Moreover, we simulated more relevant colonic incubation conditions, i.e. use of suspensions instead of solutions, which seemed to better capture the *in vivo* accumulation behaviour. Overall, this exploratory study can contribute to a better prediction of the potential of drugs and drug candidates to accumulate in colonic tissue and exert a local effect.

5.2 Introduction

The increasing prevalence in colorectal cancer on a global scale [157] inquires a deep understanding of the colonic disposition of non-steroidal anti-inflammatory drugs (NSAIDs) such as sulindac (SUL) and celecoxib (CXB) that can treat and/or prevent precursor lesions of colorectal cancer (i.e. polyps) [2,3]. In recent clinical studies with healthy volunteers, we uncovered that upon oral intake of Celebrex (celecoxib, 200 mg) or Arthrocine (sulindac, 200 mg), drug concentrations in colonic tissue are initially plasma driven, but that the anti-carcinogenic effect is likely enabled by gut-driven uptake following transit of a substantial fraction of the drugs to the colon [183,191]. The lipophilic (logP = 2.92) and weakly acidic (pKa 4.09) prodrug sulindac is characterized by a moderate intestinal solubility and permeability. Mechanistic studies clarified that incomplete absorption in the small intestine, due to high biliary clearance and incomplete dissolution, underlies its transfer to the colon. Microbiota then biotransform the prodrug into the active sulindac sulfide, which subsequently accumulates in a sufficiently high and local manner in colonic tissue. Celecoxib is a lipophilic (LogP = 4.01) drug, non-ionized across the entire physiological pH range (acidic pKa = 10.6) [192], and characterized by a high intestinal permeability [150] but low solubility [191]. Paulson et al. showed that increasing the oral dose in rats resulted in a higher recovery of celecoxib in faeces, while only 2% of the parent compound was recovered in urine and faeces upon intravenous administration [161]. This indicates that poor solubility and dissolution is a major determinant for the high undissolved caecal fraction, observed in healthy volunteers. In contrast to sulindac, however, the extent to which biliary excretions, enterocytic metabolism or extensive plasma driven colonic secretions affect the caecal concentrations of celecoxib and its metabolites has not been thoroughly examined.

The fact that substantial amounts of the NSAIDs celecoxib and sulindac can reach the colon, even without being dosed as a colon-targeted formulation, highlights the importance of evaluating the absorption and accumulation of such drugs in the colon. A study by Tannergren comprehensively reviewed human colonic absorption by analysing a large dataset of 42 drugs. They reported that most BCS I drugs (high solubility and high permeability) were well absorbed at the colon, implying sufficient dissolution and uptake. However, several BCS II drugs (low solubility and high permeability) had a lower systemic bioavailability after colonic compared to oral dosing (F_{rel} colon: $AUC_{colon,\ local\ solution}/AUC_{reference,\ oral\ administration}$), even though they were administered as a solution [52]. This suggests that the restricted colonic fluid volume can result

in precipitation. Furthermore, colonic administration of dexloxiglumide (BCS II) as a suspension resulted in a delayed maximum plasma concentration (increase in Tmax) compared to administration of a solution, suggesting the impact of non-optimal dissolution in the colonic environment [52]. In the above-mentioned clinical studies with celecoxib and sulindac, the solid drug fraction in aspirated colonic fluids indeed appeared about 3-fold higher for the poorly soluble celecoxib than for the better soluble sulindac. However, celecoxib reached substantially higher gut-driven tissue concentrations [183,191]. This emphasises the importance of evaluating the accumulation in colonic tissue, taking into account the drug's physicochemical properties and the physiological conditions in the colon. To predict the potential of drugs and drug candidates to accumulate in colonic tissue and exert a local effect, relevant non-clinical absorption models are needed, such as the Caco-2 cell line or the Ussing chambers setup with intestinal tissue biopsies.

The Caco-2 cell line and the Ussing chamber technique are routinely used as in vitro permeation screening tools, correlating well with the fraction absorbed (Fa) in humans at a small intestinal level [89,90,103,109,112,156], but also at a colonic level [52,108]. However, these systems can also provide much needed insight into the accumulation of drugs, in particular colon-targeting drugs that exert their therapeutic effect in a local manner. Moreover, several research groups have indicated that factoring in the accumulated drug fraction into the conventional apparent permeability, which can contribute to absorption later, also improves the prediction of the human fraction absorbed [103,112].

In summary, this study aimed to clarify the intestinal behaviour of NSAIDs, as to better understand their appearance in the caecum (celecoxib and carboxy celecoxib) and their accumulation in caecal tissue (celecoxib and sulindac and metabolites). Since accumulation behaviour is not routinely assessed, and no standardized protocols exist, we developed a protocol to assess drug accumulation in Caco-2 cells and human colonic tissue under relevant colonic conditions, and made a comparative analysis. Moreover, as several research groups have shown that lipophilic drugs are associated with slower diffusion through mucus [36,38], we also differentiated between mucus and tissue accumulation in human biopsies.

5.3 Materials and methods

5.3.1 Chemicals

Celecoxib was acquired via TCI Europe N.V. (Zwijndrecht, Belgium), and sulindac was ordered from Sanbio (Uden, Netherlands). Hydroxy celecoxib and carboxy celecoxib were provided to us by Toronto Research Chemicals (Toronto, Canada). Sulindac sulfide and sulindac sulfone was kindly provided to us by Janssen Pharmaceutica (Beerse, Belgium). Propyl-p-hydroxybenzoate was provided by Sigma-Aldrich (St. Louis, Missouri, USA). Chem-Lab (Zedelgem, Belgium) supplied acetic acid. Sodium acetate trihydrate was purchased from VWR (Leuven, Belgium). Sodium hydroxide (NaOH) pellets were purchased from Merck (Darmstadt, Germany). Methanol (HPLC grade), glucose and type III porcine mucin were ordered from Acros Organics (HPLC grade; Geel, Belgium). Fasted State Simulated Colonic Fluid (FaSSCoF) powder was obtained from Biorelevant (Croydon, UK). Purified water for analytical purposes was obtained using a Maxima system (Elga Ltd., High Wycombe Bucks, UK). Acetonitrile (ACN) and ammonium acetate were supplied by Fisher Scientific (Leicestershire, UK). Hanks' Balanced Salt Solution without phenol red (HBSS), Dulbecco's Modified Eagle's Medium (DMEM), 4-(2-hydroxyetheyl)-1-piperazineethanesulfonic acid (HEPES), 10.000 IU/mL penicillin, 10.000 mg/mL streptomycin, nonessential amino acid medium (NEAA), trypsin ethylenediaminetetraacetic acid (EDTA) and fetal bovine serum (FBS) were obtained from Lonza (Verviers, Belgium). D-a-tocopheryl polyethylene glycol 1000 succinate (TPGS) was supplied by Eastman Chemical Company (Kingsport, TN).

5.3.2 Media

$HBSS^+$ was prepared by dissolving 25 mM glucose in 500 mL HBSS, buffered with 10 mM HEPES and adjusted to pH 7.4 with 2 M of NaOH. 0.2% TPGS was added to this buffer solution if required for the experimental set-up.

Caco-2 cell culture medium consisted of DMEM supplemented with 10% FBS, 1% nonessential amino acids, 100 IU/mL penicillin and 100 mg/mL streptomycin ($DMEM^+$). A mucus layer, serving as a protective layer for the cells during transport/accumulation studies, consisted of type III mucin derived from porcine stomach dissolved in $HBSS^+$ (50 mg/ml) and adjusted to pH 6.5.

Fasted state simulated colonic fluid (FaSSCoF) is prepared according to standardized protocols supplied by Biorelevant. To prepare FaSSCoF, FaSSCoF powder (0.333 mg/mL) was added to blank FaSSCoF (4.8 mg/mL NaOH, 8.8 mg/mL $C_4H_4O_4$ adjusted to pH 7.8 with 2M NaOH in purified water) and left to equilibrate for 1 hour before usage.

Krebs Ringer buffer consists of 7.05 mg/mL NaCl, 1.2 mg/mL $NaHCO_3$, 2.08 mg/mL glucose, 3.32 mg/mL $NaH_2PO_4.H_2O$, 7.36 mg/mL $CaCl_2.2H_2O$, 8.8 mg/mL KCl and 4.88 mg/mL $MgCl_2.6H_2O$ in purified water. 2.08 mg/mL glucose or mannitol was added, and 0.2% TPGS was added to this buffer solution if required for the experimental set-up.

5.3.3 In situ metabolism and excretion of celecoxib and carboxy celecoxib in rat

5.3.3.1 Biotransformation of celecoxib in the gut

Rats of approximately 350 g were anaesthetized using a mixture of ketamine (87.5 mg/kg) and xylazine (0.875 mg/kg). A laparotomy was performed and a distal segment of the small intestine was isolated by inserting two glass cannulas (o.d. 4 mm, i.d. 3 mm) at the proximal and distal end of the segment. Polyethylene tubing was connected to the inlet cannula and a perfusion pump (Minipuls3, Gilson, Middleton, USA) was placed between the perfusate reservoir and the inlet cannula. After removal of the intestinal contents, the intestinal segment was pre-incubated with FaSSIF for 10 min at a perfusion flow rate of 1 mL/min before being turned into a closed loop set-up with a total volume of 10 mL FaSSIF containing celecoxib 100 µM. Perfusate samples (100 µL) were taken every 15 min for a duration of 90 min. Samples were stored at 4°C before analysis of celecoxib and metabolites.

5.3.3.2 Metabolization and excretion of celecoxib and carboxy celecoxib

A laparotomy was performed in rats to install a closed-loop set up identical to 5.3.3.1. For blood sampling, a cannula was inserted into the right external carotid, secured with a knot and connected to a piece of silastic tubing (o.d. 1.19 mm, i.d. 0.64 mm; Helix Medical, USA). To administer the drug, the right jugular vein was cannulated with a heparinized (50 IU/mL) polyethylene cannula (o.d. 1.02 mm; Portex, Kent, UK). Additionally, the bile duct was isolated and cut to collect bile throughout the experiment.

After removal of the intestinal contents, the intestinal segment was pre-incubated with FaSSIF for 10 min at a perfusion flow rate of 1 mL/min before being turned into a closed loop set-up with a total volume of 10 mL FaSSIF. A bolus of celecoxib (1 mg/kg) dissolved in DMSO (100 µL/kg) was then administered and blood and perfusate samples were taken every 15 min for a duration of 90 min. Bile was continuously collected throughout the experiment; every 15 minutes the Eppendorf tube was replaced. Sampling volumes of 100 µL and 60 µL were used for perfusate and blood samples, respectively. Samples were stored at 4°C before analysis of celecoxib and metabolites.

5.3.4 In vitro drug disposition studies in Caco-2 cells

5.3.4.1 Cell culture

Caco-2 cells were cultured with DMEM$^+$ as growth medium in cell culture flasks at 37°C in an atmosphere of 5% CO_2 and 90% relative humidity. Every 3-4 days, cells were passaged at 80–90% confluence using trypsin-EDTA. For transport experiments, Caco-2 cells were seeded on porous Costar Transwell membrane inserts (Polycarbonate 3 mm pore diameter, 12 mm diameter, 1.13 cm^2 growth area, Corning Inc., Corning, NY) at a density of 90.000 cells/cm^2. Cells (passage number 67-96) were used for transport experiments on the 18th/19th or 25th/26th day after seeding.

5.3.4.2 Drug accumulation in Caco-2 cells

To evaluate the accumulation of celecoxib, carboxy celecoxib, sulindac and sulindac sulfide, Caco-2 monolayers were first washed two times with prewarmed HBSS$^+$ to remove the growth medium (DMEM+). After washing, cells were pre-incubated with HBSS$^+$ (0.5 mL in the apical compartment, 1.5 mL in the basolateral compartment) in a shaking incubator (Thermostar, BMG Labtech, Offenburg, Germany) at 37°C and 300 rotations per minute (rpm). After 30 min, transepithelial electrical resistance (TEER) values were measured whereby only monolayers with a TEER-value higher than 250 Ω x cm^2 were used for transport experiments. After the preincubation step, 1.5 mL of TPGS (0.2% w/v) solution in HBSS$^+$ was applied to the basolateral compartment and 100 µL of mucus (50 mg/mL) was added to the apical compartment to ensure the compatibility of cells with biorelevant media [193]. After incubating the monolayers for 10 min at 37°C in a shaking incubator at 300 rpm, 0.5 mL of FaSSCoF containing 5 µM of the compound of interest was applied to the apical compartment. After 10 min, the apical and basolateral compartments were completely aspirated and rinsed three times

with warmed $HBSS^+$. The membrane was cut out and cells were scraped off, collected in 1 mL MeOH spiked with 10 µL of DMSO containing an internal standard (33.3 µM propyl-p-hydroxybenzoate) and stored at 4°C until further processing (see section 5.3.6).

5.3.4.3 Drug release from Caco-2 cells

To evaluate the release of celecoxib and sulindac from Caco-2 cells, the same protocol was applied as described in 5.3.4.2. After rinsing the apical and basolateral compartments, fresh $HBSS^+$ medium was applied to study drug release. The epithelial layer was not overlayed with fresh mucus in the release-step. After 10 min, the apical and basolateral compartments were completely aspirated and the membrane was rinsed five times with warmed $HBSS^+$ to ensure that no drug was attached to the membrane. The Caco-2 cells were then collected as previously mentioned in 5.3.4.2 to evaluate drug accumulation.

5.3.4.4 Suspension-driven drug accumulation in Caco-2 cells

To assess the accumulation of celecoxib and sulindac when applied as a suspension, the same protocol as described in 5.3.4.2 was used. An excess of celecoxib or sulindac was added to FaSSCoF (3.36 mg and 6.56 mg in 3 mL) and incubated in a shaking incubator at 175 rpm for 2 hours at 37°C before being applied to the apical compartment.

5.3.4.5 Bidirectional permeability assessment using Caco-2 cells

To evaluate the bidirectional permeation of celecoxib and sulindac across Caco-2 monolayers, the same protocol as described in 5.3.4.2. was used up until the preincubation step. After the preincubation step and measuring TEER values to check monolayer integrity, TPGS (0.2% w/v) solution in $HBSS^+$ was applied to the basolateral (1.5 mL) and apical (0.5 mL) compartment (no mucus was added). The donor compartment was spiked with 5 µM celecoxib or sulindac. Subsequently, samples of 100 µl or 50 µL were withdrawn from the acceptor compartment at 5, 15, 30 and 60 min. Withdrawn volumes were replaced by fresh TPGS (0.2% w/v) solution. After 60 min, monolayer integrity was checked again by measuring TEER values; results were not retained when the TEER value was reduced by more than 20%. Samples were analysed using HPLC (see section 5.3.7.).

5.3.5 Ex vivo drug disposition studies in human colonic biopsies

5.3.5.1 Ethics

The clinical study for the collection of human colonic biopsies followed the tenets of the Declaration of Helsinki and was approved by the Ethics Committee Research UZ/KU Leuven (reference study numbers S61127 and S61128). All volunteers provided written informed consent prior to participation. Volunteers with hepatitis B/C and/or HIV infection were excluded to guarantee the safety of the study personnel. Illness at the time of the study, medication use, a history of acute/chronic gastrointestinal disease(s), (possible) pregnancy, and/or frequent exposure to radiation during the previous year were criteria for exclusion.

5.3.5.2 Validation of drug accumulation assays in human colonic biopsies

Volunteers for whom a colonoscopy was already planned to screen for the presence of polyps or colorectal tumours were recruited prior to the study. Upon arrival, the volunteer was brought under conscious sedation (midazolam 1-5 mg and pethidine 10-50 mg i.v.). During the colonoscopy, 6 biopsies were taken with a standard biopsy forceps (Radial Jaw™3 with needle; outside diameter 2.2 mm; Boston Scientific) at the splenic flexure.

Human biopsies were transported in ice cold HBSS and excess lamina propria was carefully removed before using them for drug accumulation studies in modified 3 mL vertical Ussing chambers (Mussler Scientific Instruments, Aachen, Germany). The biopsies were mounted between two 0.4 mm polyester films with a Ø 1.5-mm opening which is equal to an exposed tissue area of 0.017 cm^2. The rounded edges and flexibility of the films reduced squeezing of the tissues at the border of the openings to minimize edge damage. The surface of the polyester was roughened with fine abrasive paper to keep the biopsies in position. After mounting, the apical and basolateral compartments were filled with 3 mL 10 mM mannitol in Krebs Ringer bicarbonate buffer. Solutions were kept at 37°C and continuously carbogenated with O_2/CO_2 (95/5%). Experiments were performed in open-circuit conditions. Transepithelial electrical resistance (TEER) was calculated from the voltage deflections induced by bipolar constant-current pulses of 16 µA every 60 s with duration of 200 ms and was recorded every 30 min over 2 h to validate the viability of tissues throughout the experiment: at the end of the experiment, only biopsies that had a TEER higher than 80% of the initial resistance after the equilibration period were considered suitable for the experiment. After a 40 min equilibration period to achieve steady-state conditions regarding transepithelial electrical resistance (TEER), the Krebs

Ringer buffer in the apical compartment was replaced with FaSSCoF containing 100 µM sulindac or celecoxib to study apical to basolateral accumulation. After exposing the tissue for 1 hour, the apical and basolateral compartments were completely aspirated and rinsed three times with warmed $HBSS^+$. The biopsies were dismounted and the exposed biopsies were divided into two groups. The mucus layer of the first group of biopsies was manually removed with a forceps and snap frozen in 1 mL methanol. The remaining tissue (in this chapter, the term 'tissue' does not include mucus) was separately snap frozen in 1 mL methanol. The second group of the biopsies was snap frozen as a whole (mucus + tissue) until further processing (see section 5.3.6).

5.3.5.3 Drug accumulation in human colonic mucosa

Volunteers were asked to follow a three-day low-fibre diet (e.g. white bread or pasta, canned fruit in heavy syrup or juice, no vegetables, clear drinks…) and to eat a last meal at 8 pm on the day before the study. To ensure fasted state conditions, volunteers could only drink water 12h to 2h prior to the colonoscopy. Upon arrival at the endoscopy unit, an enema was given to cleanse the left hemicolon and to allow visual control during the colonoscopy. The enema application is described in detail by Lemmens et al. (2020) [183]. Next, the volunteer was brought under conscious sedation (midazolam 1-5 mg and pethidine 25-50 mg i.v.). During the colonoscopy, 16 biopsies were taken with a standard biopsy forceps (Radial Jaw™3 with needle; outside diameter 2.2 mm; Boston Scientific) at the colon ascendens. Participants were not allowed to drink or consume food.

Human biopsies from the colon ascendens were mounted in Ussing chambers and allowed to equilibrate as described in section 5.3.5.2. After the equilibration period, the Krebs Ringer buffer in the apical compartment was replaced with FaSSCoF containing 100 µM sulindac or celecoxib (final concentration with 1% DMSO) to study apical to basolateral accumulation. The Krebs Ringer buffer in the basolateral compartment could also be replaced with Krebs Ringer buffer spiked with 100 µM celecoxib or sulindac to study basolateral to apical accumulation. After exposing the tissue for 1 hour, both compartments were completely aspirated and rinsed three times with warmed $HBSS^+$ samples. The biopsies were dismounted and the mucus layer of the biopsies was manually removed and snap frozen in 1 mL methanol. The remaining tissue was separately snap frozen in 1 mL methanol until further processing (see section 5.3.6).

5.3.6 Processing of biological samples

5.3.6.1 Biopsies and Caco-2 cells

To quantify drug concentrations in biopsies and Caco-2 cells (see section 5.3.4.2), 10 µL of DMSO containing an internal standard (10 µM propyl-p-hydroxybenzoate or celecoxib for experiments with test compound celecoxib and sulindac, respectively) was added to 1 mL methanol wherein biopsies and cells were collected. The biopsies and Caco-2 cells were then homogenized with a TissueLyser II (3 x 4 min, 1/30 s; Qiagen, Hilden, Germany). Subsequently, samples were centrifuged (20817 x g, 1 min, 4°C; Centrifuge 5417R; Eppendorf, Hamburg, Germany) and the supernatant was evaporated under a continuous air flow before being reconstituted in 335 µL of 25 mM NaAc pH 4.5:MeOH (55:45, v/v) or 25 mM AmAc pH 3.8:ACN (80:20, v/v) for celecoxib and carboxy celecoxib or sulindac and sulindac sulfide, respectively.

5.3.6.2 Venous blood samples

Immediately after collection, blood samples were stored on ice; at the end of the experiment, they were centrifuged (1699 x g, 15 min, 4°C; Centrifuge 5804R; Eppendorf, Hamburg, Germany) to collect plasma samples, which were stored at -26°C until analysis. To quantify drug concentrations in plasma, 5 µL of DMSO containing an internal standard (500 µM propyl-p-hydroxybenzoate) was added to 0.5 mL plasma. After adding 2 mL methanol, the mixture was thoroughly vortexed and subsequently shaken for 1 min. The samples were then centrifuged (1699 x g, 15 min, 4°C; Centrifuge 5804R; Eppendorf, Hamburg, Germany) and the supernatant was collected for LC analysis.

5.3.6.3 Bile and perfusate samples

The bile, which was continuously collected (Eppendorf tubes were replaced every 15 minutes) over 90 minutes, was weighed prior to analysis. The bile and perfusate samples from the in situ rat experiments were diluted with mobile phase of the LC-method (25 mM NaAc pH 4.5:MeOH (55:45, v/v)) in a 1:100 and 1:10 ratio before being analysed.

5.3.7 LC analysis

5.3.7.1 Celecoxib

Samples with celecoxib and carboxy celecoxib as test compound were analysed using HPLC with UV detection (252 nm). Separations were performed on a Novapak C18 column under radial compression (4 µm, 8 x 100 mm, Waters, Milford, MA, USA). A 100 µL sample was injected and eluted with a gradient of 25 mM sodium acetate buffer pH 4.5 (solvent A) and methanol (solvent B) at a flow rate of 1.0 mL/min for 18.5 min. The elution gradient was as follows: 0.0 - 1.5 min, 55% A; 2.5 – 7.0 min, 30% A; 8.0 – 13.5 min, 22% A; and 14.5 – 18.5 min, 55% A for reconditioning. Carboxy celecoxib, hydroxy celecoxib, IS, and celecoxib eluted at 6.6 min, 7.9 min, 8.6 min, and 12.5 min, respectively. Linearity was observed in a range from 20 µM to 10 nM for celecoxib and metabolites. For validation purposes, control samples were prepared containing 10 µM, 1 µM and 100 nM. Concentrations of celecoxib and metabolites could be precisely (intraday variability RSD ≤ 4.04% and interday variability RSD ≤ 7.00%) and accurately (range: 89.95 – 99.89%) determined in samples. Chromatograms were integrated with Waters Empower 2 software (Milford, MA, USA).

5.3.7.2 Sulindac

Samples with sulindac and sulindac sulfide as test compound were analysed using HPLC with UV detection (252 and 340 nm). Separations were performed on a Novapak C18 column under radial compression (4 µm, 8 x 100 mm, Waters, Milford, MA, USA). A 100 µL sample was injected and eluted with a gradient of 25 mM ammonium acetate buffer pH 3.8 (solvent A) and acetonitril (solvent B) at a flow rate of 1.0 mL/min for 16 min. The elution gradient was as follows: 0.0 - 1.5 min, 80% A; 3.5 – 6.0 min, 38% A; 7.0 – 11.0 min, 15% A; and 13.0 – 16.0 min, 80% A for reconditioning. Sulindac, sulindac sulfone, celecoxib (internal standard), and sulindac sulfide eluted at 7.1 min, 7.8 min, 10.3 min, and 11.2 min, respectively. Linearity was observed in a range from 20 µM to 10 nM. For validation purposes, control samples were prepared containing 10 µM, 1 µM and 100 nM. Concentrations of sulindac and metabolites could be precisely (intraday variability RSD ≤ 6.29% and interday variability RSD ≤ 12.54%) and accurately (range: 86.76 – 96.54%) determined in samples. Chromatograms were integrated with Waters Empower 2 software (Milford, MA, USA).

5.3.8 Data presentation

Drug concentrations accumulated in colonic biopsies and Caco-2 cells were normalized for the exposed area, and presented as the amount of accumulated compound per area (nmol/cm^2). Ussing chamber data is presented as the mean + SD (N = 6, n = 3 with N the number of different subjects and n the number of biopsies per subject). Caco-2 data is presented as mean + SD (n= 3 with n the number of monolayers from the same batch in a single experiment) All other data is presented as the mean + SD (n = 3) unless stated otherwise.

5.4 Results

5.4.1 In situ metabolism and excretion of celecoxib and carboxy celecoxib in rat

I*n situ* rat experiments [161] and *in vivo* studies in human volunteers [183] have shown that orally administered celecoxib can reach the colon through transit, because of its incomplete dissolution and absorption in the small intestine. Analysis of the human colonic aspirates also indicated a substantial presence of carboxy celecoxib, the predominant metabolite of celecoxib [183]. To better understand the potential role of other processes including biliary excretions, enterocytic metabolism or plasma-driven colonic excretions in the colonic appearance of celecoxib and, in particular, carboxy celecoxib, we performed additional *in situ* rat experiments. First, an intravenous bolus of celecoxib was administered to rats, upon which bile and plasma were sampled over time. We observed that 0.83 ± 0.44 % of the intravenous dose was recovered in bile (see section 5.3.6.3), consisting of 1.08% celecoxib, 87.62% carboxy celecoxib and 10.43% hydroxy celecoxib, even though systemic celecoxib levels were about 50-fold higher than carboxy celecoxib throughout the experiment (Fig. 5.1). These data suggest a minimal contribution of biliary clearance to the substantial fraction of celecoxib observed in the colon after oral administration. On the other hand, the relatively higher biliary excretion of carboxy celecoxib after hepatic metabolism of celecoxib may underlie its appearance in human colonic aspirations. To further substantiate this claim, we also examined whether carboxy celecoxib could be present in the lumen by extensive excretion from the systemic circulation or due to local biotransformation in the gut. Following the intravenous injection of celecoxib, the concentrations of excreted carboxy celecoxib in the ileum (perfused with blank FaSSIF) were below the LOD (100 nM) and could not explain the high amount of carboxy celecoxib that was detected in human aspirates. Upon perfusing an isolated segment of the rat ileum with 100 µM

celecoxib spiked in FaSSIF (closed loop setup), we did not detect any biotransformation to carboxy celecoxib in the perfusion solution either.

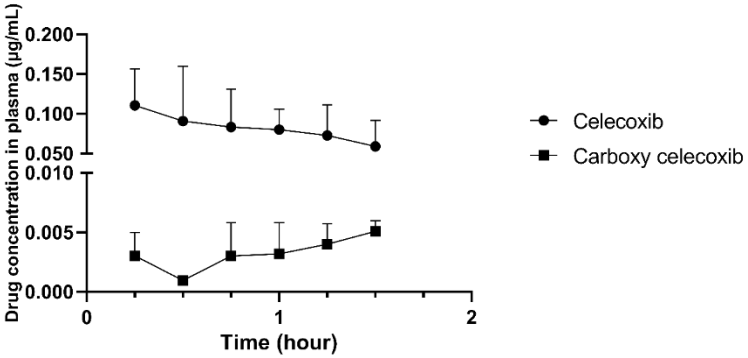

Fig. 5.1: Plasma concentration of celecoxib and carboxy celecoxib after administering an intravenous bolus (1 mg/kg in DMSO) of celecoxib in rats. Values represent mean + SD (n=3).

5.4.2 Colonic accumulation in in vitro/ex vivo intestinal models

As previously mentioned, both colon-targeted delivery systems and immediate release formulations can result in gut-driven drug uptake. However, non-clinical absorption models that closely mimic intestinal function are generally used to predict intestinal stability and permeation of drugs and potential drug candidates, but not their accumulation behaviour in cells or tissue. We selected two ubiquitously used intestinal models, the in vitro Caco-2 system and the ex vivo Ussing chamber model with human colonic biopsies, to explore the accumulation of celecoxib and sulindac. We primarily focused on the luminal accumulation behaviour, since our previous *in vivo* studies indicated that gut-driven accumulation in colonic tissue can substantially improve the anti-carcinogenic effect.

5.4.2.1 The Caco-2 model

In a series of experiments with celecoxib and sulindac, we assessed the steady state accumulation, the possible release from the cells and the impact of suspensions on the accumulation behaviour. In addition to sulindac and celecoxib, we assessed the accumulation of carboxy celecoxib and sulindac sulfide in Caco-2, since our *in vivo* studies demonstrated that these metabolites were present in the lumen of the caecum, possibly enabling gut-driven tissue accumulation [183,191]. In all accumulation experiments, the Caco-2 cell line was incubated

under conditions relevant to the colon, i.e. by applying a thick mucus layer and by using Fasted State Simulated Colonic Fluid (FaSSCoF). At the end of the experiment, the mucus layer was rinsed off, and the accumulation was assessed in the cells only. Lastly, we also evaluated the apparent permeability of celecoxib and sulindac, wherefore we used simple buffers ($HBSS^+$).

Accumulation in Caco-2 cells

Drug accumulation was studied after an exposure time of 10 minutes to ensure steady state conditions (as was shown in preliminary experiments). We observed the following accumulation of the compounds: celecoxib (0.044 nmol/cm^2); sulindac sulfide (0.013 nmol/cm^2); carboxy celecoxib (0.012 nmol/cm^2); sulindac (0.002 nmol/cm^2) (Fig. 5.2).

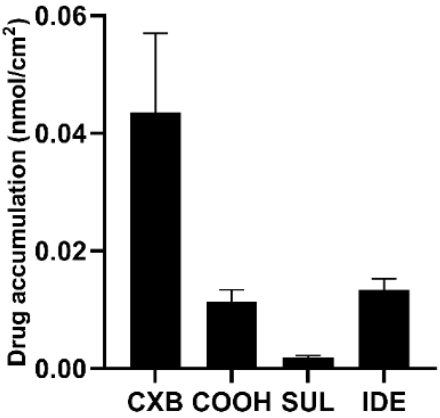

Fig. 5.2: Drug accumulation in Caco-2 monolayers after a 10-min exposure to celecoxib (CXB), carboxy celecoxib (COOH), sulindac (SUL) and sulindac sulfide (IDE). Donor concentration was 5 µM for all compounds. Bars represent mean + SD (n = 3).

Drug release from Caco-2 cells

In a follow-up experiment, we evaluated the release of celecoxib and sulindac from the Caco-2 cells after a 10-minutes accumulation as previously described. After exposing the Caco-2 cells to the drugs, we washed the cells, applied fresh $HBSS^+$ to both compartments and assessed the release after 10 min. While celecoxib accumulation dropped by 77.5% in 10 min (from 0.098 ± 0.0024 nmol/cm^2 to 0.022 ± 0.0028 nmol/cm^2), the release of sulindac was negligible (from 0.0026 ± 0.00099 nmol/cm^2 to 0.0022 ± 0.0014 nmol/cm^2) (Fig. 5.3). It is noteworthy that celecoxib accumulation after 10 min differed between the accumulation and the release experiments (Fig. 5.2 and 5.3). The difference is likely due to the different batch number and Caco-2 clone.

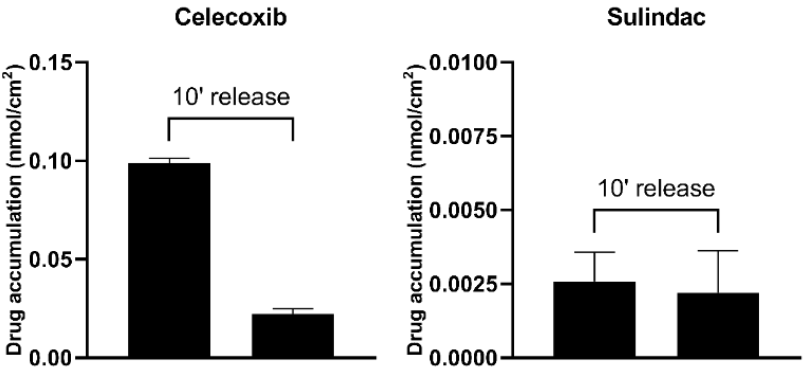

Fig. 5.3: Accumulation of celecoxib (A) and sulindac (B) in Caco-2 monolayers after (i) an apical exposure period of 10 min, and (ii) an exposure period of 10 min followed by a release period of 10 min in fresh medium. Initial donor concentration was 5 µM. Bars represent mean + SD (n = 3).

Suspension-based accumulation

Since a substantial fraction of celecoxib and sulindac in the human colonic lumen appeared undissolved [183,191], we investigated the impact of using a suspension instead of a solution on the accumulation in Caco-2 cells. An excess amount of celecoxib or sulindac was added to FaSSCoF and was then placed in a shaking incubator at 175 rpm for 2 hours at 37°C. After 2 h incubation, saturated solutions were obtained at 15.35 ± 0.82 µM for celecoxib and 601.71 ± 47.51 µM for sulindac. After a 10 min exposure of Caco-2 monolayers, we observed an

accumulation of 2.74 ± 1.53 nmol/cm^2 and 0.014 ± 0.0083 nmol/cm^2 for celecoxib and sulindac, respectively (Fig. 5.4).

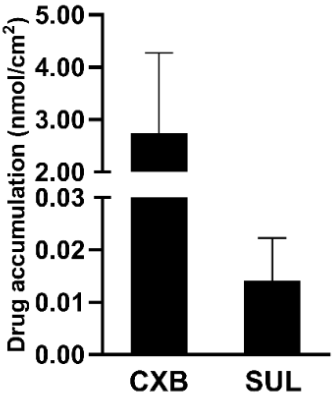

Fig. 5.4: Drug accumulation in Caco-2 monolayers after exposure to a suspension of celecoxib or sulindac in the donor compartment for 10 minutes. Bars represent mean + SD (n = 3).

Bidirectional permeation

Lastly, we evaluated the bidirectional permeation of celecoxib and sulindac across Caco-2 monolayers (Fig.5.5. We observed higher apparent permeability values for celecoxib ($17.99*10^{-6}$ ± $1.47*10^{-6}$cm/s) in the absorptive direction than in the secretory direction ($9.78*10^{-6}$ ± $2.15*10^{-6}$ cm/s). For sulindac, apparent permeability values were slightly lower: $8.08*10^{-6}$ ± $0.45*10^{-6}$ cm/s in the absorptive direction and $6.32*10^{-6}$ ± $0.41*10^{-6}$ cm/s in the secretory direction.

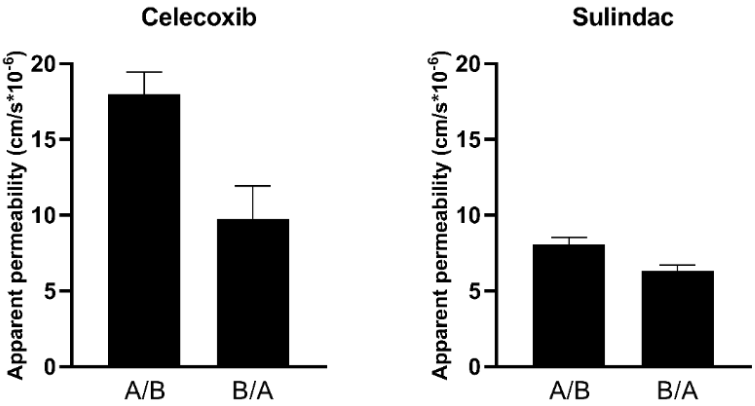

Fig. 5.5: Apparent permeability of Caco-2 cell monolayers for celecoxib and sulindac from apical to basolateral (A/B) and from basolateral to apical (B/A). Donor concentration was 5 µM. Bars represent mean + SD (n = 3).

5.4.2.2 The Ussing chamber system

In contrast to Caco-2 monolayers, which only consist of enterocytes, sampled human colonic biopsies comprise tissue with multiple cell types (goblet cells, enterocytes, enteroendocrine cells, etc.), as well as native mucus. As such, the Ussing chambers technique with human biopsies allows us to mimic the *in vivo* conditions more closely than Caco-2. Of special interest is that this technique also enables advanced studies on the effect of mucus on drug diffusion/accumulation as it can be scraped off post experiment. A preliminary experiment was performed with celecoxib to validate the separate processing of mucus and tissue. Human biopsies were exposed for 1 hour to 100 µM celecoxib in FaSSCoF. Afterwards, half of the biopsies were processed as a whole (= mucus + tissue). For the other half, mucus and tissue were analysed separately. The results indicated that processing mucus and tissue separately did not result in loss of compound, as depicted in Fig. 5.6.

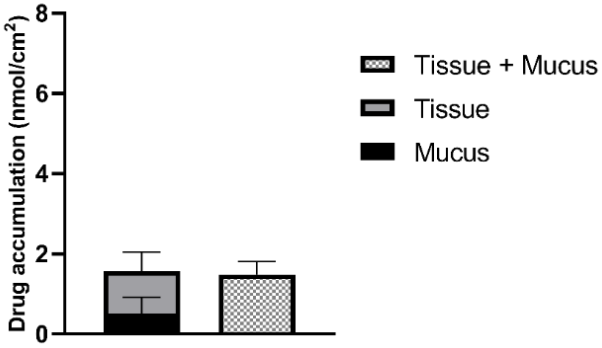

Fig. 5.6: Drug accumulation in human biopsies from the splenic flexure of the colon after exposure to celecoxib (100µM) in the donor compartment for 1 hour. Biopsies were either processed as a whole, or the mucus and tissue were processed separately. Bars represent mean + SD (N = 6, n = 3).

Then, the accumulation of celecoxib and sulindac across human colonic biopsies was assessed after apical or basolateral exposure. As shown in figure 5.7, the drug accumulation in mucus and underlying tissue after apical exposure to celecoxib is 1.34 ± 1.48 nmol/cm^2 and 3.25 ± 3.04 nmol/cm^2, respectively, and was normalized for exposed surface area. Apical driven accumulation is higher for celecoxib compared to sulindac, which reaches concentrations of 0.27 ± 0.18 nmol/cm^2 in mucus and 0.85 ± 0.35 nmol/cm^2 in tissue. The difference in accumulation of celecoxib compared to sulindac was less pronounced after basolateral exposure: celecoxib reached concentrations of 0.40 ± 0.44 nmol/cm^2 and 1.40 ± 1.11 nmol/cm^2, while the accumulation of sulindac was 0.32 ± 0.29 nmol/cm^2 and 1.06 ± 0.67 nmol/cm^2 in mucus and tissue, respectively.

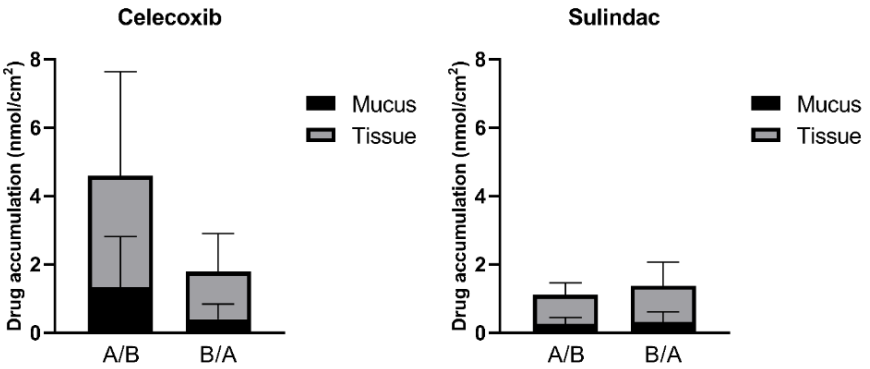

Fig. 5.7: Drug accumulation in mucus and tissue of healthy human biopsies from the ascending colon after exposure to celecoxib or sulindac for 1 hour. Mucus was manually removed and processed separately from the tissue. Donor concentration was 100 µM for both celecoxib and sulindac. A/B represents accumulation after apical exposure, B/A represents accumulation after basolateral exposure to the compound of interest. Bars represent mean + SD (N = 6, n = 3).

5.5 Discussion

Colon-targeted drug delivery systems are designed to release the drug at the colon, allowing local tissue accumulation for an efficacious treatment of colonic diseases, while minimising systemic exposure and subsequent adverse events. Conversely, immediate release formulations to target colonic diseases are assumed to rely on adequate small intestinal absorption and systemic circulation to deliver therapeutic concentrations of the drug to colonic tissue. Interestingly, recent clinical studies have revealed that the NSAIDS celecoxib and sulindac, orally administered as immediate release formulations (Celebrex and Arthrocine, respectively), can reach the caecum by transit. This results in substantial gut-driven tissue accumulation that is likely needed to induce their anti-carcinogenic effect. The substantial drug fraction arriving in the caecal lumen results from incomplete small intestinal dissolution of these moderately to poorly soluble NSAIDs, possibly combined with substantial biliary excretion. Indeed, we previously showed for sulindac, a weak acid (pKa of 4.09) with moderate intestinal solubility and permeability, that a high biliary excretion [191] contributes to its arrival in the caecum. In the present study, however, the amount of celecoxib in biliary excretions appeared negligible upon intravenous administration in rats (see section 5.4.1). This indicates that unfavourable dissolution kinetics of celecoxib along the gastrointestinal tract, due to its high lipophilicity

(logD at gastrointestinal pH: 4.01) and poor solubility, is the sole reason for the substantial and mostly undissolved fraction of celecoxib that reaches the caecum [191]. Biliary excretion does, however, contribute to the high luminal fraction of the active carboxy celecoxib metabolite in human caecal aspirates, rather than local gut biotransformation by epithelial cells or excretion from the systemic circulation. Research by the group of Van de Wiele (University of Ghent) further indicated that celecoxib remained extremely stable when incubated in feacal slurries (SHIME) (personal communication). Therefore, no bioconversion by the colonic microbiome is expected.

Our clinical studies further showed that caecal aspirates collected after oral intake of the immediate release formulations of the NSAIDs contained a relatively higher total drug content (solid + solute) of celecoxib (on average 614.3 µg/mL) compared to sulindac (on average 73.10 µg/mL). This indicates that the lower intestinal solubility of celecoxib likely enables a larger fraction of the compound to reach the caecum. Interestingly, the mean dissolved concentration in the caecal aspirates appeared lower for celecoxib (11.7 µg/mL) than for sulindac (50.6 µg/mL). This implies that the driving forces for gut-driven drug accumulation in tissue (i.e., the dissolved drug concentrations in the gut lumen) were not in line with the observed mean accumulation levels (celecoxib: 1600 ng/mg >> sulindac: 20 ng/mg). This observation emphasises the importance of considering the accumulation potential of the drugs as well. While drug permeation across the intestinal mucosa is routinely assessed through *in vitro* setups, few studies have been conducted on the accumulation behaviour of drugs in intestinal epithelia. Rozehnal et al. used the Ussing chamber model with small intestinal and colonic tissue to demonstrate that factoring in drug accumulation when determining permeability values resulted into a better correlation with the human fraction absorbed (F_a) for several compounds, including metoprolol, ibuprofen, and pravastatin [103]. Similarly, Miyake showed that the rank order of a 4k Da labeled dextran, atenolol and metoprolol only then coincided with F_a in humans [112]. In the present study, we assessed the accumulation of sulindac and celecoxib in non-clinical absorption models such as Caco-2 monolayers and the Ussing chamber system with human biopsies (consisting of mucus and tissue), as to better understand what underlies the difference in *in vivo* accumulation behaviour.

5.5.1 The intrinsic accumulation behaviour in colonic mucus and tissue

Starting from drug solutions in FaSSCoF, we observed a higher accumulation of celecoxib compared to sulindac in the mucus of human colonic biopsies (Fig. 5.7). Substantial accumulation of celecoxib in mucus can be attributed to hydrophobic interactions ($logD_{7.8}$ = 4.01) with the mucins (see Table 5.1). Conversely, the lower accumulation of sulindac can ascribed to its negative ionisation state, which impedes the hydrophobic interactions from occurring ($logD_{7.8}$ = -0.36). Our group previously reported a diffusion limiting effect of mucus on hydrophobic compounds, resulting in a more pronounced retardation of the highly lipophilic heptylparaben compared to methylparaben, which is only slightly hydrophobic [194]. In addition to the absence of hydrophobic interactions, the direct repulsion of sulindac by the negatively charged sialic acids of the heavily glycosylated protein-backbone will contribute to its lower accumulation.

Table 5.1: Physicochemical properties of celecoxib, carboxy celecoxib, sulindac, and sulindac sulfide.

	Celecoxib	Carboxy Celecoxib	Sulindac	Sulindac Sulfide
Molecular weight (g/mole)	381.37	411.36	356.41	340.41
LogP	4.01	3.15	2.92	4.82
pKa (most acidic)	10.6	3.98	4.09	4.16
LogD (pH 7.8)	4.01	-0.20	-0.38	1.54

The same physicochemical properties (Table 5.1) also underlie the higher intrinsic accumulation of celecoxib compared to sulindac in Caco-2 cells and human tissue and (Fig. 5.2 and Fig. 5.7, respectively). In contrast to the rather hydrophilic and ionized sulindac, celecoxib has favourable properties for diffusion across the lipophilic apical membrane into the enterocytes. Due to its ionization and increased hydrophilicity, the metabolite carboxy celecoxib accumulated to a lesser extent than its parent drug in Caco-2 cells (Fig. 5.2), which was also reflected in our previously reported *in vivo* accumulation data [183]. The active metabolite sulindac sulfide accumulated better compared to sulindac in the Caco-2 model (Fig. 5.2), thanks to its increased lipophilicity.

Additionally, we performed *in vitro* accumulation assays followed by release (Fig 5.3). Results indicated that celecoxib's favourable physicochemical properties for membrane diffusion not only imply a substantial intracellular accumulation but also considerable release from the cells

into fresh medium. Although the accumulation of sulindac was relatively low compared to celecoxib, only a slight drop in accumulation was observed after simulating the release. This difference in release behaviour is also reflected in our apparent permeability (Papp) experiments (Fig. 5.5), which showed that celecoxib ($18.0*10^{-6}$ cm/s) can better cross the epithelium than sulindac ($8.0*10^{-6}$ cm/s).

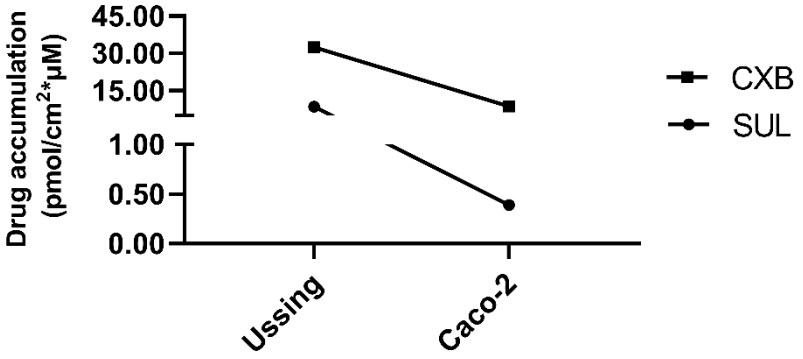

Fig. 5.8: Comparison between drug accumulation in human biopsies (Ussing chamber system) and Caco-2 monolayers after apical exposure to celecoxib or sulindac. Drug accumulation is normalized for the donor concentration.

For both celecoxib and sulindac, the amount of accumulation in tissue was consistently higher in the Ussing chamber model compared to the Caco-2 model (Fig. 5.8). It is likely that the relatively larger absorptive surface area of the human tissue enables a better accumulation compared to the 2D epithelial monolayer of the Caco-2 model, which only contains microvilli and no crypt structure. Similarly, the more pronounced accumulation of celecoxib in the Ussing chamber model after apical compared to basolateral exposure can be attributed in part to the difference in surface area. Moreover, celecoxib shows a high affinity to accumulate in the apical mucus layer, further enhancing drug accumulation in the adjacent tissue since the mucus likely acts as a depot for sustained drug release. In contrast, there was no distinct difference in the accumulation of sulindac in mucus and tissue after either apical or basolateral exposure. Presumably, the lack of good mucopenetrative properties of sulindac will likely minimise the difference between apical and basolateral driven drug accumulation. Although the accumulation difference between celecoxib and sulindac seems to depend on the intestinal

model used, both models convincingly show a stronger accumulation of celecoxib in tissue (Fig. 5.8).

5.5.2 Simulating an in vivo relevant colonic disposition – suspensions

The aforementioned solution-based permeation assays (Fig. 5.2 and 5.7) capture the intrinsic difference in accumulation between celecoxib and sulindac, which partially explains the reported higher *in vivo* accumulation of celecoxib, despite a lower dissolved concentration. *in vivo*, however, the suboptimal dissolution of celecoxib and sulindac in the scarce and scattered pockets of highly viscous content of the colonic lumen, implies that the undissolved drug fraction should be considered when simulating the accumulation behaviour. When repeating the accumulation assay with a suspension of celecoxib (Fig. 5.4), we observed a 62-fold higher accumulation compared to the solution-based assay, despite a limited three-fold higher dissolved concentration in the saturated solution (15 µM vs 5 µM). Presumably, the favourable physicochemical properties that underlie the extensive accumulation of celecoxib will be followed by a fast dissolution of the solid fraction, further enhancing drug accumulation. For sulindac, the increase in accumulation was relatively modest compared to the increase in dissolved concentration in the saturated solution, which is likely linked to the poor penetrative properties. The suspension-based accumulation assay thus indicated an increased difference in accumulation levels between celecoxib and sulindac, which is in line with the pronounced contrast in *in* vivo accumulation (1600 ng/mg vs 20 ng/mg for celecoxib and sulindac, respectively).

5.5.3 Remarks on performing accumulation assays

Since no standardized protocol is available for accumulation assays, the technique comes with various caveats. In this section we will address several of these caveats as to correctly frame the results. Attention needs to be given to the compatibility of tissue with intestinal medium, the incubation and rinsing conditions, and terminology.

For all accumulation experiments, we used Fasted State Simulated Colonic Fluid (FaSSCoF) as to better simulate physiologically relevant conditions. However, a substantial drop in Transepithelial Electrical Resistance (TEER) indicated that the Caco-2 cell-layer shows limited compatibility with FaSSCoF, despite the presence of a protective mucus layer. TEER values

reflect the integrity of intercellular tight junction dynamics, which affects the paracellular drug transport. In a permeability experiment, disruption (TEER-drop of 20%) of the tight junctions will therefore negatively impact on the validity of the results. In contrast, disruption of the tight junctions does not affect the ability of drugs to accumulate into the tissue. However, the possibility exists for the drug to diffuse to the acceptor compartment and consequently tissue will be exposed from both sides. To ensure valid test conditions, we limited the incubation period to 10 minutes in order to decrease the likelihood of severe damage. It is noteworthy that each cell model can withstand the disruptive nature of FaSSCoF to a different extent: Caco-2 cells were limited to 10 minutes, human biopsies remained viable for more than one hour, while noticeable damage to colon organoids appeared around one hour (personal communication). Since these compatibility issues dictate the incubation conditions, simple physiological buffers might be the preferred option when a comparative analysis of accumulation between models is desired.

Secondly, after incubation, HBSS (37°C) was used to rinse the tissue as to remove adsorbed drug. This procedure was repeated five times in case of a suspension, and three times in case a solution was used. However, it is likely that not all adsorbed particles were removed, and subsequently collected and processed together with the cells, possibly resulting in an overestimation of the accumulation values. In contrast, too many wash steps can extract drug from the cells, implying that drug accumulation values might be underestimated. Finding this balance is complex and drug dependent as shown by our release experiment (Fig. 5.3).

Lastly, we observed that the drug accumulation can depend on the passage number of the Caco-2 cells. One should therefore be careful in directly comparing accumulation values within and between laboratories. Furthermore, comparing accumulation values between research groups is troublesome, as no clearly defined terminology nor standard processing method exists. In our set of experiments biopsies were mechanically homogenized as a whole, therefore ‘accumulation’ includes intracellular available drug, as well as drug possibly adhering to the inter-, and extracellular matrix. Tissue also still contains mucus remnants after the mucus layer was manually scraped off. Moreover, the method of tissue homogenization (mechanic homogenization, lysis buffer, sonications) and tissue normalization (corrected for exposed surface area, protein content, dry biopsy or wet biopsy weight, etc.) differs between research groups. Consensus on tissue processing and accumulation within and between academic and industrial research would be beneficial for the drug development process.

Several of these concerns will be addressed in follow-up experiments to better understand and standardize accumulation assays.

5.6 Conclusion

Poor solubility and incomplete small intestinal dissolution, possibly combined with biliary clearance, causes a substantial fraction of orally dosed celecoxib and sulindac to reach the caecum by transit, even though both NSAIDs are not administered as colon-targeted formulations. The resulting gut-driven accumulation is likely needed to induce their anti-carcinogenic effect. This emphasises the importance of evaluating local accumulation, as to better understand and simulate how therapeutic concentrations are reached. In this study, we demonstrated the added value of both Caco-2 monolayer and the Ussing chamber model with human biopsies to evaluate the potential of drugs to accumulate in colonic mucus and tissue. We showed that the favourable physicochemical properties of celecoxib resulted in extensive accumulation in mucus and tissue as compared to sulindac, especially when closely simulating the in vivo conditions by using drug suspensions instead of solutions. The *in vitro* and *ex vivo* data are in line with a sustained and prolonged tissue exposure to celecoxib in vivo. The implementation of these accumulation assays in drug development may contribute to making informed decisions when selecting promising drug candidates aiming at local effects in colonic tissue.

CHAPTER 6 – Concluding discussion

Intake of a drug equals treatment of the colonic disease; a seemingly simple concept, but not an easy one. Firstly, after oral intake of a drug, the drug needs to traverse various segments of the gastro-intestinal tract, that each come with their own physiological variables (i.e. composition of gastrointestinal fluids, residual gastro-intestinal volumes, motility). These physiological variables are in interplay with the physicochemical properties (i.e. pKa, lipophilicity, stability, solubility, etc.) of the drug, and the disposition is dependent on the dosage form (i.e. immediate release, modified release). Colonic pathologies are often treated with colon-targeted drug delivery systems (i.e. pH-dependent, time-dependent, combination systems, etc.), which are engineered to withstand the acidic gastric environment that is typified by its plethora of enzymes (i.e. pepsin, gastric lipase) and strong contractility patterns, and the more pH neutral intestinal condition that contains endogenous surface active substances (i.e. bile salts and phospholipids) and enzymes that contribute to the degradation of lipids. By bypassing exposure to these environments, the colon-specific release will target the disease more efficaciously and minimise drug absorption and subsequent adverse effects. However, immediate release formulations often contain drugs with poor solubility and high lipophilicity, a prevalent characteristic of new drug candidates, which can result in unfavourable dissolution kinetics in the aqueous intestinal environment. These intrinsic properties of the drug can therefore hamper intestinal absorption and might subsequently expose colonic tissue in a local manner as well. Indeed, several NSAIDs such as celecoxib and sulindac, wherefore epidemiological data has shown preventive effects on the development of polyps and colorectal cancer, display these properties, and are marketed as immediate release formulations. This urged us to explore how physiology, physicochemical properties and dosage form affect colonic drug disposition, and how sufficiently high tissue concentrations are reached (systemically, or locally). To elucidate local colonic drug disposition, several small-scale clinical studies with healthy volunteers were performed. Since colonic *in vivo* data is difficult to obtain, we also simulated colonic disposition through multiple *in vitro* models (Caco-2 cell line and the Ussing Chamber technique). We focused on assessing the accumulation behaviour, aside of exploring standard parameters including solubility and permeability, as to better understand the disposition.

6.1 Understanding how high colonic concentrations are reached: gut versus systemic driven uptake

A first part of this dissertation is dedicated to understanding how the NSAIDs celecoxib and sulindac reach sufficiently high colonic concentrations to exert their effect on colorectal cancer progression. The lipophilic and poorly soluble nature of sulindac and celecoxib can imply incomplete intestinal dissolution, allowing an undissolved fraction to reach the colon through transit and contribute to colonic tissue accumulation. In chapter 4, we simulated the *in vivo* intestinal dissolution by performing an *in vitro* transfer experiment in which a pH-shift was present. In the experiment, one Arthrocine tablet (immediate release, 200 mg sulindac) or one Celebrex capsule (immediate release, 200 mg celecoxib) was first exposed to gastric (FaSSGF, pH 1.5) conditions, and then to intestinal (FaSSIF, pH 6.5) and colonic (FaSSIF, pH 6.0) relevant conditions. Results showed that the extent of dissolution was pronouncedly higher for Arthrocine® (sulindac) than for Celebrex® (celecoxib). Sulindac as a weak acid (pKa 4.09) undergoes a change in ionisation state upon transfer, which concurred with going from a low solubility (gastric pH) to a high solubility (intestinal and colonic pH). The intestinal conditions were thus favourable for the pronounced drug dissolution. For the more lipophilic celecoxib, which maintains the same ionisation state (neutral) in all intestinal compartments due to the high pKa value (10.6), a remarkably low dissolution was observed. These *in vitro* experiments were a first indication that low solubility can possibly result in the caecal arrival of an undissolved fraction. Considering the incomplete intestinal dissolution, colonic tissue concentrations might therefore originate from both absorption (gut-driven uptake) and distribution (systemic-driven uptake) after uptake in the small intestine. To validate this finding, we needed to establish an *in vivo* protocol that allowed us to simultaneously sample caecal content, plasma, and caecal biopsies.

To date, only one other research group has been able to collect colonic content, indicating the scarcity and difficulty of the procedure. The group of Vertzoni (University of Athens) used a colon preparation procedure that existed of administration of bisacodyl, a stimulant laxative. More specifically, volunteers were given 10 mg of bisacodyl 50 h and 10 mg of bisacodyl 44 h before the colonoscopy. The effects of bisacodyl on the intraluminal content were shown to be eliminated by the time of colonoscopy, during which colonic content was collected [64]. In our *in vivo* set-ups an array of techniques was tested (retrieval pouch, various aspiration catheters),

and ultimately, we chose to rectally administer a one-time enema of 250 mL tap water to cleanse the left hemi-colon while ensuring an undisturbed right hemi-colon. This procedure allowed us to sample physiologically relevant samples of colonic content through the colonoscope. However, due to the viscous nature of caecal content, we were limited to a one-time aspiration of colonic content at the end of the colonoscopy. It was not feasible to aspirate as a function of time, which is routinely done for aspiration studies of the upper GI tract.

To validate the importance of caecal concentrations on the net tissue accumulation of compounds, we needed to discern plasma from gut-driven tissue accumulation after oral intake of Celebrex® or Arthrocine®. To this end, clinical studies were designed for the drug's systemic T_{max} to drop in-between two colonoscopy phases (chapter 3 and 4), both during which caecal tissue and colonic contents were collected. In the first phase (between 1 and 2.5 h post drug intake), plasma levels are expected to increase and drive caecal tissue accumulation. In the second phase (between 6 and 7.5 h post drug intake), plasma levels of celecoxib are expected to decrease. Tissue concentrations could be systemically driven (in which case they would decrease as well), but also gut driven if celecoxib arrived at the caecal lumen through transit. For both celecoxib and sulindac caecal tissue concentrations remained relatively low despite an increasing plasma concentration during phase 1, and were in most cases not detected in the luminal contents of the caecum, collected after 2.5 h. In contrast, during phase 2 tissue concentrations were substantially higher than in phase 1 which is in accordance with the high concentrations in the content. These data clearly indicated that accumulation of celecoxib and sulindac in caecal tissue seem to occur concomitantly with high luminal concentrations, independent of the systemic profile. The accumulation can thus be gut driven once the drug reaches the caecal lumen.

Apart from incomplete intestinal dissolution, other pharmacokinetic processes including extensive biliary excretion, secretion from the systemic circulation, and local biotransformation can also underlie the appearance of celecoxib and sulindac in the caecum (chapter 3 and 4). For sulindac, rat *in situ* experiments showed that upon an injection of an intravenous bolus of sulindac, biliary excretions predominantly contain sulindac and little to no metabolites. Apart from incomplete intestinal dissolution and absorption, these data indicated that biliary excretion likely contributes to the caecal arrival of drugs via transit. For celecoxib, we found that bile mainly contained the hepatically formed carboxy celecoxib, but no or little celecoxib, even

though systemic celecoxib levels were about 50-fold higher than carboxy celecoxib throughout the experiment. In this case, data suggested that the poor solubility of celecoxib throughout the gastrointestinal tract mainly underlies its arrival in the colon [187].

Apart from celecoxib, also high concentrations of carboxy celecoxib were found in caecal aspirations (chapter 3). However, we showed that local enterocytic metabolism or plasma-driven colonic excretions cannot explain the high *in vivo* caecal concentration. Moreover, recent results from the group of Van de Wiele (Ghent University) showed that celecoxib remained extremely stable when incubated in feacal slurries in the SHIME (personal communication). Therefore, no bioconversion by the colonic microbiome is expected.

6.2 Implications for colon-targeting drugs

The presence of an undissolved caecal fraction is the first direct indication of possible gut-driven uptake, despite being labelled as an immediate release formulation. Nevertheless, the extent of drug accumulation differs substantially between compounds. The observed accumulation behaviour is reliant on an array of variables, including the bioaccessible fraction, the physicochemical properties of the drug (ionisation state, lipophilicity, etc.), the effective permeability, etc. Firstly, the limited volume of colonic fluids in scarce and scattered pockets (median 2 mL) and their relatively high viscosity are not ideal to keep drugs and metabolites in solution, affecting the subsequent absorption. This implies that while low intestinal solubility enables a large fraction of the compound to reach the caecum, it also limits the bioaccessibility. Indeed, while the poorly soluble celecoxib reached higher total concentrations in the caecal lumen than sulindac (614.3 ± 614.5 µg/mL versus 73.10 ± 103.38 µg/mL total drug content), dissolved concentrations were higher for sulindac (celecoxib: 11.7 ± 12.5 µg/mL; sulindac: 50.63 ± 70.95 µg/mL solute). Interestingly, *in vivo* studies showed that the extent of tissue accumulation (celecoxib reached on average 1600 ng per mg biopsy (dry weight) compared to 20 ng/mg for sulindac during the second colonoscopy period) is more in line with the total drug concentrations (solid + solute) in caecal aspirations, but not with dissolved concentrations. This indicates that the physicochemical properties need to be considered. As previously mentioned, the lipophilic celecoxib has a net-zero charge ($logD_{7.8}$ of 4.01) that enables it to traverse the mucins and to partition into the lipophilic plasma membrane. In contrast, the negative charge of sulindac ($logD_{7.8}$ of -0.38) will explain its relatively poor accumulation. This is also reflected

in two independent studies that reported the effective permeability (P_{eff}) for celecoxib [195] and sulindac [196]. By using single pass *in situ* perfusion in rats, they showed that P_{eff} values were $0.639 \pm 0.064 \times 10^{-4}$ cm/s for celecoxib and $0.154 \pm 0.040 \times 10^{-4}$ cm/s for sulindac [195,196]. This indicates that celecoxib can better partition into the mucosa compared to sulindac, which is in agreement with the observed tissue accumulation. However, it should be noted that although similar perfusion solutions were used, the intestinal region differed (ileum versus jejunum).

When considering therapeutic efficacy, it is noteworthy that the concentrations of celecoxib and sulindac that are required to get an anti-carcinogenic effect in cell culture experiments are generally between 10 µM and 100 µM [170], which are not reached in plasma by administering a single 200 mg dose. In this respect, the relatively high levels of celecoxib and sulindac in the colonic lumen and the resulting accumulation in colonic tissue seem essential to obtain the reported anti-carcinogenic effects. However, it is important to remark that the interplay between the drug's physicochemical properties and the colonic physiology can result in a region-dependent accumulation behaviour, and therefore a region-dependent therapeutic effect. In chapter 3, we evaluated the tissue concentration of celecoxib in several colonic regions, and at several time points after oral intake. We observed an increase from 4 to 8 h after intake of the drug in all sampled regions (caecum – hepatic flexure – splenic flexure – sigmoid) except for the hepatic flexure where the highest accumulation was seen at 6 h. Moreover, the caecal tissue concentrations at 8 h were consistently higher compared to the other regions. This indicates that the more chyme-like consistency- hence a higher water content – at the caecum will likely contribute to a better dissolution and subsequent absorption of the drug into the tissue. In contrast, as chyme moves more distally, the content will become more solid and harbour less water, which is seen translated into a lower uptake. As such, apart from the gut-driven uptake that can enable an anticarcinogenic effect, it needs to be considered in combination with the distinctive longitudinal drug dissolution and accumulation behaviour. To ensure that the entire colon is treated, colon-targeted formulations can be used. For example, Choi et al. (2015) reported that delivery of budesonide using a pH-dependent nanoparticle system was mostly restricted to the rat caecum. However, using a dual pH- and time-dependent system resulted in a better exposure to the more distal parts of the colon as well, and not just the caecum [197]. Similarly for rectal delivery systems: the site of action of the different topical formulations varies, with suppositories dispersing in the rectum, foam reaching the sigmoid and descending

colon, and enemas reaching up to the splenic flexure. Rectal drug delivery systems thus target only the distal parts of the colon.

Apart from the regional colonic disposition of the parent compounds, attention also needs to be directed towards a possible local bioconversion that can affect local accumulation. Considering sulindac and sulindac sulfide, our *in vivo* studies showed a shift in drug composition over time (phase 1 versus phase 2 in chapter 4), most likely caused by colonic microbial metabolism that gradually converts sulindac into sulindac sulfide by sulfoxide reduction of the thioethers [180]. Analysis of human faecal samples by the group of Duggan showed that sulindac only makes up 5% of the total dose in faeces [179]. These results suggest that the fraction of sulindac sulfide depends on the colonic residence time in the presence of microflora. Consequently, it can be assumed that proximal colonic regions will be exposed to higher amount of sulindac compared to more distal regions and the inverse is true for sulindac sulfide.

While oral intake of 200 mg Celebrex resulted in an incomplete intestinal absorption, allowing a substantial fraction of solid material to arrive at the caecum, it bears repeating that colonic disposition is dependent on the drug dosage form, in particular when a poorly soluble compound is of interest. Paulson et al. (2000) studied the disposition of a single 300 mg dose of celecoxib in humans, but administered as a fine suspension reconstituted in 80 mL of apple juice/Tween 80/ethanol mixture instead of a capsule, and found that a mere 2.56% of the dose was excreted as celecoxib in either urine or faeces [198]. By using a fine suspension of celecoxib, the disintegration and dissolution is facilitated, substantially impacting the pharmacokinetic profile of the poorly soluble compound. In the study of Paulson, the therapeutic effect of celecoxib and metabolites will depend to a larger extent on systemic exposure, opposed to our *in vivo* studies where we witnessed that high caecal fractions of celecoxib resulted in a more pronounced gut-driven tissue accumulation, possibly enabling the anti-carcinogenic effect. Moreover, when Paulson et al. (2001) administered varying oral doses in rats, higher doses resulted in higher fractions of celecoxib that could be retrieved in the faeces [199]. Since we reported high caecal fractions for 200 mg, and it is not uncommon to prescribe 400 mg of Celebrex, it can be presumed that this observation can be extended to humans.

6.3 Implications for colonic drug disposition in pathophysiology

Although NSAIDs such as celecoxib and sulindac are preventive drugs for the development of colorectal cancer, in which a healthy human physiology is to be considered, they can also be used for treatments. However, the altered physiology in patients with colonic diseases will impact the drug disposition in numerous manners. It has been reported that inflammatory bowel disease (IBD), especially in case of ongoing inflammation, is linked to an abnormal gut barrier [200] that subsequently also affects drug absorption. For example, Johansson and colleagues showed that colonic mucus properties can be modulated in Crohn's disease (CD) and Ulcerative Colitis (UC) animal models and sigmoid colon tissue of active UC patients, thereby also allowing bacteria to penetrate the inner mucus layer, and come in close contact with the epithelium [28]. Furthermore, microbial dysbiosis in IBD, which is characterised by reduced diversity and temporal stability, and a decrease in *Firmicutes* and an increase in *Proteobacteria* at phylogenetic level, can dysregulate barrier function [201]. It is also apparent that dysbiosis is associated with colorectal cancer, often as a result from the ingested dietary components [202]. Moreover, patients with colorectal cancer may have slower bowel movements, since this has been associated with an increased risk in developing the disease [203]. The potential slower transit will impact the release of the drug and its exposure to the colonic mucosa. In contrast, UC and CD are linked to a shortened transit time (on average 24 h in UC and CD and 52 h in healthy volunteers) [53], which can be especially detrimental for formulations with slow release or dissolution of the drug. A shortened transit time can potentially alter the local pH since the pH can increase when the microbiome produces less SCFA due to time constraints and alter the ionisation state of drugs. It has been reported that a lack of SCFA can cause bacteria to produce lactic acid, which can decrease pH [55]. As such, numerous physiological variables (pH, microbiome composition, transit time, and others) are affected by colonic diseases, which subsequently also alter drug absorption.

6.4 Implementation of in vitro accumulation assays in drug development tests

In vitro models for the early stage assessment of drug candidates are ubiquitously used in pharmaceutical industry, allowing elimination of underperforming compounds and preventing late stage attrition. In doing so, the drug development process is optimized, both from an economical (decreasing time and expenses spend) and ethical (reduced preclinical testing) point of view. Most routinely available models are engineered to capture the intra gastric or small intestinal drug behaviour. However, few traditional *in vitro* tools exist that address the complexity of the colonic environment and their implication for drug disposition, and consequently, colon-targeting compounds and formulations suffer from inconsistent performance. With the recent advances made over the past 5 – 10 years in culturing technologies and bioengineering of stem cell derived systems, colonic systems enabling simultaneous permeability and stability assessment of drugs seem to be on the way or already achieved, but still at low throughput capacity and not fully characterized. When assessing those novel systems in their capability to accurately capture colonic drug disposition one should also consider the importance of accumulation studies. This is specifically crucial for colon-targeted drugs since they often aim to directly target the epithelium or immune cells of the lamina propria and are less desired to enter the blood stream. Scarcely addressed in current literature, chapter 5 gives insight into the accumulation behaviour of celecoxib and sulindac in two *in vitro* models, including the traditional Caco-2 cell line and human biopsies in the Ussing chamber model. Our research aim was three-fold:

1) To investigate the accumulation behaviour in mucus (colonic biopsies in the Ussing Chamber model)
2) To assess the accumulation in intestinal tissue (Caco-2, Ussing chamber)
3) To simulate suspension driven accumulation (Caco-2)

We assessed the apical driven accumulation of celecoxib and sulindac in the Caco-2 model (10 min, 5µM) and in the Ussing chamber model (1 h, 100µM) wherefore human colonic biopsies were used. In all accumulation experiments, relevant colonic conditions were simulated, i.e. by applying a thick mucus layer (Caco-2), by using FaSSCoF (Caco-2, UC) and by creating sink conditions through the addition of TPGS (0.2%) to the basolateral compartment (Caco-2,

UC). We observed that the extent of celecoxib accumulation surpasses sulindac in both mucus (Ussing chambers) and tissue across all tested models. Also *in vivo*, we reported a higher accumulation for celecoxib. This distinct observation is underpinned by the physicochemical properties (pKa, lipophilicity) of the drugs.

Substantial accumulation of celecoxib in mucus can be attributed to hydrophobic interactions ($logD_{7.8}$ = 4.01) with the mucins. Conversely, the relatively low accumulation of sulindac can ascribed to its negative ionisation state, which impedes the hydrophobic interactions from occurring ($logD_{7.8}$ = -0.36). Moreover, sulindac can get repulsed by the mucins of the mucus layer as the sialic acids of the heavily glycosylated protein-backbone are negatively charged as well, contributing to the low accumulation. Similar to mucus, we also observed a higher accumulation of celecoxib compared to sulindac in human tissue and Caco-2 cells. Again, this is likely due to celecoxib being an unionized drug with favourable physicochemical properties, allowing it to permeate the lipophilic cell membrane by transcellular diffusion. Due to its ionization and increased hydrophilicity, celecoxib accumulated better compared to its main metabolite carboxy celecoxib ($LogD_{7.8}$ of -0.20) in the Caco-2 model, which was also reflected in our previously reported *in vivo* accumulation data. The higher lipophilicity of the active sulindac sulfide metabolite ($LogD_{7.8}$ of 1.54) likely underlies its better accumulation compared to sulindac ($LogD_{7.8}$ of -0.38) in the Caco-2 model.

For both celecoxib and sulindac, the amount of accumulation in human tissue was consistently higher in the Ussing chamber model compared to the Caco-2 model. However, attention needs to be given to the varying properties of mucus and epithelial layers across models to correctly compare and interpret the data. Mucus, for which we have shown that it can serve as a drug depot and likely enables sustained drug release to the adjacent tissue, differs vastly between models. For instance, intestinal cell line models such as Caco-2 are routinely used in drug permeability experiments, yet do not have goblet cells and thus lack a mucus layer. In our series of experiments we applied a mucus layer of porcine origin as to circumvent this limitation [10], yet the single and uniformly distributed layer does not accurately represent the colonic mucus that is organized as a thick two-layer system [11]. Although human colonic biopsies in Ussing chambers serve as a physiologically relevant model for studying drug accumulation, the downside is that *ex vivo* conditions stimulate mucus production [198,199]. These considerations also need to be applied to the colonic models that are emerging. For example, recent progress

has been made to culture intestinal crypts into gut organoids that represent a close approximation of the *in vivo* situation, with VanDussen's group reporting that ileal and rectal organoids are capable of expressing a MUC2-rich and double layered mucus. The colonic organoids retained the complex and resistant mucus inner layer after a "disruption" experiment, while the loose outer mucus layer was removed. However, the 36 µm thick mucus layer in the organoid monolayers does not accurately represent the thickness of the human mucus layer, which is approximately 400–600 µm [204,205]. The human colon chip that uses microfluidic culture technology has been successful in reproducing a physiologically relevant bilayered mucus structure with a total thickness of 500–600 µm [130]. Indeed, these dimensions are closer to the living human colon, and will therefore contribute to a more *in vivo* relevant accumulation. It should be noted however that mucus thickness is region-dependent, even in the colon. For many models such as the EpiIntestinal, there has been limited characterization and therefore it is still questionable whether a mucus layer is present and relevant for the *in vivo* situation (no imaging of mucus layers in the EpiIntestinal has been performed, although the presence of MUC-2 through staining likely indicates its presence).

Furthermore, differences between accumulation values in models can be attributed to physiological properties such as the absorptive surface area, the tightness of the tissue, and the expression of transporters and drug metabolizing enzymes. The TEER values measured with EpiIntestinal™ ($152.5 \pm 39\ \Omega*cm^2$) are in close proximation to human intestinal *ex vivo* tissue ($50–100\ \Omega*cm^2$) indicating that structural features may more closely mimic intestinal tissue than Caco-2 cell monolayers with TEER values ranging from $250–2400\ \Omega*cm^2$ [206], likely generating more relevant *in vivo* like accumulation. The higher accumulation of celecoxib in human tissue can also be enabled by the relatively larger absorptive surface area compared to the 2D epithelial monolayer of the Caco-2 model, which only contains microvilli and no crypt structure. Similarly, accumulation of celecoxib was higher in the EpiIntestinal model (personal communication) compared to the Caco-2 system, which is likely due to the presence of the ileal crypt-villi architecture.

Overall, these studies have shown that the intrinsic accumulation differences between celecoxib and sulindac can be captured by *in vitro* models, and highlighted the importance of mucus on drug accumulation. However, differences in the mucus and tissue composition need to be accounted for when interpreting drug accumulation and permeation.

While the intrinsic difference in accumulation between celecoxib and sulindac was captured by solution-based *in vitro* assays, it is important to realise that the colonic lumen contains scarce and scattered pockets of highly viscous content that can result in a suboptimal dissolution and a substantial solid fraction of poorly soluble compounds. To this end, we used suspensions to account for undissolved drug fractions. We observed that while the concentration of the saturated celecoxib solution (15 µM) in the suspension experiment was only three-fold higher compared to experiments where a solution was used (5 µM), accumulation was 62 fold higher. Presumably, the favourable physicochemical properties that underlie the extensive accumulation of celecoxib will be followed by a fast dissolution from the undissolved powder, further enhancing drug accumulation. For sulindac, the increase in accumulation was relatively modest compared to the increase in dissolved concentration in the saturated solution, which is likely linked to the poor penetrative properties. The suspension-based accumulation assay thus indicated an increased difference in accumulation levels between celecoxib and sulindac, which is in line with the pronounced contrast in *in* vivo accumulation (1600 ng/mg vs 20 ng/mg for celecoxib and sulindac during the second colonoscopy period, respectively).

In general, both the Caco-2 model and the Ussing chamber model are promising *in vitro* tools to study drug accumulation and were able to distinguish between the tissue accumulation of celecoxib and sulindac. However, human tissue samples are short-lived (± 4 hours) and require invasive endoscopy which is not feasible for routine applications in drug absorption studies. Therefore, the low throughput nature of the Ussing chamber technique restricts its application in early stages of drug discovery. Nevertheless, it can ameliorate the prediction of drug absorption in late discovery or early development stage and contribute to the optimization of the lead compounds. In contrast, the Caco-2 model remains ubiquitously used in industrial and academical settings, given its high throughput nature, standardized protocols, and since it generates robust and reproducible data. Also for accumulation assays, the Caco-2 experiments resulted in the least variable drug concentrations. Therefore, Caco-2 accumulation assays will be easier to implement in the early stages of drug discovery. Recent accumulation assays such as the EpiIntestinal also have low throughput capacity and are not fully characterized for their use in permeability and metabolism studies.

Although promising, the optimization need of emerging colonic *in vitro* models impede its usefulness in the pharmaceutical industry and academia. To this end, the complexity of the

colonic environment and the implication for colonic drug disposition can be better captured through a combination of *in vitro* experiments with physiologically based pharmacokinetic modelling. To date, several software packages are commercially available that can be used to predict the oral drug disposition of colon-targeting compounds or formulations in humans (e.g. SimCYP®, Gastroplus ®). In particular, they can be of significant value to discern potential drug candidates that have a high prospect to accumulate in colonic tissue, and thereby achieve optimal target exposure. Since the colonic territory is still largely uncharted, data sets regarding the physiological/anatomical (tissue volumes, blood flow rate, enzyme abundance, etc.) and biochemical/physicochemical properties (distribution, clearance, and absorption) do require further exploration. For example, one prominent problem that current preclinical models cannot predict well is the partitioning of the luminal drug into the colonic tissue. Models such as GastroPlus do not account for tissue concentrations that originate from distribution. Although this feature is possible in SimCYP, SimCYP does not consider concentration gradients (gut-driven versus systemic-driven). Lastly, in the absence of colonic disposition data, the predictions are often not validated. In this regard, *in vivo* reference data that encompasses drug absorption characteristics such as solubility, permeability, biliary excretion, and tissue accumulation on a colonic level are essential. This doctoral dissertation is a first step, but further academic and industrial research is needed.

Supplementary Figure

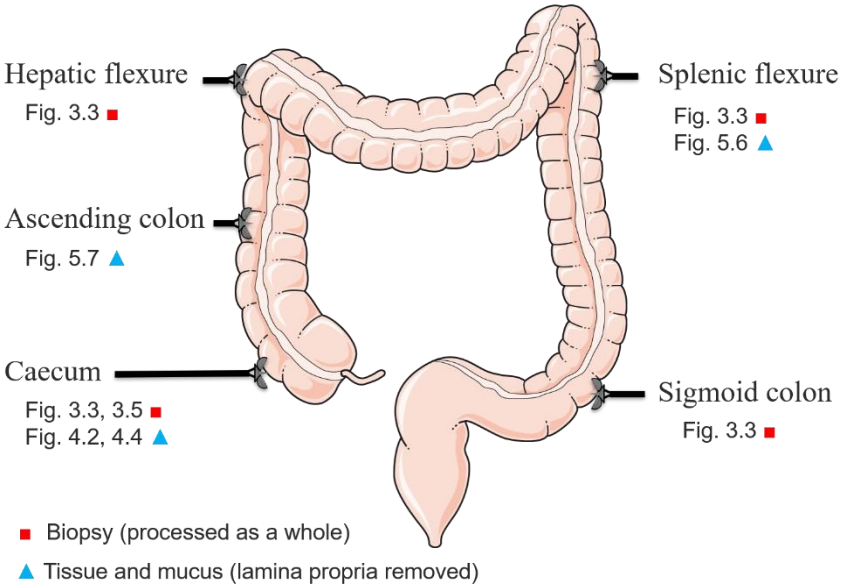

Fig. S1: Schematic representation of the region where biopsies were sampled and how biopsies were processed (■: biopsies were processed as a whole; ▲ the lamina propria was removed prior to exposure, and the mucus was scraped off post experiment).

English summary

Over the past 20–30 years, the incidence of inflammatory bowel disease has increased substantially. Similarly, colorectal cancer (CRC) cases are continuously rising, especially in developing countries, with CRC being the third leading cause of cancer death and the fourth most diagnosed cancer in the world. Epidemiological data has shown preventive effects on the development of colorectal cancer for the NSAIDs celecoxib and sulindac, which are commonly being used as immediate release formulations; however, it is not known how sufficiently high concentrations in colonic tissue are realised. For immediate release formulations, research has focused mostly on clarifying the drug disposition at the small intestine as it is the main site of absorption, allowing drugs to reach the targeted site through the systemic circulation (systemic driven accumulation). However, since some NSAIDs display poor solubility and high lipophilicity, a common characteristic of new drug candidates, incomplete absorption in the small intestine can allow a drug to reach the colon and enable local exposure to the colonic tissue (gut driven accumulation). Therefore, this dissertation explores whether colonic accumulation is gut-driven or systemic driven and wants to clarify the dissolution and accumulation behaviour through *in vitro* tools that emulate the colonic environment.

First we clarified how the *in vitro* characteristics of celecoxib and sulindac could potentially underlie the arrival of a fraction of the drug to the colon through transit. Since the pH of the intraluminal environment can affect the solubility of a drug, we first performed an *in vitro* transfer experiment in which the pH-shift along the gastrointestinal tract (stomach – small intestine – colon) was simulated (FaSSGF, pH 1.5 - FaSSIF, pH 6.5 - FaSSIF: pH 6.0). We found a remarkably low release of celecoxib from the capsule (Celebrex®) at all stages. In contrast to the neutral celecoxib, sulindac is a weak acid (pKa 4.09) with moderate permeability that undergoes a change in ionisation state upon transfer from the acidic stomach to the more neutral environment of the small intestine. This concurs with a low solubility (gastric pH) to a high solubility (intestinal and colonic pH) due to a change in ionisation state. Indeed, the *in vitro* transfer experiment showed a more pronounced, yet still incomplete, dissolution of sulindac compared to celecoxib. This *in vitro* experiment was a first indication that the incomplete dissolution of celecoxib and sulindac can possibly result in the caecal arrival of the drug, potentially enabling local drug accumulation in colonic tissue.

To evaluate whether *in vivo* tissue accumulation is systemic and/or gut-driven, blood, colonic contents and tissue had to be sampled simultaneously in human volunteers. To this end, a preliminary study was performed to establish a colon preparation procedure and sampling technique to collect contents and tissue. To ensure that the physiological state of the proximal colon remains undisturbed, we opted to administer rectal enemas after volunteers had followed a three-day low fibre diet. By varying the frequency and volume of the enemas, we observed that a one-time enema of 250 mL of water appeared sufficient to cleanse the left hemicolon while avoiding spill over to the right hemicolon where then physiologically relevant samples could be taken. Using the suction channel of the colonoscope turned out to be the most reliable way to collect the contents from the proximal colon. However, we found that the viscosity of the colonic contents limits this technique to one sample per colonoscopy. To follow tissue accumulation, we decided to collect biopsies in a time dependent way. This procedure was then applied to two clinical studies where we aimed to distinguish systemic from gut-driven tissue accumulation after oral intake of Celebrex® (celecoxib) or Arthrocine® (sulindac), as to clarify what pharmacokinetic processes underlie the anticarcinogenic effect. More specifically, the clinical studies were designed so that the systemic T_{max} of the drug was situated between two colonoscopy periods (90 minutes), both during which caecal tissue and colonic content was collected. Plasma levels are expected to increase in the first period (between 1 and 2.5 h post drug intake) and drive caecal tissue accumulation. In the second period (between 6 and 7.5 h post drug intake), plasma levels are expected to decrease. Tissue concentrations could be systemically driven (in which case they would decrease as well in the second period), but also gut driven if the drug arrived at the caecal lumen through transit.

In a first clinical study, healthy human volunteers were given one capsule of Celebrex® (celecoxib) with 240 mL of tap water. We found during the first period that caecal tissue concentrations remained relatively low in spite of increasing plasma concentrations; and celecoxib was not detected in the luminal contents of the caecum, collected after 2.5 h. In contrast, during the second period, tissue concentrations were substantially higher than during the first period which is in accordance with the high concentrations in the contents. *In situ* experiments with rats furthermore showed that biliary excretion (upon absorption, systemically available drug can be excreted through the bile duct back into the small intestine) does not underlie the high caecal concentrations, as bile contained mostly liver-mediated metabolites.

Taken together, *in vivo and in vitro* data clearly indicated that accumulation of celecoxib in caecal tissue is due to the presence of high luminal concentrations, which is a result from poor intestinal solubility and absorption. The accumulation is thus not solely dependent on the systemic profile and can be gut driven once the drug reaches the caecal lumen.

In a second clinical study, we monitored the concentrations of sulindac and metabolites in the systemic circulation, the caecal lumen and caecal tissue following oral intake of an Arthrocine® tablet (200 mg sulindac). Similar as to the celecoxib study, we observed that sulindac can arrive at the colonic lumen which then accumulates in a high and local manner in the colonic tissue. However, and in line with high dissolution in the *in vitro* transfer experiment resulting in intestinal absorption, we observed that the caecal concentrations of sulindac are considerably lower than for celecoxib. *In situ* rat experiments indicated that biliary excretions almost exclusively consisted of sulindac after intravenous injection of a bolus of sulindac or sulindac sulfide, and that metabolites were non-existent or limited respectively. The fraction of sulindac that reaches the caecum of healthy volunteers following oral administration therefore probably results from incomplete small intestinal dissolution, which is due to the relatively low intrinsic solubility and the more pronounced biliary excretion of sulindac compared to celecoxib.

When considering therapeutic efficacy, it is noteworthy that the concentrations of celecoxib and sulindac that are required to get an anti-carcinogenic effect in cell culture experiments are generally between 10 µM and 100 µM, which are not reached in plasma by administering a single 200 mg dose. In this respect, the relatively high levels of celecoxib and sulindac in the colonic lumen and the resulting accumulation in colonic tissue seem essential to obtain the reported anti-carcinogenic effects.

Interestingly, celecoxib reached substantially higher drug concentrations in caecal contents and gut-driven tissue concentrations compared to sulindac. This emphasises the importance of evaluating the accumulation in colonic tissue, taking into account the drug's physicochemical properties and the physiological conditions in the colon. To predict the potential of drugs and drug candidates to accumulate in colonic tissue and exert a local effect, relevant non-clinical absorption models are needed, such as the Caco-2 cell model or the Ussing chambers setup with excised intestinal tissue. In a series of experiments, we assessed the accumulation in mucus

and tissue, and studied the possible release from the cells and the impact of using suspensions on the accumulation behaviour in the Caco-2 system under relevant colonic conditions.

We found that *in vitro* tools were capable of predicting the *in vivo* accumulation behaviour to some extent; the amount of celecoxib accumulation surpasses sulindac in both mucus and tissue, and across all tested models, which is in line with the higher *in vivo* accumulation for celecoxib. This distinct observation is underpinned by the physicochemical properties (pKa, lipophilicity) of the compounds. For mucus, the negative ionisation state of sulindac at a colonic pH infers interaction filtering, as the drug can be repulsed by the mucins that also carry a negative charge. In contrast, celecoxib as a net-neutral compound (pKa 10.6) likely experiences a better mucopenetration. Similarly for tissue, lipophilic and unionized low molecular weight drugs such as celecoxib can partition through the lipophilic cell membrane by passive diffusion.

While the intrinsic difference in accumulation between celecoxib and sulindac was captured by solution-based *in vitro* assays, it is important to realise that the colonic lumen contains scarce and scattered pockets of highly viscous content that can result in a suboptimal dissolution and a substantial solid fraction of poorly soluble compounds. To this end, we used suspensions to account for undissolved drug fractions, which indeed generated values more in line with *in vivo* accumulation data.

In conclusion, we demonstrated that incomplete intestinal dissolution of immediate release formulations can underlie the caecal arrival of drugs via transit, enabling local accumulation in colonic tissue that is likely needed to induce remission. Furthermore, we were able to clarify the colonic accumulation behaviour through *in vitro* tools such as the Caco-2 system and the Ussing chamber model. In a next stage, the combination of *in vivo/ in vitro* data with *in silico* tools can provide valuable early screening of drug candidate formulations, preventing late-stage attrition.

Nederlandstalige samenvatting

In de voorbije 20 tot 30 jaar worden inflammatoire darmziekten en colorectale kanker steeds vaker vastgesteld. Colorectale kanker is zelfs de derde grootste oorzaak van kanker-gerelateerde sterfgevallen, en de vierde meest gestelde diagnose op wereldschaal. Epidemiologische data hebben aangetoond dat NSAIDs (non-steroidal anti-inflammatory drugs) zoals celecoxib en sulindac een preventieve werking uitoefenen op de ontwikkeling van colorectale kanker. Het is echter niet geweten op welke manier therapeutische concentraties worden bereikt in het dikke darmweefsel. Dit kan enerzijds via systemische blootstelling na opname van het geneesmiddel in de dunne darm, of anderzijds door directe blootstelling aan het geneesmiddel in de dikke darm. Aangezien NSAIDs vaak lipofiel (vetoplosbaar) en slecht oplosbaar zijn in de waterige intraluminale inhoud van de dunne darm, net zoals vele nieuwe kandidaat geneesmiddelen, is onvolledige intestinale opname plausibel. Het geneesmiddel kan vervolgens de dikke darm bereiken, waarna er lokale blootstelling plaatsvindt. Het onderzoek in deze thesis tracht te verklaren of accumulatie van celecoxib en sulindac in dikke darmweefsel afkomstig is van lokale of systemische bloostelling, gaat dieper in op de dispositie van geneesmiddelen in de dikke darm, en kadert het accumulatiegedrag van de geneesmiddelen aan de hand van relevante *in vitro* modellen.

Eerst bestudeerden we of de fysicochemische eigenschappen van celecoxib en sulindac mogelijks kunnen leiden tot een onopgeloste caecale fractie. Aangezien de pH van de verschillende gastro-intestinale segmenten de opgeloste concentratie van het geneesmiddel en de vrijzetting ervan uit de formulering kan beïnvloeden, voerden we eerst een *in vitro* transfer experiment uit dat de pH-fluctuaties in het gastro-intestinaal systeem nabootst. Na één capsule Celebrex® aan te brengen in het *in vitro* systeem (maag: FaSSGF pH 1.5; dunne darm: FaSSIF pH 6.5; dikke darm: FaSSIF pH 6.0), vonden we opmerkelijk lage hoeveelheden van celecoxib in al de segmenten. Sulindac is een zwak zuur (pKa 4.09) met middelmatige permeabiliteit, en verkrijgt een negatieve lading wanneer het van de zure maaginhoud naar de meer neutrale omgeving van de dunne darm gaat. Dit gaat gepaard met een verandering in oplosbaarheid: van een lage (gastrische pH) naar een hoge oplosbaarheid (pH in de dunne en dikke darm). Inderdaad, het *in vitro* experiment toonde een substantiële, doch onvolledige, vrijgave van sulindac in vergelijking met het neutrale celecoxib. Dit *in vitro* experiment was een eerste

indicatie dat de gelimiteerde oplosbaarheid van celecoxib en sulindac kan resulteren in een fractie dat de dikke darm kan bereiken via de transit, en vervolgens lokaal kan accumuleren in het weefsel.

Om te bepalen of luminale of systemische blootstelling resulteert in accumulatie na orale inname van het geneesmiddel, moeten we dikke darmvochten en -biopsies verzamelen, en gelijktijdig bloedstalen afnemen. Hiertoe dienden we eerst de darmvoorbereiding en vochtcollectie te optimaliseren. Om de fysiologische toestand van het proximale colon te behouden, werden rectale lavementen toegediend aan vrijwilligers die voorheen een vezelarm dieet hadden gevolgd. Door de frequentie en volume van het lavement te variëren, concludeerden we dat een eenmalig lavement van 250 mL voldoende is om het linker hemicolon te reinigen en verstoring van het rechter hemicolon te vermijden. Het suctiekanaal van de coloscoop werd dan gebruikt om de dikke darmvochten te verzamelen. Omwille van de hoge viscositeit van de darmvochten kan er echter maar één staal per coloscopie geaspireerd worden. Om weefselaccumulatie op te volgen verzamelden we daarom biopsies op regelmatige tijdstippen. Deze techniek werd vervolgens toegepast om te achterhalen of weefselaccumulatie van celecoxib en sulindac via systemische en/of luminale blootstelling bereikt wordt. Meer specifiek: de klinische studies werden opgesteld zodat de systemische T_{max} van het geneesmiddel tussen twee coloscopie periodes (90 min) valt. Plasmaconcentraties werden verwacht te stijgen in de eerste periode (tussen 1 en 2.5u na orale inname van het geneesmiddel) waardoor er weefselaccumulatie plaatsvindt. In de tweede periode (tussen 6 en 7.5u na inname), werden plasmaconcentraties verwacht te dalen. Weefselconcentraties kunnen dan opgebouwd worden door systemische blootstelling (waardoor ze dalen tijdens de tweede periode) maar ook opgebouwd worden door directe en lokale blootstelling nadat het geneesmiddel in het caecale lumen terechtkomt.

In een eerste klinische studie werd aan gezonde vrijwilligers één capsule Celebrex® (celecoxib) gegeven met 240 mL water. We observeerden dat caecale weefselconcentraties relatief laag bleven ondanks een toename in plasmaconcentraties gedurende de eerste periode; celecoxib werd niet gedetecteerd in de luminale vochten, welke verzameld werden na 2.5u. Tijdens de tweede periode waren weefselconcentraties substantieel hoger dan tijdens de eerste periode, wat overeenstemt met de hoge hoeveelheden aan celecoxib in de vochten. Bovendien toonden we met *in situ* rat experimenten aan dat galexcreties (systemisch beschikbaar geneesmiddel kan

opnieuw geëxcreteerd worden in de dunne darm na opname) voornamelijk metabolieten bevatten, en niet celecoxib, en dus weinig zal bijdragen tot de hoge caecale concentraties. Ook lokale omzetting door de epitheelcellen en microbioom werd uitgesloten. De bekomen data tonen dus dat accumulatie van celecoxib in caecaal weefsel gedreven kan worden door luminale concentraties, welke voornamelijk het gevolg zijn van een slechte oplosbaarheid en onvolledige absorptie in de dunne darm. De weefselaccumulatie is dus niet enkel afhankelijk van de systemische concentraties.

In een tweede klinische studie bepaalden we de concentraties van sulindac en de metabolieten in de systemische circulatie, het lumen, en in dikke darmweefsel na inname van Arthrocine® (200 mg sulindac). We observeerden dat sulindac het lumen van de dikke darm kan bereiken via de transit, gelijkaardig aan celecoxib, en lokaal kan accumuleren. In lijn met de goede vrijzetting van sulindac in het *in vitro* transfer experiment en absorptie in de dunne darm, zijn de caecale concentraties van sulindac aanzienlijk lager dan voor celecoxib. Bovendien toonden *in situ* rat experimenten aan dat galexcreties voornamelijk sulindac en niet metabolieten bevatten. De fractie die het caecum bereikt is daardoor grotendeels te danken aan onvolledige dissolutie/absorptie in de dunne darm, en dit omwille van een gelimiteerde intrinsieke oplosbaarheid en de relatief grotere galexcretie van sulindac in vergelijking met celecoxib.

Voor zowel celecoxib als sulindac is het opmerkelijk dat de anti-carcinogene effecten in celcultuurexperimenten meestal bekomen worden na blootstelling aan 10-100 µM. Zulke concentraties worden echter niet bereikt in het bloed na inname van één enkele 200 mg dosis. Dit impliceert dat de hogere concentraties in het lumen hoogstwaarschijnlijk vereist zijn opdat therapeutisch werkzame concentraties in het weefsel bereikt kunnen worden.

Tot op heden worden *in vitro* modellen die de *in vivo* situatie simuleren voornamelijk gebruikt om de dispositie in de dunne darm te bestuderen, waarbij de focus op permeatie/absorptie en stabiliteit ligt. Voor celecoxib en sulindac, of voor colon-gerichte formuleringen dewelke een uitgestelde afgifte beogen, is absorptie of systemische beschikbaarheid echter niet het primaire doel, aangezien directe blootstelling kan leiden tot lokale accumulatie. Hiertoe gingen we in het tweede luik van deze studie na hoe relevante niet-klinische absorptiemodellen zoals het Caco-2 model en de Ussing chamber setup met humaan weefsel het *in vivo* accumulatie gedrag kunnen voorspellen. In een reeks van experimenten gingen we de accumulatie in mucus en

weefsel na, bestudeerden we de mogelijke vrijzetting uit de cellen, en trachtten we het effect van relevante incubatiecondities (suspensies) op accumulatie te bestuderen.

We observeerden dat *in vitro* modellen het *in vivo* accumulatie gedrag tot een zekere graad kunnen voorspellen: de accumulatie van celecoxib was aanzienlijk hoger dan sulindac in mucus en weefsel, wat overeenkomt met de resultaten van *in vivo* studies. Bovendien werd dit waargenomen in al de gebruikte modellen. Dit kan verklaard worden door de fysicochemische eigenschappen van de geneesmiddelen. Sulindac heeft een negatieve lading bij een pH van 7.8, waardoor het molecule afgestoten kan worden door de mucus die eveneens negatieve ladingen draagt. In tegenstelling tot sulindac is celecoxib een neutraal molecule bij dezelfde pH, wat gunstig is voor een goede mucopenetratie. Deze redenering is eveneens van toepassing op weefsel, waarbij lipofiele en niet-geïoniseerde moleculen zoals celecoxib het celmembraan kunnen kruisen door passieve diffusie.

Hoewel het intrinsieke verschil in accumulatie tussen celecoxib en sulindac gevat kan worden door *in vitro* modellen waarin er gebruikt wordt gemaakt van oplossingen, is het belangrijk om te beseffen dat dikke darmvochten visceus zijn, gekenmerkt worden door een laag volume, en verdeeld zijn in individuele 'pockets', wat leidt tot een suboptimale dissolutie van slecht oplosbare geneesmiddelen en een substantiële vaste fractie. Inderdaad, het gebruik van suspensies waarin onopgeloste partikels aanwezig zijn stelt daarom een meer fysiologisch relevante testconditie voor. Wanneer we een *in vitro* accumulatie experiment met suspensies in plaats van oplossingen uitvoerden, bleken deze meer in lijn te liggen met *in vivo* accumulatie data.

Afsluitend kunnen we stellen dat onvolledige intestinale dissolutie en absorptie van slecht oplosbare geneesmiddelen kan leiden tot fracties van het geneesmiddel die het colon kunnen bereiken via darmtransit, en vervolgens lokaal kunnen accumuleren zodat een anti-carcinogeen effect kan bekomen worden. Bovendien toonden we aan dat *in vitro* modellen zoals Caco-2 en Ussing Chambers gebruikt kunnen worden om het *in vivo* accumulatie gedrag te verhelderen. In een volgende stap zal de combinatie van *in vivo*/*in vitro* data met *in silico* methodes zeer waardevol zijn ter verbetering van de selectie van kandidaat geneesmiddelen.

Bibliography

1. Rawla, P.; Sunkara, T.; Barsouk, A. Epidemiology of Colorectal Cancer: Incidence, Mortality, Survival, and Risk Factors. *Przeglad Gastroenterol.* **2019**, *14*, 89–103, doi:10.5114/pg.2018.81072.
2. Bertagnolli, M.M.; Eagle, C.J.; Zauber, A.G.; Redston, M.; Solomon, S.D.; Kim, K.; Tang, J.; Rosenstein, R.B.; Wittes, J.; Corle, D.; et al. Celecoxib for the Prevention of Sporadic Colorectal Adenomas. *N. Engl. J. Med.* **2006**, *355*, 873–884, doi:10.1056/NEJMoa061355.
3. Herendeen, J.M.; Lindley, C. Use of NSAIDs for the Chemoprevention of Colorectal Cancer. *Ann. Pharmacother.* 2003.
4. Clevers, H. The Intestinal Crypt, a Prototype Stem Cell Compartment. *Cell* **2013**, *154*, 274–284, doi:10.1016/j.cell.2013.07.004.
5. Van Eyken, P.; Fanni, D.; Gerosa, C.; Ambu, R. The Normal Biopsy: Mucosa and Submucosa. In *Colitis: A Practical Approach to Colon Biopsy Interpretation*; Geboes, K., Nemolato, S., Leo, M., Faa, G., Eds.; Springer International Publishing: Cham, 2014; pp. 1–16 ISBN 978-3-319-08028-4.
6. Ayabe, T.; Satchell, D.P.; Wilson, C.L.; Parks, W.C.; Selsted, M.E.; Ouellette, A.J. Secretion of Microbicidal α-Defensins by Intestinal Paneth Cells in Response to Bacteria. *Nat. Immunol.* **2000**, *1*, 113–118, doi:10.1038/77783.
7. Latorre, R.; Sternini, C.; De Giorgio, R.; Greenwood-Van Meerveld, B. Enteroendocrine Cells: A Review of Their Role in Brain-Gut Communication. *Neurogastroenterol. Motil.* **2016**, *28*, 620–630, doi:10.1111/nmo.12754.
8. Nicoletti, C. Unsolved Mysteries of Intestinal M Cells. *Gut* **2000**, *47*, 735–739, doi:10.1136/gut.47.5.735.
9. Kim, Y.S.; Ho, S.B. Intestinal Goblet Cells and Mucins in Health and Disease: Recent Insights and Progress. **2010**, doi:10.1007/s11894-010-0131-2.
10. Cheng, H. Origin, Differentiation and Renewal of the Four Main Epithelial Cell Types in the Mouse Small Intestine II. Mucous Cells. *Am. J. Anat.* **1974**, *141*, 481–501, doi:10.1002/aja.1001410404.
11. Johansson, M.E.V.; Larsson, J.M.H.; Hansson, G.C. The Two Mucus Layers of Colon Are Organized by the MUC2 Mucin, Whereas the Outer Layer Is a Legislator of Host–Microbial Interactions. *Proc. Natl. Acad. Sci. U. S. A.* **2011**, *108*, 4659–4665, doi:10.1073/pnas.1006451107.
12. Sellers, R.S.; Morton, D. The Colon: From Banal to Brilliant. *Toxicol. Pathol.* **2014**, *42*, 67–81, doi:10.1177/0192623313505930.
13. Johansson, M.E.V.; Sjövall, H.; Hansson, G.C. The Gastrointestinal Mucus System in Health and Disease. *Nat. Rev. Gastroenterol. Hepatol.* **2013**, *10*, 352–361, doi:10.1038/nrgastro.2013.35.
14. Rahner, C.; Mitic, L.L.; Anderson, J.M. Heterogeneity in Expression and Subcellular Localization of Claudins 2, 3, 4, and 5 in the Rat Liver, Pancreas, and Gut. *Gastroenterology* **2001**, *120*, 411–422, doi:10.1053/GAST.2001.21736.
15. Hewitt, K.J.; Agarwal, R.; Morin, P.J. The Claudin Gene Family: Expression in Normal and Neoplastic Tissues. *BMC Cancer* **2006**, *6*, 186, doi:10.1186/1471-2407-6-186.
16. Lu, Z.; Ding, L.; Lu & Yan-Hua Chen, Q. Tissue Barriers Claudins in Intestines. *Claudins Intest. Tissue Barriers* **2013**, *1*, 3, doi:10.4161/tisb.24978.

17. Xu, J.; Lin, Y.; Boulas, P.; Peterson, M.L. Low Colonic Absorption Drugs: Risks and Opportunities in the Development of Oral Extended Release Products. *Expert Opin. Drug Deliv.* **2018**, *15*, 197–211, doi:10.1080/17425247.2018.1389889.
18. Mandagere, A.K.; Thompson, T.N.; Hwang, K.-K. Graphical Model for Estimating Oral Bioavailability of Drugs in Humans and Other Species from Their Caco-2 Permeability and in Vitro Liver Enzyme Metabolic Stability Rates. *J. Med. Chem.* **2002**, *45*, 304–311, doi:10.1021/jm010152k.
19. Youhanna, S.; Lauschke, V.M. The Past , Present and Future of Intestinal In Vitro Cell Systems for Drug Absorption Studies. *J. Pharm. Sci.* **2020**, 1–16, doi:10.1016/j.xphs.2020.07.001.
20. Kararli, T.T.; Searle, G.D. *REVIEW ARTICLE COMPARISON OF THE GASTROINTESTINAL ANATOMY, PHYSIOLOGY, AND BIOCHEMISTRY OF HUMANS AND COMMONLY USED LABORATORY ANIMALS*; 1995; Vol. 16;.
21. Thomson, A.; Smart, K.; Somerville, M.S.; Lauder, S.N.; Appanna, G.; Horwood, J.; Sunder Raj, L.; Srivastava, B.; Durai, D.; Scurr, M.J.; et al. The Ussing Chamber System for Measuring Intestinal Permeability in Health and Disease. *BMC Gastroenterol.* **2019**, *19*, 98, doi:10.1186/s12876-019-1002-4.
22. Krug, S.M.; Schulzke, J.D.; Fromm, M. Tight Junction, Selective Permeability, and Related Diseases. *Semin. Cell Dev. Biol.* **2014**, *36*, 166–176, doi:10.1016/j.semcdb.2014.09.002.
23. Drozdzik, M.; Busch, D.; Lapczuk, J.; Müller, J.; Ostrowski, M.; Kurzawski, M.; Oswald, S. Protein Abundance of Clinically Relevant Drug Transporters in the Human Liver and Intestine: A Comparative Analysis in Paired Tissue Specimens. *Clin. Pharmacol. Ther.* **2019**, *105*, 1204–1212, doi:10.1002/cpt.1301.
24. Fritz, A.; Busch, D.; Lapczuk, J.; Ostrowski, M.; Drozdzik, M.; Oswald, S. Expression of Clinically Relevant Drug-Metabolizing Enzymes along the Human Intestine and Their Correlation to Drug Transporters and Nuclear Receptors: An Intra-Subject Analysis. *Basic Clin. Pharmacol. Toxicol.* **2019**, *124*, 245–255, doi:10.1111/bcpt.13137.
25. Drozdzik, M.; Busch, D.; Lapczuk, J.; Müller, J.; Ostrowski, M.; Kurzawski, M.; Oswald, S. Protein Abundance of Clinically Relevant Drug-Metabolizing Enzymes in the Human Liver and Intestine: A Comparative Analysis in Paired Tissue Specimens. *Clin. Pharmacol. Ther.* **2018**, *104*, 515–524, doi:10.1002/cpt.967.
26. Drozdzik, M.; Gröer, C.; Penski, J.; Lapczuk, J.; Ostrowski, M.; Lai, Y.; Prasad, B.; Unadkat, J.D.; Siegmund, W.; Oswald, S. Protein Abundance of Clinically Relevant Multidrug Transporters along the Entire Length of the Human Intestine. *Mol. Pharm.* **2014**, *11*, 3547–3555, doi:10.1021/mp500330y.
27. Li, M.; De Graaf, I.A.M.; Van De Steeg, E.; De Jager, M.H.; Groothuis, G.M.M. The Consequence of Regional Gradients of P-Gp and CYP3A4 for Drug-Drug Interactions by P-Gp Inhibitors and the P-Gp/CYP3A4 Interplay in the Human Intestine Ex Vivo. *Toxicol. In Vitro* **2016**, *40*, 26–33, doi:10.1016/j.tiv.2016.12.002.
28. Johansson, M.E.V.; Gustafsson, J.K.; Holmén-Larsson, J.; Jabbar, K.S.; Xia, L.; Xu, H.; Ghishan, F.K.; Carvalho, F.A.; Gewirtz, A.T.; Sjövall, H.; et al. Bacteria Penetrate the Normally Impenetrable Inner Colon Mucus Layer in Both Murine Colitis Models and Patients with Ulcerative Colitis. *Gut* **2014**, *63*, 281–291, doi:10.1136/gutjnl-2012-303207.

29. Bajka, B.H.; Rigby, N.M.; Cross, K.L.; Macierzanka, A.; Mackie, A.R. The Influence of Small Intestinal Mucus Structure on Particle Transport Ex Vivo. *Colloids Surf. B Biointerfaces* **2015**, *135*, 73–80, doi:10.1016/J.COLSURFB.2015.07.038.
30. Szentkuti, L.; Lorenz, K. The Thickness of the Mucus Layer in Different Segments of the Rat Intestine. *Histochem. J.* **1995**, *27*, 466–72.
31. Varum, F.J.O.; McConnell, E.L.; Sousa, J.J.S.; Veiga, F.; Basit, A.W. Mucoadhesion and the Gastrointestinal Tract. *Crit. Rev. Ther. Drug Carrier Syst.* 2008, *25*, 207–258.
32. McConnell, E.L.; Fadda, H.M.; Basit, A.W. Gut Instincts: Explorations in Intestinal Physiology and Drug Delivery. *Int. J. Pharm.* **2008**, *364*, 213–226, doi:10.1016/j.ijpharm.2008.05.012.
33. Strugala, V.; Dettmar, P.W.; Pearson, J.P. Thickness and Continuity of the Adherent Colonic Mucus Barrier in Active and Quiescent Ulcerative Colitis and Crohn's Disease. *Int. J. Clin. Pract.* **2008**, *62*, 762–769, doi:10.1111/j.1742-1241.2007.01665.x.
34. Desai, M.A.; Vadgama, P. Estimation of Effective Diffusion Coefficients of Model Solutes through Gastric Mucus: Assessment of a Diffusion Chamber Technique Based on Spectrophotometric Analysis. *ET J.* **1991**, *116*, 1113–1116, doi:10.1039/AN9911601113.
35. Araújo, F.; Martins, C.; Azevedo, C. Chemical Modification of Drug Molecules as Strategy to Reduce Interactions with Mucus. *Adv. Drug Deliv. Rev.* **2018**, *124*, 98–106, doi:10.1016/J.ADDR.2017.09.020.
36. Behrens, I.; Stenberg, P.; Artursson, P.; Kissel, T. Transport of Lipophilic Drug Molecules in a New Mucus-Secreting Cell Culture Model Based on HT29-MTX Cells. *Pharm. Res.* **2001**, *18*, 1138–45.
37. Wikman, A.; Karlsson, J.; Carlstedt, I.; Artursson, P. A Drug Absorption Model Based on the Mucus Layer Producing Human Intestinal Goblet Cell Line HT29-H. *Pharm. Res.* **1993**, *10*, 843–52.
38. Matthes, I.; Nimmerfall, F.; Vonderscher, J.; Sucker, H. [Mucus models for investigation of intestinal absorption mechanisms. 4. Comparison of mucus models with absorption models in vivo and in situ for prediction of intestinal drug absorption]. *Pharm.* **1992**, *47*, 787–791.
39. Desai, M.A.; Mutlu, M.; Vadgama, P. A Study of Macromolecular Diffusion through Native Porcine Mucus. *Experientia* **1992**, *48*, 22–6.
40. Lai, S.K.; Wang, Y.-Y.; Cone, R.; Wirtz, D.; Hanes, J. Altering Mucus Rheology to "Solidify" Human Mucus at the Nanoscale. *PLOS ONE* **2009**, *4*, e4294, doi:10.1371/journal.pone.0004294.
41. Tang, B.C.; Dawson, M.; Lai, S.K.; Wang, Y.-Y.; Suk, J.S.; Yang, M.; Zeitlin, P.; Boyle, M.P.; Fu, J.; Hanes, J. Biodegradable Polymer Nanoparticles That Rapidly Penetrate the Human Mucus Barrier. *Proc. Natl. Acad. Sci.* **2009**, *106*, 19268–19273, doi:10.1073/pnas.0905998106.
42. Shamat, M.A. The Role of the Gastrointestinal Microflora in the Metabolism of Drugs. *Int. J. Pharm.* **1993**, *97*, 1–13, doi:10.1016/0378-5173(93)90121-U.
43. Pei, L. yan; Ke, Y. shi; Zhao, H. hu; Wang, L.; Jia, C.; Liu, W. zhi; Fu, Q. hui; Shi, M. ni; Cui, J.; Li, S. chun Role of Colonic Microbiota in the Pathogenesis of Ulcerative Colitis. *BMC Gastroenterol.* **2019**, *19*, doi:10.1186/s12876-019-0930-3.
44. Zoetendal, E.G.; Von Wright, A.; Vilpponen-Salmela, T.; Ben-Amor, K.; Akkermans, A.D.L.; De Vos, W.M. Mucosa-Associated Bacteria in the Human Gastrointestinal Tract Are Uniformly Distributed along the Colon and Differ from the Community

Recovered from Feces. *Appl. Environ. Microbiol.* **2002**, *68*, 3401–3407, doi:10.1128/AEM.68.7.3401-3407.2002.
45. Eckburg, P.B.; Bik, E.M.; Bernstein, C.N.; Purdom, E.; Dethlefsen, L.; Sargent, M.; Gill, S.R.; Nelson, K.E.; Relman, D.A. Diversity of the Human Intestinal Microbial Flora. *Science* **2005**, *308*, 1635–1638, doi:10.1126/science.1110591.
46. Zimmermann, M.; Zimmermann-Kogadeeva, M.; Wegmann, R.; Goodman, A.L. Mapping Human Microbiome Drug Metabolism by Gut Bacteria and Their Genes. *Nature* **2019**, *570*, 462–467, doi:10.1038/s41586-019-1291-3.
47. Cummings, J.H.; Hill, M.J.; Bone, E.S.; Branch, W.J.; Jenkins, D.J. The Effect of Meat Protein and Dietary Fiber on Colonic Function and Metabolism. II. Bacterial Metabolites in Feces and Urine. *Am. J. Clin. Nutr.* **1979**, *32*, 2094–2101, doi:10.1093/ajcn/32.10.2094.
48. Joossens, M.; Huys, G.; Cnockaert, M.; De Preter, V.; Verbeke, K.; Rutgeerts, P.; Vandamme, P.; Vermeire, S. Dysbiosis of the Faecal Microbiota in Patients with Crohn's Disease and Their Unaffected Relatives. *Gut* **2011**, *60*, 631–637, doi:10.1136/gut.2010.223263.
49. Murray, K.; Hoad, C.L.; Mudie, D.M.; Wright, J.; Heissam, K.; Abrehart, N.; Pritchard, S.E.; Al Atwah, S.; Gowland, P.A.; Garnett, M.C.; et al. Magnetic Resonance Imaging Quantification of Fasted State Colonic Liquid Pockets in Healthy Humans. *Mol. Pharm.* **2017**, *14*, 2629–2638, doi:10.1021/acs.molpharmaceut.7b00095.
50. Schiller, C.; FROHLICH, C.-P.; GIESSMANN, T.; SIEGMUND, W.; MONNIKES, H.; HOSTEN, N.; WEITSCHIES, W. Intestinal Fluid Volumes and Transit of Dosage Forms as Assessed by Magnetic Resonance Imaging. *Aliment. Pharmacol. Ther.* **2005**, *22*, 971–979, doi:10.1111/j.1365-2036.2005.02683.x.
51. Diakidou, A.; Vertzoni, M.; Goumas, K.; Söderlind, E.; Abrahamsson, B.; Dressman, J.; Reppas, C. Characterization of the Contents of Ascending Colon to Which Drugs Are Exposed After Oral Administration to Healthy Adults. *Pharm. Res. N. Y.* **2009**, *26*, 2141–51, doi:http://dx.doi.org/10.1007/s11095-009-9927-x.
52. Tannergren, C.; Bergendal, A.; Lennernäs, H.; Abrahamsson, B. Toward an Increased Understanding of the Barriers to Colonic Drug Absorption in Humans: Implications for Early Controlled Release Candidate Assessment. *Mol. Pharm.* **2009**, *6*, 60–73, doi:10.1021/mp800261a.
53. Broesder, A.; Woerdenbag, H.J.; Prins, G.H.; Nguyen, D.N.; Frijlink, H.W.; Hinrichs, W.L.J. PH-Dependent Ileocolonic Drug Delivery, Part I: In Vitro and Clinical Evaluation of Novel Systems. *Drug Discov. Today* **2020**, *25*, 1362–1373, doi:10.1016/j.drudis.2020.06.011.
54. Evans, D.F.; Pye, G.; Bramley, R.; Clark, A.G.; Dyson, T.J.; Hardcastle, J.D. Measurement of Gastrointestinal PH Profiles in Normal Ambulant Human Subjects. *Gut* **1988**, *29*, 1035–1041, doi:10.1136/gut.29.8.1035.
55. SG, N.; D, K.; DS, R.; DF, E. Intestinal Luminal PH in Inflammatory Bowel Disease : Possible Determinants and Implications for Therapy with Aminosalicylates and Other Drugs. *Gut* **2001**, *48*, 571–577.
56. Koziolek, M.; Grimm, M.; Becker, D.; Iordanov, V.; Zou, H.; Shimizu, J.; Wanke, C.; Garbacz, G.; Weitschies, W. Investigation of PH and Temperature Profiles in the GI Tract of Fasted Human Subjects Using the Intellicap(®) System. *J. Pharm. Sci.* **2015**, *104*, 2855–2863, doi:10.1002/jps.24274.

57. McDougall, C.J.; Wong, R.; Scudera, P.; Lesser, M.; DeCosse, J.J. Colonic Mucosal PH in Humans. *Dig. Dis. Sci.* **1993**, *38*, 542–545, doi:10.1007/BF01316512.
58. Deloose, E.; Janssen, P.; Depoortere, I.; Tack, J. The Migrating Motor Complex: Control Mechanisms and Its Role in Health and Disease. *Nat. Rev. Gastroenterol. Hepatol.* **2012**, *9*, 271–285, doi:10.1038/nrgastro.2012.57.
59. Grivel, M.L.; Ruckebusch, Y. The Propagation of Segmental Contractions along the Small Intestine. *J. Physiol.* **1972**, *227*, 611–625, doi:10.1113/jphysiol.1972.sp010050.
60. Maurer, A.H. Gastrointestinal Motility, Part 2: Small-Bowel and Colon Transit. *J. Nucl. Med. Technol.* **2016**, *44*, 12–18, doi:10.2967/jnumed.113.134551.
61. Phillips, S.F. Functions of the Large Bowel: An Overview. *Scand. J. Gastroenterol. Suppl.* **1984**, *93*, 1–12.
62. Hens, B.; Corsetti, M.; Spiller, R.; Marciani, L.; Vanuytsel, T.; Tack, J.; Talattof, A.; Amidon, G.L.; Koziolek, M.; Weitschies, W.; et al. Exploring Gastrointestinal Variables Affecting Drug and Formulation Behavior: Methodologies, Challenges and Opportunities. *Int. J. Pharm.* **2017**, *519*, 79–97, doi:10.1016/j.ijpharm.2016.11.063.
63. Pentafragka, C.; Symillides, M.; McAllister, M.; Dressman, J.; Vertzoni, M.; Reppas, C. The Impact of Food Intake on the Luminal Environment and Performance of Oral Drug Products with a View to in Vitro and in Silico Simulations: A PEARRL Review. *J. Pharm. Pharmacol.* **2019**, *71*, 557–580, doi:10.1111/jphp.12999.
64. Reppas, C.; Karatza, E.; Goumas, C.; Markopoulos, C.; Vertzoni, M. Characterization of Contents of Distal Ileum and Cecum to Which Drugs/Drug Products Are Exposed during Bioavailability/Bioequivalence Studies in Healthy Adults. *Pharm. Res.* **2015**, doi:10.1007/s11095-015-1710-6.
65. Ingels, F.; Deferme, S.; Destexhe, E.; Oth, M.; Van Den Mooter, G.; Augustijns, P. Simulated Intestinal Fluid as Transport Medium in the Caco-2 Cell Culture Model. *Int. J. Pharm.* **2002**, *232*, 183–192, doi:10.1016/S0378-5173(01)00897-3.
66. Birch, D.; Diedrichsen, R.G.; Christophersen, P.C.; Mu, H.; Nielsen, H.M. Evaluation of Drug Permeation under Fed State Conditions Using Mucus-Covered Caco-2 Cell Epithelium. *Eur. J. Pharm. Sci. Off. J. Eur. Fed. Pharm. Sci.* **2018**, *118*, 144–153, doi:10.1016/j.ejps.2018.02.032.
67. Pelaseyed, T.; Bergström, J.H.; Gustafsson, J.K.; Ermund, A.; Birchenough, G.M.H.; Schütte, A.; van der Post, S.; Svensson, F.; Rodríguez-Piñeiro, A.M.; Nyström, E.E.L.; et al. The Mucus and Mucins of the Goblet Cells and Enterocytes Provide the First Defense Line of the Gastrointestinal Tract and Interact with the Immune System. *Immunol. Rev.* **2014**, *260*, 8–20, doi:10.1111/imr.12182.
68. Vertzoni, M.; Diakidou, A.; Chatzilias, M.; Söderlind, E.; Abrahamsson, B.; Dressman, J.B.; Reppas, C. Biorelevant Media to Simulate Fluids in the Ascending Colon of Humans and Their Usefulness in Predicting Intracolonic Drug Solubility. *Pharm. Res.* **2010**, *27*, 2187–2196, doi:10.1007/s11095-010-0223-6.
69. Georgaka, D.; Butler, J.; Kesisoglou, F.; Reppas, C.; Vertzoni, M. Evaluation of Dissolution in the Lower Intestine and Its Impact on the Absorption Process of High Dose Low Solubility Drugs. *Mol. Pharm.* **2017**, *14*, 4181–4191, doi:10.1021/acs.molpharmaceut.6b01129.
70. Markopoulos, C.; Vertzoni, M.; Symillides, M.; Kesisoglou, F.; Reppas, C. Two-Stage Single-Compartment Models to Evaluate Dissolution in the Lower Intestine. *J. Pharm. Sci.* **2015**, *104*, 2986–2997, doi:10.1002/jps.24485.

71. Hawksworth, G.; Drasar, B.S.; Hill, M.J. Intestinal Bacteria and the Hydrolysis of Glycosidic Bonds. *J. Med. Microbiol.* **1971**, *4*, 451–459, doi:10.1099/00222615-4-4-451.
72. Prasad, Y.V.R.; Krishnaiah, Y.S.R.; Satyanarayana, S. In Vitro Evaluation of Guar Gum as a Carrier for Colon-Specific Drug Delivery. *J. Controlled Release* **1998**, *51*, 281–287, doi:10.1016/S0168-3659(97)00181-8.
73. Rubinstein, A.; Radai, R.; Ezra, M.; Pathak, S.; Rokem, J.S. In Vitro Evaluation of Calcium Pectinate: A Potential Colon-Specific Drug Delivery Carrier. *Pharm. Res.* **1993**, *10*, 258–263, doi:10.1023/A:1018995029167.
74. Jain, A.; Gupta, Y.; Jain, S.K. Potential of Calcium Pectinate Beads for Target Specific Drug Release to Colon. *J. Drug Target.* **2007**, *15*, 285–294, doi:10.1080/10611860601146134.
75. Bashardoust, N.; Jenita, J.L.; Zakeri-Milani, P. Preparation and In Vitro Investigation of Chitosan Compressed Tablets for Colon Targeting. *Adv. Pharm. Bull.* **2011**, *1*, 87–92, doi:10.5681/apb.2011.013.
76. Tiwari, A.; Ramteke, S.; Shukla, R.D. and R. Preparation and Characterization of Satranidazole Loaded Calcium Pectinate Microbeads for Colon Specific Delivery; Application of Response Surface Methodology Available online: https://www.eurekaselect.com/74540/article (accessed on 21 August 2020).
77. Shukla, R.K.; Ramteke, S.; Trivedi, P.; Tiwari, A. Enteric Coated Guar Gum Microspheres of Ornidazole for Colonic Delivery. *Curr. Nanosci.* **2012**, *8*, 571–580, doi:10.2174/157341312801784186.
78. Wahlgren, M.; Axenstrand, M.; Håkansson, Å.; Marefati, A.; Lomstein Pedersen, B. In Vitro Methods to Study Colon Release: State of the Art and An Outlook on New Strategies for Better In-Vitro Biorelevant Release Media. *Pharmaceutics* **2019**, *11*, doi:10.3390/pharmaceutics11020095.
79. Milojevic, S.; Newton, J.M.; Cummings, J.H.; Gibson, G.R.; Louise Botham, R.; Ring, S.G.; Stockham, M.; Allwood, M.C. Amylose as a Coating for Drug Delivery to the Colon: Preparation and in Vitro Evaluation Using 5-Aminosalicylic Acid Pellets. *J. Controlled Release* **1996**, *38*, 75–84, doi:10.1016/0168-3659(95)00112-3.
80. Gibson, G.R.; Cummings, J.H.; Macfarlane, G.T. Use of a Three-Stage Continuous Culture System to Study the Effect of Mucin on Dissimilatory Sulfate Reduction and Methanogenesis by Mixed Populations of Human Gut Bacteria. *Appl. Environ. Microbiol.* **1988**, *54*, 2750–2755.
81. Macfarlane, S.; Quigley, M.E.; Hopkins, M.J.; Newton, D.F.; Macfarlane, G.T. Polysaccharide Degradation by Human Intestinal Bacteria during Growth under Multi-Substrate Limiting Conditions in a Three-Stage Continuous Culture System. *FEMS Microbiol. Ecol.* **1998**, *26*, 231–243, doi:10.1016/S0168-6496(98)00039-7.
82. Sousa, T.; Paterson, R.; Moore, V.; Carlsson, A.; Abrahamsson, B.; Basit, A.W. The Gastrointestinal Microbiota as a Site for the Biotransformation of Drugs. *Int. J. Pharm.* **2008**, *363*, 1–25, doi:10.1016/j.ijpharm.2008.07.009.
83. Vertzoni, M.; Kersten, E.; van der Mey, D.; Muenster, U.; Reppas, C. Evaluating the Clinical Importance of Bacterial Degradation of Therapeutic Agents in the Lower Intestine of Adults Using Adult Fecal Material. *Eur. J. Pharm. Sci.* **2018**, *125*, 142–150, doi:10.1016/j.ejps.2018.09.019.
84. Tannergren, C.; Borde, A.; Boreström, C.; Abrahamsson, B.; Lindahl, A. Evaluation of an in Vitro Faecal Degradation Method for Early Assessment of the Impact of

Colonic Degradation on Colonic Absorption in Humans. *Eur. J. Pharm. Sci. Off. J. Eur. Fed. Pharm. Sci.* **2014**, *57*, 200–206, doi:10.1016/j.ejps.2013.10.001.
85. Vertzoni, M.; Carlsson, A.; Abrahamsson, B.; Goumas, K.; Reppas, C. Degradation Kinetics of Metronidazole and Olsalazine by Bacteria in Ascending Colon and in Feces of Healthy Adults. *Int. J. Pharm.* **2011**, *413*, 81–86, doi:10.1016/j.ijpharm.2011.04.028.
86. Vince, A.; Killingley, M.; Wrong, O.M. Effect of Lactulose on Ammonia Production in a Fecal Incubation System. *Gastroenterology* **1978**, *74*, 544–549, doi:10.1016/0016-5085(78)90293-7.
87. Lemmens, G.; Van Camp, A.; Kourula, S.; Vanuytsel, T.; Augustijns, P. Drug Disposition in the Lower Gastrointestinal Tract: Targeting and Monitoring. *Pharmaceutics* **2021**, *13*, 161, doi:10.3390/pharmaceutics13020161.
88. Hubatsch, I.; Ragnarsson, E.G.E.; Artursson, P. Determination of Drug Permeability and Prediction of Drug Absorption in Caco-2 Monolayers. *Nat. Protoc.* **2007**, *2*, 2111–2120.
89. Pham-The, H.; Cabrera-Pérez, M.Á.; Nam, N.-H.; Castillo-Garit, J.A.; Rasulev, B.; Le-Thi-Thu, H.; Casañola-Martin, G.M. In Silico Assessment of ADME Properties: Advances in Caco-2 Cell Monolayer Permeability Modeling. *Curr. Top. Med. Chem.* **2018**, *18*, 2209–2229, doi:10.2174/1568026619666181130140350.
90. Han van de Waterbeemd, Bernard Testa, Raimund Mannhold, et al *Drug Bioavailability: Estimation of Solubility, Permeability, Absorption and Bioavailability, Volume 40, 2nd Edition* -; ISBN 978-3-527-32051-6.
91. Artursson, P.; Karlsson, J. Correlation between Oral Drug Absorption in Humans and Apparent Drug Permeability Coefficients in Human Intestinal Epithelial (Caco-2) Cells. *Biochem. Biophys. Res. Commun.* **1991**, *175*, 880–885, doi:10.1016/0006-291X(91)91647-U.
92. Tavelin, S.; Taipalensuu, J.; Söderberg, L.; Morrison, R.; Chong, S.; Artursson, P. Prediction of the Oral Absorption of Low-Permeability Drugs Using Small Intestine-Like 2/4/A1 Cell Monolayers. *Pharm. Res.* **2003**, *20*, 397–405, doi:10.1023/A:1022699920043.
93. Sánchez, A.B.; Calpena, A.C.; Mallandrich, M.; Clares, B. Validation of an Ex Vivo Permeation Method for the Intestinal Permeability of Different BCS Drugs and Its Correlation with Caco-2 In Vitro Experiments. *Pharmaceutics* **2019**, *11*, doi:10.3390/pharmaceutics11120638.
94. Cui, Y.; Claus, S.; Schnell, D.; Runge, F.; Maclean, C. In-Depth Characterization of Epiintestinal Microtissue as a Model for Intestinal Drug Absorption and Metabolism in Human. *Pharmaceutics* **2020**, *12*, doi:10.3390/pharmaceutics12050405.
95. Englund, G.; Rorsman, F.; Rönnblom, A.; Karlbom, U.; Lazorova, L.; Gråsjö, J.; Kindmark, A.; Artursson, P. Regional Levels of Drug Transporters along the Human Intestinal Tract: Co-Expression of ABC and SLC Transporters and Comparison with Caco-2 Cells. *Eur. J. Pharm. Sci.* **2006**, *29*, 269–277, doi:10.1016/j.ejps.2006.04.010.
96. Behrens, I.; Kamm, W.; Dantzig, A.H.; Kissel, T. Variation of Peptide Transporter (PepT1 and HPT1) Expression in Caco-2 Cells as a Function of Cell Origin. *J. Pharm. Sci.* **2004**, *93*, 1743–1754, doi:10.1002/jps.20062.
97. Behrens, I.; Kissel, T. Do Cell Culture Conditions Influence the Carrier-Mediated Transport of Peptides in Caco-2 Cell Monolayers? *Eur. J. Pharm. Sci. Off. J. Eur. Fed. Pharm. Sci.* **2003**, *19*, 433–442, doi:10.1016/s0928-0987(03)00146-5.

98. Bravo, S.A.; Nielsen, C.U.; Amstrup, J.; Frokjaer, S.; Brodin, B. In-Depth Evaluation of Gly-Sar Transport Parameters as a Function of Culture Time in the Caco-2 Cell Model. *Eur. J. Pharm. Sci. Off. J. Eur. Fed. Pharm. Sci.* **2004**, *21*, 77–86, doi:10.1016/s0928-0987(03)00205-7.
99. Lennernäs, H. Human Intestinal Permeability. *J. Pharm. Sci.* **1998**, *87*, 403–410, doi:10.1021/js970332a.
100. Lozoya-Agullo, I.; Araújo, F.; González-Álvarez, I.; Merino-Sanjuán, M.; González-Álvarez, M.; Bermejo, M.; Sarmento, B. Usefulness of Caco-2/HT29-MTX and Caco-2/HT29-MTX/Raji B Coculture Models To Predict Intestinal and Colonic Permeability Compared to Caco-2 Monoculture. *Mol. Pharm.* **2017**, *14*, 1264–1270, doi:10.1021/acs.molpharmaceut.6b01165.
101. Lennernäs, H. Human Jejunal Effective Permeability and Its Correlation with Preclinical Drug Absorption Models. *J. Pharm. Pharmacol.* **1997**, *49*, 627–638, doi:10.1111/j.2042-7158.1997.tb06084.x.
102. Makhey, V.D.; Guo, A.; Norris, D.A.; Hu, P.; Yan, J.; Sinko, P.J. Characterization of the Regional Intestinal Kinetics of Drug Efflux in Rat and Human Intestine and in Caco-2 Cells. *Pharm. Res.* **1998**, *15*, 1160–1167, doi:10.1023/a:1011971303880.
103. Rozehnal, V.; Nakai, D.; Hoepner, U.; Fischer, T.; Kamiyama, E.; Takahashi, M.; Yasuda, S.; Mueller, J. Human Small Intestinal and Colonic Tissue Mounted in the Ussing Chamber as a Tool for Characterizing the Intestinal Absorption of Drugs. *Eur. J. Pharm. Sci.* **2012**, *46*, 367–373, doi:10.1016/j.ejps.2012.02.025.
104. Stephens, R.H.; O'Neill, C.A.; Warhurst, A.; Carlson, G.L.; Rowland, M.; Warhurst, G. Kinetic Profiling of P-Glycoprotein-Mediated Drug Efflux in Rat and Human Intestinal Epithelia. *J. Pharmacol. Exp. Ther.* **2001**, *296*, 584–591.
105. Ungell, A.-L.; Nylander, S.; Bergstrand, S.; Sjöberg, Å.; Lennernäs, H. Membrane Transport of Drugs in Different Regions of the Intestinal Tract of the Rat. *J. Pharm. Sci.* **1998**, *87*, 360–366, doi:10.1021/js970218s.
106. Wu-Pong, S.; Livesay, V.; Dvorchik, B.; Barr, W.H. Oligonucleotide Transport in Rat and Human Intestine Ussing Chamber Models. *Biopharm. Drug Dispos.* **1999**, *20*, 411–416, doi:10.1002/1099-081x(199912)20:9<411::aid-bdd208>3.0.co;2-4.
107. Westerhout, J.; Wortelboer, H.; Verhoeckx, K. Ussing Chamber. In *The Impact of Food Bioactives on Health: In Vitro and Ex Vivo Models*; Springer International Publishing, 2015; pp. 263–273 ISBN 9783319161044.
108. Sjöberg, Å.; Lutz, M.; Tannergren, C.; Wingolf, C.; Borde, A.; Ungell, A.-L. Comprehensive Study on Regional Human Intestinal Permeability and Prediction of Fraction Absorbed of Drugs Using the Ussing Chamber Technique. *Eur. J. Pharm. Sci.* **2013**, *48*, 166–180, doi:10.1016/J.EJPS.2012.10.007.
109. Haslam, I.S.; O'Reilly, D.A.; Sherlock, D.J.; Kauser, A.; Womack, C.; Coleman, T. Pancreatoduodenectomy as a Source of Human Small Intestine for Ussing Chamber Investigations and Comparative Studies with Rat Tissue. *Biopharm. Drug Dispos.* **2011**, *32*, 210–221, doi:10.1002/bdd.751.
110. Ungell, A.-L.; Abrahamsson, B. Biopharmaceutical Support in Candidate Drug Selection. **2001**, 129–171, doi:10.1201/b14413-6.
111. Watanabe, E.; Takahashi, M.; Hayashi, M. A Possibility to Predict the Absorbability of Poorly Water-Soluble Drugs in Humans Based on Rat Intestinal Permeability Assessed by an in Vitro Chamber Method. *Eur. J. Pharm. Biopharm.* **2004**, *58*, 659–665, doi:10.1016/j.ejpb.2004.03.029.

112. Miyake, M.; Toguchi, H.; Nishibayashi, T.; Higaki, K.; Sugita, A.; Koganei, K.; Kamada, N.; Kitazume, M.T.; Hisamatsu, T.; Sato, T.; et al. Establishment of Novel Prediction System of Intestinal Absorption in Humans Using Human Intestinal Tissues. *J. Pharm. Sci.* **2013**, *102*, 2564–2571, doi:10.1002/jps.23609.
113. Kisser, B.; Mangelsen, E.; Wingolf, C.; Partecke, L.I.; Heidecke, C.-D.; Tannergren, C.; Oswald, S.; Keiser, M. The Ussing Chamber Assay to Study Drug Metabolism and Transport in the Human Intestine. *Curr. Protoc. Pharmacol.* **2017**, *77*, 7.17.1-7.17.19, doi:10.1002/cpph.22.
114. Zimmermann, C.; Gutmann, H.; Hruz, P.; Gutzwiller, J.-P.; Beglinger, C.; Drewe, J. Mapping of Multidrug Resistance Gene 1 and Multidrug Resistance-Associated Protein Isoform 1 to 5 MRNA Expression along the Human Intestinal Tract. *Drug Metab. Dispos. Biol. Fate Chem.* **2005**, *33*, 219–224, doi:10.1124/dmd.104.001354.
115. Sato, T.; Vries, R.G.; Snippert, H.J.; van de Wetering, M.; Barker, N.; Stange, D.E.; van Es, J.H.; Abo, A.; Kujala, P.; Peters, P.J.; et al. Single Lgr5 Stem Cells Build Crypt-Villus Structures in Vitro without a Mesenchymal Niche. *Nature* **2009**, *459*, 262–265, doi:10.1038/nature07935.
116. Sato, T.; Stange, D.E.; Ferrante, M.; Vries, R.G.J.; Es, J.H. van; Brink, S. van den; Houdt, W.J. van; Pronk, A.; Gorp, J. van; Siersema, P.D.; et al. Long-Term Expansion of Epithelial Organoids From Human Colon, Adenoma, Adenocarcinoma, and Barrett's Epithelium. *Gastroenterology* **2011**, *141*, 1762–1772, doi:10.1053/j.gastro.2011.07.050.
117. Basak, O.; Beumer, J.; Wiebrands, K.; Seno, H.; van Oudenaarden, A.; Clevers, H. Induced Quiescence of Lgr5+ Stem Cells in Intestinal Organoids Enables Differentiation of Hormone-Producing Enteroendocrine Cells. *Cell Stem Cell* **2017**, *20*, 177-190.e4, doi:10.1016/j.stem.2016.11.001.
118. Yin, X.; Farin, H.F.; van Es, J.H.; Clevers, H.; Langer, R.; Karp, J.M. Niche-Independent High-Purity Cultures of Lgr5 + Intestinal Stem Cells and Their Progeny. *Nat. Methods* **2014**, *11*, 106–112, doi:10.1038/nmeth.2737.
119. Mizutani, T.; Nakamura, T.; Morikawa, R.; Fukuda, M.; Mochizuki, W.; Yamauchi, Y.; Nozaki, K.; Yui, S.; Nemoto, Y.; Nagaishi, T.; et al. Real-Time Analysis of P-Glycoprotein-Mediated Drug Transport across Primary Intestinal Epithelium Three-Dimensionally Cultured in Vitro. *Biochem. Biophys. Res. Commun.* **2012**, *419*, 238–243, doi:10.1016/j.bbrc.2012.01.155.
120. Zhang, L.; Zhao, J.; Liang, C.; Liu, M.; Xu, F.; Wang, X. A Novel Biosensor Based on Intestinal 3D Organoids for Detecting the Function of BCRP. *Drug Deliv.* **2017**, *24*, 1453–1459, doi:10.1080/10717544.2017.1381199.
121. Onozato, D.; Yamashita, M.; Nakanishi, A.; Akagawa, T.; Kida, Y.; Ogawa, I.; Hashita, T.; Iwao, T.; Matsunaga, T. Generation of Intestinal Organoids Suitable for Pharmacokinetic Studies from Human Induced Pluripotent Stem Cells. *Drug Metab. Dispos.* **2018**, *46*, 1572–1580, doi:10.1124/dmd.118.080374.
122. Moon, C.; VanDussen, K.L.; Miyoshi, H.; Stappenbeck, T.S. Development of a Primary Mouse Intestinal Epithelial Cell Monolayer Culture System to Evaluate Factors That Modulate IgA Transcytosis. *Mucosal Immunol.* **2014**, *7*, 818–828, doi:10.1038/mi.2013.98.
123. VanDussen, K.L.; Marinshaw, J.M.; Shaikh, N.; Miyoshi, H.; Moon, C.; Tarr, P.I.; Ciorba, M.A.; Stappenbeck, T.S. Development of an Enhanced Human Gastrointestinal Epithelial Culture System to Facilitate Patient-Based Assays. *Gut* **2015**, *64*, 911–920, doi:10.1136/gutjnl-2013-306651.

124. Noben, M.; Vanhove, W.; Arnauts, K.; Santo Ramalho, A.; Van Assche, G.; Vermeire, S.; Verfaillie, C.; Ferrante, M. Human Intestinal Epithelium in a Dish: Current Models for Research into Gastrointestinal Pathophysiology. *United Eur. Gastroenterol. J.* **2017**, *5*, 1073–1081, doi:10.1177/2050640617722903.
125. Kim, H.J.; Huh, D.; Hamilton, G.; Ingber, D.E. Human Gut-on-a-Chip Inhabited by Microbial Flora That Experiences Intestinal Peristalsis-like Motions and Flow. *Lab. Chip* **2012**, *12*, 2165–2174, doi:10.1039/C2LC40074J.
126. Kim, H.J.; Ingber, D.E. Gut-on-a-Chip Microenvironment Induces Human Intestinal Cells to Undergo Villus Differentiation. *Integr. Biol. Quant. Biosci. Nano Macro* **2013**, *5*, 1130–1140, doi:10.1039/c3ib40126j.
127. Trietsch, S.J.; Naumovska, E.; Kurek, D.; Setyawati, M.C.; Vormann, M.K.; Wilschut, K.J.; Lanz, H.L.; Nicolas, A.; Ng, C.P.; Joore, J.; et al. Membrane-Free Culture and Real-Time Barrier Integrity Assessment of Perfused Intestinal Epithelium Tubes. *Nat. Commun.* **2017**, *8*, 262, doi:10.1038/s41467-017-00259-3.
128. Kim, S.H.; Lee, J.W.; Choi, I.; Kim, Y.-C.; Lee, J.B.; Sung, J.H. A Microfluidic Device with 3-d Hydrogel Villi Scaffold to Simulate Intestinal Absorption. *J. Nanosci. Nanotechnol.* **2013**, *13*, 7220–7228, doi:10.1166/jnn.2013.8088.
129. Yu, J.; Carrier, R.L.; March, J.C.; Griffith, L.G. Three Dimensional Human Small Intestine Models for ADME-Tox Studies. *Drug Discov. Today* **2014**, *19*, 1587–1594, doi:10.1016/j.drudis.2014.05.003.
130. Sontheimer-Phelps, A.; Chou, D.B.; Tovaglieri, A.; Ferrante, T.C.; Duckworth, T.; Fadel, C.; Frismantas, V.; Sutherland, A.D.; Jalili-Firoozinezhad, S.; Kasendra, M.; et al. Human Colon-on-a-Chip Enables Continuous In Vitro Analysis of Colon Mucus Layer Accumulation and Physiology. *Cell. Mol. Gastroenterol. Hepatol.* **2020**, *9*, 507–526, doi:10.1016/j.jcmgh.2019.11.008.
131. Kozuka, K.; He, Y.; Koo-McCoy, S.; Kumaraswamy, P.; Nie, B.; Shaw, K.; Chan, P.; Leadbetter, M.; He, L.; Lewis, J.G.; et al. Development and Characterization of a Human and Mouse Intestinal Epithelial Cell Monolayer Platform. *Stem Cell Rep.* **2017**, *9*, 1976–1990, doi:10.1016/j.stemcr.2017.10.013.
132. Ayehunie, S.; Landry, T.; Stevens, Z.; Armento, A.; Hayden, P.; Klausner, M. Human Primary Cell-Based Organotypic Microtissues for Modeling Small Intestinal Drug Absorption. *Pharm. Res.* **2018**, *35*, 72, doi:10.1007/s11095-018-2362-0.
133. Peters, M.F.; Landry, T.; Pin, C.; Maratea, K.; Dick, C.; Wagoner, M.P.; Choy, A.L.; Barthlow, H.; Snow, D.; Stevens, Z.; et al. Human 3D Gastrointestinal Microtissue Barrier Function As a Predictor of Drug-Induced Diarrhea. *Toxicol. Sci. Off. J. Soc. Toxicol.* **2019**, *168*, 3–17, doi:10.1093/toxsci/kfy268.
134. Srinivasan, B.; Kolli, A.R.; Esch, M.B.; Abaci, H.E.; Shuler, M.L.; Hickman, J.J. TEER Measurement Techniques for in Vitro Barrier Model Systems. *J. Lab. Autom.* **2015**, *20*, 107–126, doi:10.1177/2211068214561025.
135. Kasendra, M.; Luc, R.; Yin, J.; Manatakis, D.V.; Kulkarni, G.; Lucchesi, C.; Sliz, J.; Apostolou, A.; Sunuwar, L.; Obrigewitch, J.; et al. Duodenum Intestine-Chip for Preclinical Drug Assessment in a Human Relevant Model. *eLife* **2020**, *9*, doi:10.7554/eLife.50135.
136. Venema, K. The TNO In Vitro Model of the Colon (TIM-2). In *The Impact of Food Bioactives on Health: in vitro and ex vivo models*; Verhoeckx, K., Cotter, P., López-Expósito, I., Kleiveland, C., Lea, T., Mackie, A., Requena, T., Swiatecka, D., Wichers, H., Eds.; Springer International Publishing: Cham, 2015; pp. 293–304 ISBN 978-3-319-16104-4.

137. Van de Wiele, T.; Van den Abbeele, P.; Ossieur, W.; Possemiers, S.; Marzorati, M. The Simulator of the Human Intestinal Microbial Ecosystem (SHIME®). In *The Impact of Food Bioactives on Health: in vitro and ex vivo models*; Verhoeckx, K., Cotter, P., López-Expósito, I., Kleiveland, C., Lea, T., Mackie, A., Requena, T., Swiatecka, D., Wichers, H., Eds.; Springer International Publishing: Cham, 2015; pp. 305–317 ISBN 978-3-319-16104-4.
138. Shah, P.; Fritz, J. V.; Glaab, E.; Desai, M.S.; Greenhalgh, K.; Frachet, A.; Niegowska, M.; Estes, M.; Jäger, C.; Seguin-Devaux, C.; et al. A Microfluidics-Based in Vitro Model of the Gastrointestinal Human-Microbe Interface. *Nat. Commun.* **2016**, *7*, doi:10.1038/ncomms11535.
139. Minekus, M.; Smeets-Peeters, M.; Bernalier, A.; Marol-Bonnin, S.; Havenaar, R.; Marteau, P.; Alric, M.; Fonty, G.; Huis in't Veld, J.H.J. A Computer-Controlled System to Simulate Conditions of the Large Intestine with Peristaltic Mixing, Water Absorption and Absorption of Fermentation Products. *Appl. Microbiol. Biotechnol.* **1999**, *53*, 108–114, doi:10.1007/s002530051622.
140. Nuenen, M.H.M.C. van; Meyer, P.D.; Venema, K. The Effect of Various Inulins and Clostridium Difficile on the Metabolic Activity of the Human Colonic Microbiota in Vitro. *Microb. Ecol. Health Dis.* **2003**, *15*, 137–144, doi:10.1080/08910600310018959.
141. Venema, K.; Nuenen, M. van; Smeets-Peeters, M.; Minekus, M.; Havenaar, R. TNO's in Vitro Large Intestinal Model: An Excellent Screening Tool for Functional Food and Pharmaceutical Research. *Ernährung* **2000**, *24*, 558–564.
142. Molly, K.; Vande Woestyne, M.; Verstraete, W. Development of a 5-Step Multi-Chamber Reactor as a Simulation of the Human Intestinal Microbial Ecosystem. *Appl. Microbiol. Biotechnol.* **1993**, *39*, 254–258, doi:10.1007/BF00228615.
143. Peppercorn, M.A.; Goldman, P. The Role of Intestinal Bacteria in the Metabolism of Salicylazosulfapyridine. *J. Pharmacol. Exp. Ther.* **1972**, *181*, 555–562.
144. Van den Abbeele, P.; Van de Wiele, T.; Verstraete, W.; Possemiers, S. The Host Selects Mucosal and Luminal Associations of Coevolved Gut Microorganisms: A Novel Concept. *FEMS Microbiol. Rev.* **2011**, *35*, 681–704, doi:10.1111/j.1574-6976.2011.00270.x.
145. Van den Abbeele, P.; Belzer, C.; Goossens, M.; Kleerebezem, M.; De Vos, W.M.; Thas, O.; De Weirdt, R.; Kerckhof, F.-M.; Van de Wiele, T. Butyrate-Producing Clostridium Cluster XIVa Species Specifically Colonize Mucins in an in Vitro Gut Model. *ISME J.* **2013**, *7*, 949–961, doi:10.1038/ismej.2012.158.
146. Vermeiren, J.; Van den Abbeele, P.; Laukens, D.; Vigsnaes, L.K.; De Vos, M.; Boon, N.; Van de Wiele, T. Decreased Colonization of Fecal Clostridium Coccoides/Eubacterium Rectale Species from Ulcerative Colitis Patients in an in Vitro Dynamic Gut Model with Mucin Environment. *FEMS Microbiol. Ecol.* **2012**, *79*, 685–696, doi:10.1111/j.1574-6941.2011.01252.x.
147. Jalili-Firoozinezhad, S.; Gazzaniga, F.S.; Calamari, E.L.; Camacho, D.M.; Fadel, C.W.; Bein, A.; Swenor, B.; Nestor, B.; Cronce, M.J.; Tovaglieri, A.; et al. A Complex Human Gut Microbiome Cultured in an Anaerobic Intestine-on-a-Chip. *Nat. Biomed. Eng.* **2019**, *3*, 520–531, doi:10.1038/s41551-019-0397-0.
148. Kim, H.J.; Li, H.; Collins, J.J.; Ingber, D.E. Contributions of Microbiome and Mechanical Deformation to Intestinal Bacterial Overgrowth and Inflammation in a Human Gut-on-a-Chip. *Proc. Natl. Acad. Sci.* **2016**, *113*, E7–E15, doi:10.1073/pnas.1522193112.

149. Pfizer CELEBREX- Celecoxib Capsule Available online: http://labeling.pfizer.com/ShowLabeling.aspx?id=793 (accessed on 10 January 2020).
150. Paulson, S.K.; Vaughn, M.B.; Jessen, S.M.; Lawal, Y.; Gresk, C.J.; Yan, B.; Maziasz, T.J.; Cook, C.S.; Karim, A. Pharmacokinetics of Celecoxib after Oral Administration in Dogs and Humans: Effect of Food and Site of Absorption. *J. Pharmacol. Exp. Ther.* **2001**, *297*.
151. Yazdanian, M.; Briggs, K.; Jankovsky, C.; Hawi, A. The "High Solubility" Definition of the Current FDA Guidance on Biopharmaceutical Classification System May Be Too Strict for Acidic Drugs. *Pharm. Res.* **2004**, *21*, 293–299, doi:10.1023/B:PHAM.0000016242.48642.71.
152. Duggan, D.E.; Hare, L.E.; Ditzler, C.A.; Lei, B.W.; Kwan, K.C. The Disposition of Sulindac. *Clin. Pharmacol. Ther.* **1977**, *21*, 326–335, doi:10.1002/cpt1977213326.
153. Edsbäcker, S.; Larsson, P.; Wollmer, P. Gut Delivery of Budesonide, a Locally Active Corticosteroid, from Plain and Controlled-Release Capsules. *Eur. J. Gastroenterol. Hepatol.* **2002**, *14*, 1357–1362, doi:10.1097/00042737-200212000-00012.
154. Kesisoglou, F.; Xia, B.; Agrawal, N.G.B. Comparison of Deconvolution-Based and Absorption Modeling IVIVC for Extended Release Formulations of a BCS III Drug Development Candidate. *AAPS J.* **2015**, *17*, 1492–1500, doi:10.1208/s12248-015-9816-7.
155. Yu, A.; Baker, J.R.; Fioritto, A.F.; Wang, Y.; Luo, R.; Li, S.; Wen, B.; Bly, M.; Tsume, Y.; Koenigsknecht, M.J.; et al. Measurement of in Vivo Gastrointestinal Release and Dissolution of Three Locally Acting Mesalamine Formulations in Regions of the Human Gastrointestinal Tract. *Mol. Pharm.* **2017**, *14*, 345–358, doi:10.1021/acs.molpharmaceut.6b00641.
156. Nejdfors, P.; Ekelund, M.; Jeppsson, B.; Weström, B.R. Mucosal in Vitro Permeability in the Intestinal Tract of the Pig, the Rat, and Man: Species- and Region-Related Differences. *Scand. J. Gastroenterol.* **2000**, *35*, 501–507, doi:10.1080/003655200750023769.
157. Bray, F.; Ferlay, J.; Soerjomataram, I.; Siegel, R.L.; Torre, L.A.; Jemal, A. Global Cancer Statistics 2018: GLOBOCAN Estimates of Incidence and Mortality Worldwide for 36 Cancers in 185 Countries. *CA. Cancer J. Clin.* **2018**, *68*, 394–424, doi:10.3322/caac.21492.
158. Gong, L.; Thorn, C.F.; Bertagnolli, M.M.; Grosser, T.; Altman, R.B.; Klein, T.E. Celecoxib Pathways: Pharmacokinetics and Pharmacodynamics. *Pharmacogenet. Genomics* **2012**, *22*, 310–8, doi:10.1097/FPC.0b013e32834f94cb.
159. Burn, J.; Sheth, H. The Role of Aspirin in Preventing Colorectal Cancer. *Br. Med. Bull.* 2016.
160. Fujimura, T.; Ohta, T.; Oyama, K.; Miyashita, T.; Miwa, K.; Miyashita, T.-M.; Surgery, G. Gastrointestinal Tract Cancers: A Review and Report of Personal Experience DEVELOPMENT OF SELECTIVE COX-2 IN-HIBITORS. *China World J Gastroenterol* **2345**, *12*, 1336–1345.
161. Paulson, S.K.; Zhang, J.Y.; Breau, A.P.; Hribar, J.D.; Liu, N.W.; Jessen, S.M.; Lawal, Y.M.; Cogburn, J.N.; Gresk, C.J.; Markos, C.S.; et al. Pharmacokinetics, Tissue Distribution, Metabolism, and Excretion of Celecoxib in Rats. *Drug Metab. Dispos. Biol. Fate Chem.* **2000**, *28*, 514–21.
162. Werner, U.; Werner, D.; Pahl, A.; Mundkowski, R.; Gillich, M.; Brune, K. Investigation of the Pharmacokinetics of Celecoxib by Liquid Chromatography-Mass Spectrometry. *Biomed. Chromatogr.* **2002**, *16*, 56–60, doi:10.1002/bmc.115.

163. Youle, M.S.; Read, N.W. Effect of Painless Rectal Distension on Gastrointestinal Transit of Solid Meal. *Dig. Dis. Sci.* **1984**, *29*, 902–906, doi:10.1007/BF01312478.
164. Mistiaen, W.; Blockx, P.; Van Hee, R.; Bortier, H.; Harrisson, F. The Effect of Stress on Gastric Emptying Rate Measured with a Radionuclide Tracer. *Hepatogastroenterology.* **2002**, *49*, 1457–60.
165. Greenwood-Van Meerveld, B.; Johnson, A.C.; Grundy, D. Gastrointestinal Physiology and Function. In; Springer, Cham, 2017; pp. 1–16.
166. Worsøe, J.; Fynne, L.; Gregersen, T.; Schlageter, V.; Christensen, L.A.; Dahlerup, J.F.; Rijkhoff, N.J.M.; Laurberg, S.; Krogh, K. Gastric Transit and Small Intestinal Transit Time and Motility Assessed by a Magnet Tracking System. *BMC Gastroenterol.* **2011**, *11*, 145, doi:10.1186/1471-230X-11-145.
167. Penning, T.D.; Talley, J.J.; Bertenshaw, S.R.; Carter, J.S.; Collins, P.W.; Docter, S.; Graneto, M.J.; Lee, L.F.; Malecha, J.W.; Miyashiro, J.M.; et al. Synthesis and Biological Evaluation of the 1,5-Diarylpyrazole Class of Cyclooxygenase-2 Inhibitors: Identification of 4-[5-(4-Methylphenyl)-3- (Trifluoromethyl)-1 *H* - Pyrazol-1-Yl]Benzenesulfonamide (SC-58635, Celecoxib). *J. Med. Chem.* **1997**, *40*, 1347–1365, doi:10.1021/jm960803q.
168. Vaish, V.; Sanyal, S.N. Role of Sulindac and Celecoxib in the Regulation of Angiogenesis during the Early Neoplasm of Colon: Exploring PI3-K/PTEN/Akt Pathway to the Canonical Wnt/β-Catenin Signaling. *Biomed. Pharmacother.* **2012**, *66*, 354–367, doi:10.1016/J.BIOPHA.2012.01.004.
169. Egashira, I.; Takahashi-Yanaga, F.; Nishida, R.; Arioka, M.; Igawa, K.; Tomooka, K.; Nakatsu, Y.; Tsuzuki, T.; Nakabeppu, Y.; Kitazono, T.; et al. Celecoxib and 2,5-Dimethylcelecoxib Inhibit Intestinal Cancer Growth by Suppressing the Wnt/β-Catenin Signaling Pathway. *Cancer Sci.* **2017**, *108*, 108–115, doi:10.1111/cas.13106.
170. Grösch, S.; Maier, T.J.; Schiffmann, S.; Geisslinger, G. Cyclooxygenase-2 (COX-2)–Independent Anticarcinogenic Effects of Selective COX-2 Inhibitors. *JNCI J. Natl. Cancer Inst.* **2006**, *98*, 736–747, doi:10.1093/jnci/djj206.
171. Liggett, J.L.; Choi, C.K.; Donnell, R.L.; Kihm, K.D.; Kim, J.S.; Min, K.W.; Noegel, A.A.; Baek, S.J. Nonsteroidal Anti-Inflammatory Drug Sulindac Sulfide Suppresses Structural Protein Nesprin-2 Expression in Colorectal Cancer Cells. *Biochim. Biophys. Acta - Gen. Subj.* **2014**, *1840*, 322–331, doi:10.1016/j.bbagen.2013.09.032.
172. Bottone, F.G.; Martinez, J.M.; Collins, J.B.; Afshari, C.A.; Eling, T.E. Gene Modulation by the Cyclooxygenase Inhibitor, Sulindac Sulfide, in Human Colorectal Carcinoma Cells. Possible Link to Apoptosis. *J. Biol. Chem.* **2003**, *278*, 25790–25801, doi:10.1074/jbc.M301002200.
173. Taylor, M.T.; Lawson, K.R.; Ignatenko, N.A.; Marek, S.E.; Stringer, D.E.; Skovan, B.A.; Gerner, E.W. *Sulindac Sulfone Inhibits K-Ras-Dependent Cyclooxygenase-2 Expression in Human Colon Cancer Cells 1*; 2000; Vol. 60;.
174. Giuliano, F.; Warner, T.D. Ex Vivo Assay to Determine the Cyclooxygenase Selectivity of Non-Steroidal Anti-Inflammatory Drugs. *Br. J. Pharmacol.* **1999**, *126*, 1824–1830, doi:10.1038/sj.bjp.0702518.
175. Lawson, K.R.; Ignatenko, N.A.; Piazza, G.A.; Cui, H.; Gerner, E.W. Influence of K-Ras Activation on the Survival Responses of Caco-2 Cells to the Chemopreventive Agents Sulindac and Difluoromethylornithine. *Cancer Epidemiol. Biomark. Prev. Publ. Am. Assoc. Cancer Res. Cosponsored Am. Soc. Prev. Oncol.* **2000**, *9*, 1155–62.

176. Li, X.; Pathi, S.S.; Safe, S. Sulindac Sulfide Inhibits Colon Cancer Cell Growth and Downregulates Specificity Protein Transcription Factors. *BMC Cancer* **2015**, *15*, 1, doi:10.1186/s12885-015-1956-8.
177. Piazza, G.A.; Rahm, A.K.; Finn, T.S.; Fryer, B.H.; Li, H.; Stoumen, A.L.; Pamukcu, R.; Ahnen, D.J. Apoptosis Primarily Accounts for the Growth-Inhibitory Properties of Sulindac Metabolites and Involves a Mechanism That Is Independent of Cyclooxygenase Inhibition, Cell Cycle Arrest, and P53 Induction. *Cancer Res.* **1997**, *57*, 2452–9.
178. Williams, C.S.; Goldman, A.P.; Sheng, H.; Morrow, J.D.; DuBois, R.N. Sulindac Sulfide, but Not Sulindac Sulfone, Inhibits Colorectal Cancer Growth. *Neoplasia* **1999**, *1*, 170–176, doi:10.1038/sj.neo.7900024.
179. Dobrinska, M.R.; Furst, D.E.; Spiegel, T.; Vincek, W.C.; Tompkins, R.; Duggan, D.E.; Davies, R.O.; Paulus, H.E. Biliary Secretion of Sulindac and Metabolites in Man. *Biopharm. Drug Dispos.* **1983**, *4*, 347–358, doi:10.1002/bdd.2510040407.
180. Van De Steeg, E.; Schuren, F.H.J.; Obach, R.S.; Van Woudenbergh, C.; Walker, G.S.; Heerikhuisen, M.; Nooijen, I.H.G.; Vaes, W.H.J. An Ex Vivo Fermentation Screening Platform to Study Drug Metabolism by Human Gut Microbiota. *Drug Metab. Dispos.* **2018**, *46*, 1596–1607, doi:10.1124/dmd.118.081026.
181. Grimm, M.; Koziolek, M.; Kühn, J.; Weitschies, W. Interindividual and Intraindividual Variability of Fasted State Gastric Fl Uid Volume and Gastric Emptying of Water. *Eur. J. Pharm. Biopharm.* **2018**, *127*, 309–317.
182. Mann, J.; Dressman, J.; Rosenblatt, K.; Ashworth, L.; Muenster, U.; Frank, K.; Hutchins, P.; Williams, J.; Klumpp, L.; Wielockx, K.; et al. Validation of Dissolution Testing with Biorelevant Media : An OrBiTo Study. **2017**, doi:10.1021/acs.molpharmaceut.7b00198.
183. Lemmens, G.; Brouwers, J.; Snoeys, J.; Augustijns, P.; Vanuytsel, T. Insight into the Colonic Disposition of Celecoxib in Humans. *Eur. J. Pharm. Sci.* **2020**, *145*, doi:10.1016/j.ejps.2020.105242.
184. ChemAxon Available online: https://www.drugbank.ca/drugs/DB00605 (accessed on 27 April 2020).
185. Reid, J.M.; Mandrekar, S.J.; Carlson, E.C.; Harmsen, W.S.; Green, E.M.; McGovern, R.M.; Szabo, E.; Ames, M.M.; Boring, D.; Limburg, P.J. Comparative Bioavailability of Sulindac in Capsule and Tablet Formulations. *Cancer Epidemiol. Biomarkers Prev.* **2008**, *17*, 674–679, doi:10.1158/1055-9965.EPI-07-2510.
186. Braeckmans, M.; Brouwers, J.; Masuy, I.; Servais, C.; Tack, J.; Augustijns, P. The Influence of Gastric Motility on the Intraluminal Behavior of Fosamprenavir. *Eur. J. Pharm. Sci.* **2020**, *142*, 105117, doi:10.1016/j.ejps.2019.105117.
187. Vertzoni, M.; Augustijns, P.; Grimm, M.; Koziolek, M.; Lemmens, G.; Parrott, N.; Pentafragka, C.; Reppas, C.; Rubbens, J.; Van Den Abeele, J.; et al. Impact of Regional Differences along the Gastrointestinal Tract of Healthy Adults on Oral Drug Absorption: An UNGAP Review. *Eur. J. Pharm. Sci.* **2019**, *134*, doi:10.1016/j.ejps.2019.04.013.
188. Davies, N.M.; Watson, M.S. Clinical Pharmacokinetics of Sulindac: A Dynamic Old Drug. *Clin. Pharmacokinet.* 1997, *32*, 437–459.
189. Birmingham, B.; Buvanendran, A. Nonsteroidal anti-inflammatory drugs, acetaminophen, and COX-2 inhibitors. In *Practical Management of Pain: Fifth Edition*; Elsevier Inc., 2013; p. 553.e5-568.e5 ISBN 9780323083409.

190. Duggan, D.E.; Hooke, K.F.; Noll, R.M.; Hucker, H.B.; Gordan Van Arman, C. *COMPARATIVE DISPOSITION OF SULINDAC AND METABOLITES IN FIVE SPECIES*; 1977; Vol. 27;.
191. Lemmens, G.; Brouwers, J.; Snoeys, J.; Augustijns, P.; Vanuytsel, T. Insight into the Colonic Disposition of Sulindac in Humans. *J. Pharm. Sci.* **2020**, doi:10.1016/j.xphs.2020.09.034.
192. Shono, Y.; Jantratid, E.; Janssen, N.; Kesisoglou, F.; Mao, Y.; Vertzoni, M.; Reppas, C.; Dressman, J.B. Prediction of Food Effects on the Absorption of Celecoxib Based on Biorelevant Dissolution Testing Coupled with Physiologically Based Pharmacokinetic Modeling. **2009**, doi:10.1016/j.ejpb.2009.05.009.
193. Wuyts, B.; Riethorst, D.; Brouwers, J.; Tack, J.; Annaert, P.; Augustijns, P. Evaluation of Fasted State Human Intestinal Fluid as Apical Solvent System in the Caco-2 Absorption Model and Comparison with FaSSIF. *Eur. J. Pharm. Sci.* **2015**, *67*, 126–135, doi:10.1016/j.ejps.2014.11.010.
194. Stappaerts, J.; Berben, P.; Cevik, I.; Augustijns, P. The Effect of 2-Hydroxypropyl-β-Cyclodextrin on the Intestinal Permeation through Mucus. *Eur. J. Pharm. Sci.* **2018**, *114*, 238–244, doi:10.1016/j.ejps.2017.12.014.
195. Song, W.H.; Yeom, D.W.; Lee, D.H.; Lee, K.M.; Yoo, H.J.; Chae, B.R.; Song, S.H.; Choi, Y.W. In Situ Intestinal Permeability and in Vivo Oral Bioavailability of Celecoxib in Supersaturating Self-Emulsifying Drug Delivery System. *Arch. Pharm. Res.* **2014**, *37*, 626–635, doi:10.1007/s12272-013-0202-7.
196. Varma, M.V.S.; Panchagnula, R. Prediction of in Vivo Intestinal Absorption Enhancement on P-Glycoprotein Inhibition, from Rat in Situ Permeability. *J. Pharm. Sci.* **2005**, *94*, 1694–1704, doi:10.1002/jps.20309.
197. Choi, M.; Cao, J.; Lee, Y.; Ikram, M. Colon-Targeted Delivery of Budesonide Using Dual PH- and Time-Dependent Polymeric Nanoparticles for Colitis Therapy. **2015**, 3789–3799.
198. Paulson, S.K.; Hribar, J.D.; Liu, N.W.; Hajdu, E.; Bible, R.H.; Piergies, A.; Karim, A. Metabolism and Excretion of [(14)C]Celecoxib in Healthy Male Volunteers. *Drug Metab. Dispos. Biol. Fate Chem.* **2000**, *28*, 308–14.
199. Paulson, S.K.; Vaughn, M.B.; Jessen, S.M.; Lawal, Y.; Gresk, C.J.; Yan, B.; Maziasz, T.J.; Cook, C.S.; Karim, A. Pharmacokinetics of Celecoxib after Oral Administration in Dogs and Humans: Effect of Food and Site of Absorption. *J. Pharmacol. Exp. Ther.* **2001**, *297*.
200. Sugita, K.; Kabashima, K. Tight Junctions in the Development of Asthma, Chronic Rhinosinusitis, Atopic Dermatitis, Eosinophilic Esophagitis, and Inflammatory Bowel Diseases. *J. Leukoc. Biol.* **2020**, *107*, 749–762, doi:10.1002/JLB.5MR0120-230R.
201. Matsuoka, K.; Kanai, T. The Gut Microbiota and Inflammatory Bowel Disease. *Semin. Immunopathol.* **2015**, *37*, 47–55, doi:10.1007/s00281-014-0454-4.
202. Loke, Y.L.; Chew, M.T.; Ngeow, Y.F.; Lim, W.W.D.; Peh, S.C. Colon Carcinogenesis: The Interplay Between Diet and Gut Microbiota. *Front. Cell. Infect. Microbiol.* **2020**, *10*, doi:10.3389/fcimb.2020.603086.
203. Nakamura, G.J.; Schneiderman, L.J.; Klauber, M.R. Colorectal Cancer and Bowel Habits. *Cancer* **1984**, *54*, 1475–1477, doi:10.1002/1097-0142(19841001)54:7<1475::AID-CNCR2820540743>3.0.CO;2-M.
204. VanDussen, K.L.; Marinshaw, J.M.; Shaikh, N.; Miyoshi, H.; Moon, C.; Tarr, P.I.; Ciorba, M.A.; Stappenbeck, T.S. Development of an Enhanced Human

Gastrointestinal Epithelial Culture System to Facilitate Patient-Based Assays. *Gut* **2015**, *64*, 911–920, doi:10.1136/gutjnl-2013-306651.

205. Johansson, M.E. V; Gustafsson, J.K.; Holmén-Larsson, J.; Jabbar, K.S.; Xia, L.; Xu, H.; Ghishan, F.K.; Carvalho, F.A.; Gewirtz, A.T.; Sjövall, H.; et al. Bacteria Penetrate the Normally Impenetrable Inner Colon Mucus Layer in Both Murine Colitis Models and Patients with Ulcerative Colitis. *Gut* **2014**, *63*, 281–291, doi:10.1136/gutjnl-2012-303207.

206. Srinivasan, B.; Kolli, A.R.; Esch, M.B.; Abaci, H.E.; Shuler, M.L.; Hickman, J.J. TEER Measurement Techniques for in Vitro Barrier Model Systems. *J. Lab. Autom.* **2015**, *20*, 107–126, doi:10.1177/2211068214561025.

Author contributions, scientific acknowledgements and conflict of interest

Author contributions

Chapter 1 – introduction: *Drug disposition in the lower gastrointestinal tract: targeting and monitoring (review)*

- **Manuscript writing:** Glenn Lemmens, Arno van Camp, Stephanie Kourula, Tim Vanuytsel, Patrick Augustijns

Chapter 3 – *Insight into the colonic disposition of celecoxib in humans*

- **Experimental Design:** Glenn Lemmens, Joachim Brouwers, Patrick Augustijns, Tim Vanuytsel
- **Execution of experiments:** Glenn Lemmens
- **Data analysis:** Glenn Lemmens
- **Manuscript writing:** Glenn Lemmens, Joachim Brouwers, Patrick Augustijns, Tim Vanuytsel
- **Medical supervision:** Tim Vanuytsel

Chapter 4 - *Insight into the colonic disposition of sulindac in humans*

- **Experimental Design:** Glenn Lemmens, Joachim Brouwers, Patrick Augustijns, Tim Vanuytsel
- **Execution of experiments:** Glenn Lemmens, Raf Mols
- **Data analysis:** Glenn Lemmens
- **Manuscript writing:** Glenn Lemmens, Joachim Brouwers, Patrick Augustijns, Tim Vanuytsel
- **Medical supervision:** Tim Vanuytsel

Chapter 5 – *In vitro assessment of colonic accumulation of NSAIDs used to treat colon cancer*

- **Experimental Design:** Glenn Lemmens, Joachim Brouwers, Ricard Farré, Patrick Augustijns, Tim Vanuytsel
- **Execution of experiments:** Glenn Lemmens, Raf Mols
- **Data analysis:** Glenn Lemmens
- **Manuscript writing:** Glenn Lemmens, Joachim Brouwers, Ricard Farré, Patrick Augustijns, Tim Vanuytsel
- **Medical supervision:** Tim Vanuytsel

Scientific acknowledgements

Raf Mols provided technical guidance for the analytical aspect during this project, and performed the *in situ* experiments. The authors are furthermore grateful for the medical assistance of hospital personnel during the clinical trials, as well as for the healthy volunteers that participated.

Conflict of interest

This work has received support from Flanders Innovation & Entrepreneurship (Vlaio) (Grant No. 155042) and KU Leuven Internal Funds (C24/17/076). Tim Vanuytsel is a senior clinical investigator of the Flanders Research Foundation (FWO Vlaanderen). The authors have no conflicts of interest to declare.

Curriculum vitae

Glenn LEMMENS

(°12 January 1993, Leuven, Belgium)

Education

- **2014 – 2016:** Master of Science in Biochemistry & Biotechnology, KU Leuven
- **2011 – 2014:** Bachelor of Science in Biochemistry & Biotechnology, KU Leuven
- **2005 – 2011:** Science-Mathematics, Sancta Maria, Leuven

Bibliography

Articles in internationally review journals

Lemmens, G.; Brouwers, J.; Snoeys, J.; Augustijns, P.; Vanuytsel, T. In vitro assessment of colonic accumulation of NSAIDs used to treat colon cancer. *Pharmaceutics.* **2021**, (in preparation)

Lemmens, G.; Van Camp, A.; Kourula, S.; Vanuytsel, T.; Augustijns, P. Drug Disposition in the Lower Gastrointestinal Tract: Targeting and Monitoring. *Pharmaceutics* **2021**, *13*, 161. https://doi.org/10.3390/pharmaceutics13020161

Lemmens, G.; Brouwers, J.; Snoeys, J.; Augustijns, P.; Vanuytsel, T. Insight into the Colonic Disposition of Sulindac in Humans. *J. Pharm. Sci.* **2020**, *110*, 259–267, doi:10.1016/j.xphs.2020.09.034.

Lemmens, G.; Brouwers, J.; Snoeys, J.; Augustijns, P.; Vanuytsel, T. Insight into the Colonic Disposition of Celecoxib in Humans. *Eur. J. Pharm. Sci.* **2020**, *145*, 105242, doi:10.1016/j.ejps.2020.105242.

Vertzoni, M.; Augustijns, P.; Grimm, M.; Koziolek, M.; **Lemmens, G.**; Parrott, N.; Pentafragka, C.; Reppas, C.; Rubbens, J.; Van Den Abeele, J.; et al. Impact of Regional Differences along the Gastrointestinal Tract of Healthy Adults on Oral Drug Absorption: An UNGAP Review. Eur. J. Pharm. Sci. 2019, 134, doi:10.1016/j.ejps.2019.04.013.

Meeting abstracts, presented at international scientific conferences and symposia

Lemmens, G.; Brouwers, J.; Snoeys, J.; Farré, R.; Augustijns, P.; Vanuytsel, T. Understanding colonic disposition of low solubility compounds. ULLA. Finland, 30 June – 6 July 2019

Lemmens, G.; Brouwers, J.; Snoeys, J.; Farré, R; Augustijns, P.; Vanuytsel, T. Pharmacokinetic disposition of celecoxib used for the prevention and treatment of colorectal cancer. UNGAP. Bulgaria, 12-13 February 2019

Lemmens, G.; Brouwers, J.; Snoeys, J.; Farré, R.; Augustijns, P.; Vanuytsel, T. Pharmacokinetic disposition of celecoxib used for the prevention and treatment of colorectal cancer. GPEN. Singapore, 26-29 September 2018

Meetings abstracts, presented at other scientific conferences and symposia

Lemmens, G.; Brouwers, J.; Snoeys, J.; Farré, R.; Augustijns, P.; Vanuytsel, T. Pharmacokinetic disposition of celecoxib used for the prevention and treatment of colorectal cancer. UNGAP. Bulgaria, 5-7 March 2018

Lemmens, G.; Brouwers, J.; Snoeys, J.; Farré, R.; Augustijns, P.; Vanuytsel, T. Pharmacokinetic disposition of celecoxib used for the prevention and treatment of colorectal cancer. Biopharmacy Day. Woluwe Saint-Lamber, 8 december 2017.

Lemmens, G.; Brouwers, J.; Snoeys, J.; Farré, R.; Augustijns, P.; Vanuytsel, T. Pharmacokinetics of COX-inhibitors for the prevention and treatment of colorectal cancer. ULLA. Leuven, 08 – 15 July 2017